Probing the Influence of the Tp′ Ligand on Reactions of Pt(II) and Pt(IV)

Kristi L. Engelman

A dissertation submitted to the faculty of the University of North Carolina at Chapel Hill in partial fulfillment of the requirements for the degree of Doctor of Philosophy in the Department of Chemistry.

Chapel Hill
2010

Approved by:

Advisor: Professor Joseph L. Templeton

Professor Maurice Brookhart

Professor Cynthia Schauer

Professor Valerie Ashby

Professor Wenbin Lin

ABSTRACT

Kristi Engelman: Probing the Influence of the Tp′ Ligand on Reactions of Pt(II) and Pt(IV)
(Under the direction of Professor Joseph L. Templeton)

Transformations of platinum(II) to platinum(IV) using organic reagents have been studied. A tridentate ligand system, hydridotris(3,5-dimethylpyrazolyl)borate - Tp′, was shown to promote reactions at the platinum center. Three types of organic reagents have been investigated: alkynes, carbon monoxide, and isonitriles.

Reaction of the Tp′PtMe fragment with terminal alkynes results in η^2-binding of the alkyne. Oxidative addition of the alkyne occurs upon gentle heating. Kinetic studies indicate that electron donating groups on the alkyne increase the rate of oxidative addition and that approaching the transition state increases the entropy. The proposed mechanism of oxidative addition proceeds through a transition state in which the third arm of the Tp′ ligand is dechelated, a process that would be made easier by an electron donating group on the alkyne. In contrast, the reaction of alkynes (both terminal and internal) with the Tp′PtPh fragment does not produce η^2-bound alkyne adducts. Instead, phenyl migration to the alkyne followed by *ortho* C-H bond activation occurs resulting in formation of unsaturated metallacycles.

Conversion of Tp′Pt(Me)(CO) to the acyl complex, Tp′Pt(C(Me)=O)MeH has been accomplished by nucleophilic attack with MeLi followed by addition of HCl. The Pt(IV) acyl complex reacts with adventitious water in the presence of CO to produce the

acyl dihydride product, Tp′Pt(C(Me)=O)H_2, from a proposed metal mediated water gas shift reaction. Upon addition of acid, formation of dihydrogen is observed. An analogous carboxamido complex, Tp′Pt((C=O)NHR)Me_2, has also been synthesized. Deprotonation of the carboxamido ligand followed by acidification produces Tp′PtMe_2H, presumably after elimination of free isocyanate.

Reaction of the Tp′PtMe fragment with 2,6-dimethylphenyl isonitrile produces a four-coordinate σ-bound isonitrile complex. This complex is susceptible to nucleophilic attack at the carbon of the isonitrile, producing an iminoacyl moiety. Protonation at the nitrogen of the iminoacyl complex results in an aminocarbene complex. The availability of the lone pair at the nitrogen of the free pyrazole arm of the Tp′ ligand provides access to rare six-coordinate iminoacyl and aminocarbene complexes.

ACKNOWLEDGEMENTS

I would like to thank my advisor Prof. Joseph L. Templeton. Many thanks go to Dr. David Harris and Dr. Marc ter Horst for all the NMR assistance, witty banter, and maintaining the NMR facilities so superbly. I would also like to thank Dr. Peter White for solving my crystal structures (whether good or bad) and for being so accommodating to all my requests. And to round out the facilities people, I would like to thank Dr. Sohrab Habibi for the assistance with mass spectroscopy.

I would like to thank current and previous members of the Templeton lab. Abby O'Connor, Andy Jackson, Ned West, and Chetna Khosla provided an enthusiastic work environment in which I truly enjoyed chemistry and being at work. They also provided loads of both mental and emotional support and are certainly the people I will instantly think of when I reflect on my time at UNC. Margaret MacDonald, Andrew Garrett, and Anne Saunders took me in when I was but a little first year and welcomed me into the lab. It has been great to work with Bryan Frauhiger, Leah Pranger, Mat Finnis, Mike Norris, and Matt Ondisco. Jonah Jurss and Meredith Hampton have gone through it together with me and I look forward to finding out what life brings us during the next few years. Perhaps the two people who had the greatest influence during my time at UNC were Dr. Marc Walter and Dr. Wes Bernskoetter, who enjoyed making fun of the ditzy blond as much as they enjoyed suggesting reactions for me to do.

In addition, several other people have come into my life during UNC and meant a tremendous amount to me. Andrea Palmieri, Anna Belle, Laurel Clark, Rebecca Moorhouse, Natalie Bjorge, Jessica Bailey, and Jessica Schreiber have supported me throughout my time at UNC. Of course, I cannot forget Mandi Carlton, Christan Rowland Flaherty, Sara Varnum Barnes, and Elizabeth Mobley who knew me back when I was just another girl in a pledge t-shirt.

Most importantly, I would like to thank my family: my brothers Shawn and Nic, sister-in-law Heather, nephews Andrew and Liam and most importantly my parents. All of them have believed in me from day one, supported me, and above all loved me. My parents are truly the single reason that I am here today.

TABLE OF CONTENTS

LIST OF FIGURES AND SCHEMES

LIST OF TABLES

LIST OF ABBREVIATIONS AND SYMBOLS

°	degree(s)
•	perpendicular
•	parallel
α	Greek alpha: crystallographic angle
β	Greek beta: crystallographic angle
γ	Greek gamma: crystallographic angle
δ	Greek delta: denotes chemical shift reference scale
η	Greek eta: ligand hapticity
κ	Greek kappa: denotes coordination to metal by x atoms
ν	Greek mu: IR absorption band frequency
π	Greek pi: denotes bond
θ	Greek theta: general angle
σ	Greek sigma: denotes coordination to a metal via a single atom
ν_{XY}	Greek nu: denotes infrared absorbance band corresponding to the stretching of the bond between atoms X and Y
Δ	Greek capital delta: denotes separation between values or applied heat
a,b,c	crystallographic unit cell parameters
Å	angstrom(s)
acac	acetylacetonate
Ar	general aromatic
ax	axial
BAr'_4	tetrakis(3,5-trifluoromethylphenyl)borate

br	broad
C	Celsius
cm^{-1}	wavenumber
d	doublet
$\Delta G°$	standard Gibbs energy
$\Delta G^{‡}$	Gibbs energy of activation
dppm	1,1-bis(diphenylphosphino)methane
dppe	1,2-bis(diphenylphosphino)ethane
dr	diastereomeric ratio
dtbpe	1,2-bis(di-tert-butylphosphino)ethane
dtc	dithiocarbamate
eq	equatorial (NMR data)
eq	equation
equiv	equivalents
ESI	ElectroSpray Ionization
Et	ethyl, $-CH_2CH_3$
h	hour(s)
HMQC	Heteronuclear Multiple Quantum Coherence
HRMS	high resolution mass spectroscopy
Hz	Hertz
IR	infrared
$^{x}J_{YZ}$	magnetic coupling between atoms X and Y through a distance of x bonds
K	Kelvin

kcal	kilocalorie
L	general ligand, usually 2 e^- donor
M	general metal atom
m	multiplet
m	meta
Me	methyl, $-CH_3$
min	minute(s)
mol	mole
MS	mass spectroscopy
*n*Bu	*n*-butyl, $-C_4H_9$
NMR	nuclear magnetic resonance
o	ortho
ORTEP	Oak Ridge Thermal Ellipsoid Plot
OTf	triflate, trifluoromethane sulfonate: $CF_3SO_3^-$
p	para
Ph	phenyl, $-C_6H_5$
ppm	parts per million
q	quartet
R	general alkyl group
R, R_W	crystallographic refinement quality indicators
s	singlet (NMR data)
s	second
t	triplet

^{t}Bu	tertiary butyl, -C(CH_3)$_3$
THF	tetrahydrofuran
TMS	trimethylsilyl, -Si(CH_3)$_3$
Tp	hydridotrispyrazolylborate
Tp'	hydridotris(3,5-dimethylpyrazolyl)borate
X	general halogen atom

Chapter 1

Transformations between Pt(II) and Pt(IV) utilizing the Tp'PtR Fragment

Transition Metal Mediated Transformations: Transition metals catalyze numerous important reactions. This thesis will explore some of the diverse array of reactivity patterns demonstrated by group 10 metals, particularly platinum. A plethora of reviews and books have been written solely dedicated to the organometallic chemistry of platinum, known for high catalytic activity, chemical robustness, and an extensive range of reactions.[1-4]

One reaction that exemplifies the importance of platinum chemistry is Shilov's oxidation of methane to methanol, one of the first examples of alkane functionalization (Scheme 1.1).[5] Although Shilov's reaction is not industrially feasible due to its stoichiometric consumption of platinum as a sacrificial oxidant, it demonstrates the potential of group ten metals to provide access to valuable small organic molecules. Numerous systems have been modeled after Shilov's system in an attempt to achieve functionalization of sp^3 hybridized carbons under mild conditions.[6-15]

Scheme 1.1. Shilov Oxidation of Methane to Methanol

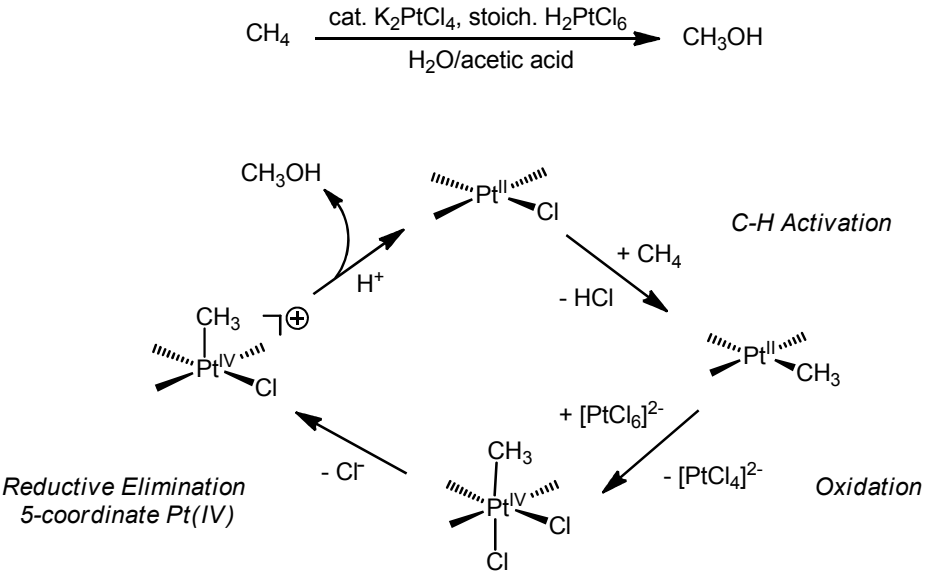

The mechanism of Shilov's system has been extensively studied. The mechanism proposed by Bercaw and Labinger highlights the central role of transition metal complexes.[16] First, C-H bond activation of methane occurs to form a Pt(II) methyl complex. Second, the metal is oxidized from Pt(II) to Pt(IV) and transforms from a four-coordinate square planar geometry to a six-coordinate octahedral geometry. Ligand loss from this complex produces a five-coordinate complex. From this five-coordinate complex, reductive elimination of methanol occurs and the metal center is reduced from Pt(IV) to Pt(II).

As in Shilov's cycle, transformations from Pt(II) to Pt(IV) provide access to a wide array of complexes. However, in catalytic reactions, these transformations occur rapidly and are difficult to study. Stoichiometric oxidations of Pt from Pt(II) to Pt(IV) are better suited for mechanistic studies. Herein, we present studies of oxidative addition and reductive elimination of organic molecules from a platinum center.

Classical and Coordinatively Unsaturated Pt(II) and Pt(IV): Conventional Pt(II) complexes have a d^8 electron count and adopt a square planar geometry. On the other hand Pt(IV) complexes have a d^6 electron count and are generally octahedral. (Figure 1.1)

Figure 1.1. Classical Pt(II) and Pt(IV)

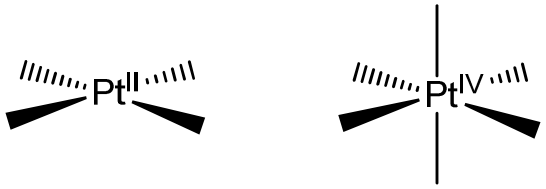

Complexes of Pt(II) and Pt(IV) have been known for over a century. Conversions from four-coordinate Pt(II) to six-coordinate Pt(IV) are common and can

readily be achieved by oxidative addition. More recently, coordinatively unsaturated three- and five-coordinate Pt complexes have been reported. These complexes require a delicate balance of ligands in order to stabilize the unusual metal coordination number. Three-coordinate complexes are either Pt(II) or Pt(0). The most common geometry is T-shaped and the metal center is stabilized by an agostic interaction.[17-21] Although these complexes are considered three-coordinate, the agostic interaction can be viewed as occupying the fourth coordination site. There are only a handful of examples of three-coordinate platinum complexes: one is Baratta's 14-electron platinum (II) complex which is stabilized by an agostic interaction from a methyl group (Eq. 1).[17]

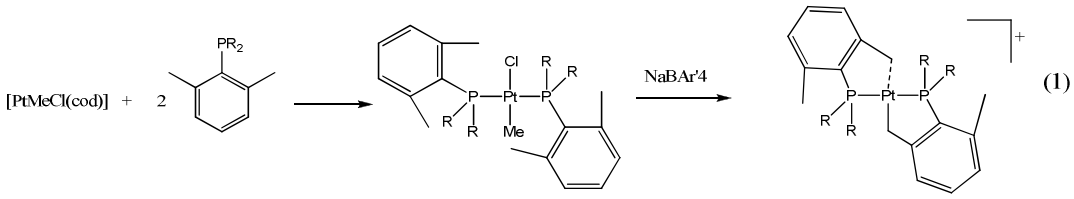

(1)

Although the first five-coordinate Pt(II) complex was reported nearly 50 years ago[22], they still remain relatively rare. One common route to five-coordinate Pt(II) complexes is addition of a π-acid ligand to a metal complex with a multidentate ligand system. The π-acid acts as a two-electron donor and a two- or four-electron acceptor. These complexes often adopt a pseudo-trigonal bipyramidal geometry (Eq. 2).[23]

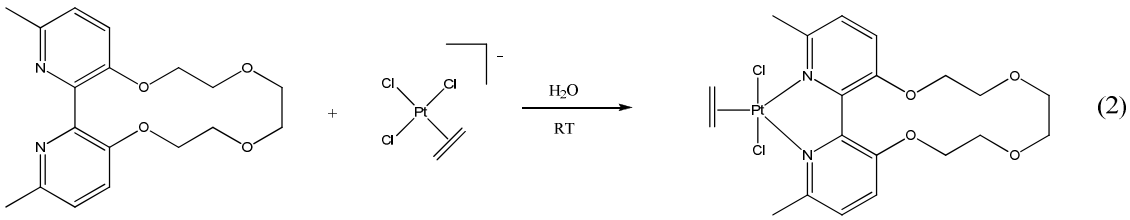

(2)

Goldberg has done extensive research in the realm of five-coordinate Pt(IV) complexes. In 2001, she reported a stable five-coordinate Pt(IV) alkyl complex.[24] The geometry of this complex is square pyramidal. Thermolysis of this complex in ethylene

results in reductive elimination of ethane and methane and formation of a platinum (II) metallocycle (Eq. 3).[25]

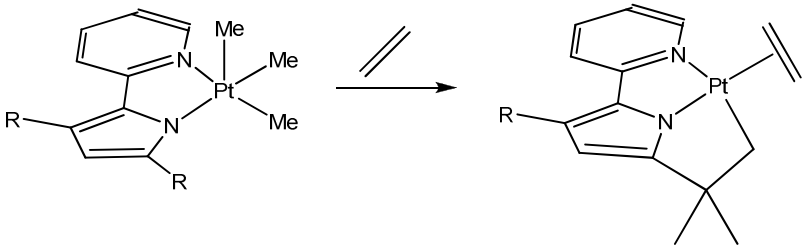

(3)

Our group has synthesized a Pt(IV) five-coordinate species starting from Tp′PtMeH_2. Reductive elimination of methane followed by oxidative addition of triethylsilane produces a five-coordinate platinum dihydride complex (Eq. 4).[26]

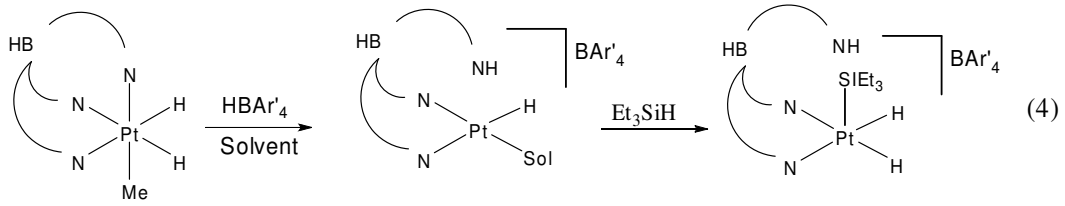

(4)

In addition, we recently reported the synthesis of a five-coordinate Cl-nacnac platinum complex (Cl-nacnac = *N*-*p*-Cl-phenyl-*β*-diiminate) which undergoes cycloaddition with phosphaalkyne to produce a six-coordinate phosphalkenyl product (Eq. 5).[27]

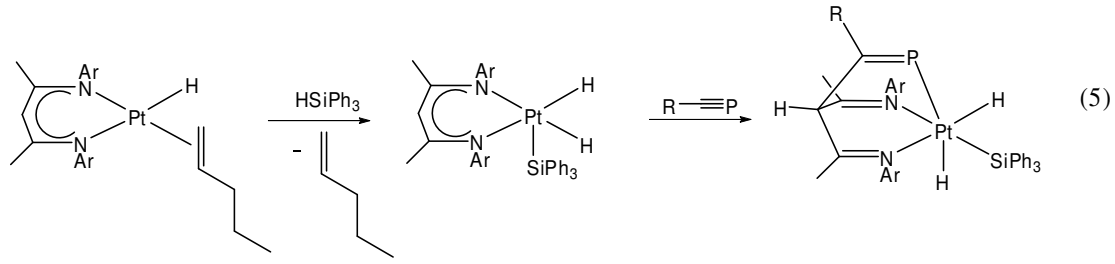

(5)

Tilley has synthesized a similar dihydrosilyl platinum complex using PyPyr (PyPyr = 3,5-diphenyl-2-(2-pyridyl)pyrrolide).[28] This complex reacts with 4-dimethylaminopyridine (DMAP) to give the six-coordinate DMAP complex, while

reaction with trimethylphosphine results in reductive elimination of silane producing the four-coordinate phosphine complex (Eq. 6).

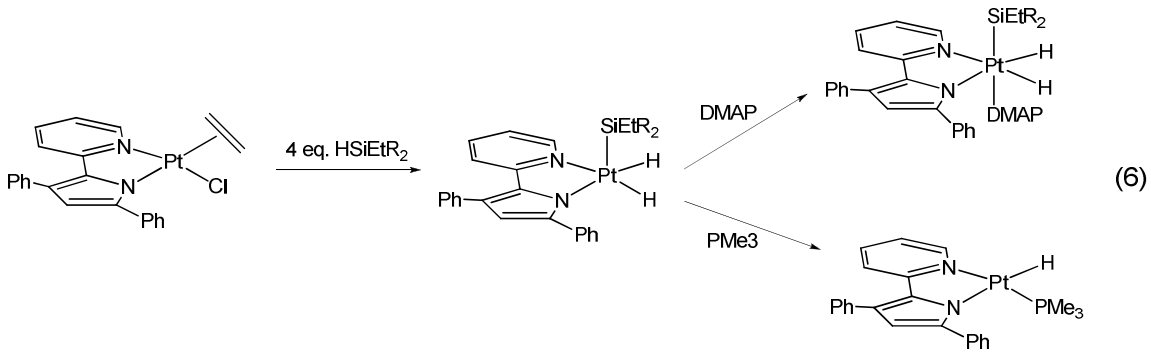

(6)

Coordinatively and electronically unsaturated Pt(II) and Pt(IV) complexes are of interest because they are often proposed as intermediates in catalytic cycles.[29] These Pt(IV) complexes have shown promise as precursors to desirable Pt(II) products. However, coordinatively unsaturated species are often highly reactive and difficult to isolate. In later chapters, both five-coordinate products and putative intermediates will be discussed.

Scorpionate Ligands: Developed in the 1960s by Trofimenko,[30,31] scorpionate ligands have been widely studied due to their ability to dechelate one arm to provide access to reactive species in organometallic transformations.[32] Scorpionates consist of a tridentate ligand system in which each arm is bound to a central atom such as boron or carbon. The ligand generally binds either in the traditional tridentate facially coordinating mode, especially in six-coordinate complexes, or in a bidentate mode in which one of the arms is free. Conversion between these two modes, hereafter referred to as κ^3 or κ^2, often has a low energy barrier and readily provides access to reactive intermediates, such as five-coordinate platinum complexes.

Figure 1.2. Tp′ - hydridotris(3,5-dimethylpyrazolyl)borate

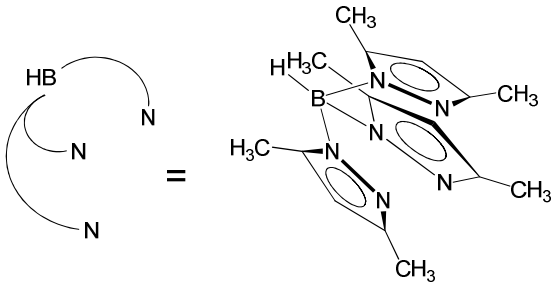

Since the report of the first scorpionate (Tp = trispyrazolylborate),[31] research utilizing scorpionates has grown exponentially. Aside from the κ^3 or κ^2 conversions, the tunability of the scorpionate ligand is another asset. By varying the identity of the central atom one can prepare either a monoanionic ligand or a neutral ligand. Also, the ring size, type, and substituents can be altered to influence the ligand's electronic properties. The research presented in this thesis has all been performed with Tp′, hydridotris(3,5-dimethylpyrazolyl)borate, a first generation scorpionate (Figure 1.2). This monoanionic scorpionate has been extensively studied and has provided an array of stable platinum complexes.[32]

Transformations Between Pt(IV) and Pt(II) Utilizing the Tp′PtR Fragment - Reductive Elimination of Small Molecules: The synthesis of Tp′$PtMe_2H$, first reported by our group in 1996,[33] opened the door for the preparation of numerous platinum complexes due to the ability of Tp′$PtMe_2H$ to reductively eliminate methane. Protonation of one of the arms of the Tp′ ligand causes dechelation and produces a reactive five-coordinate complex. This intermediate readily reductively eliminates one equivalent of methane, even at -78°C (Eq. 7).[34] The solvent molecule is weakly bound, so a variety of ligands can then be introduced into the coordination sphere, including π-acids.

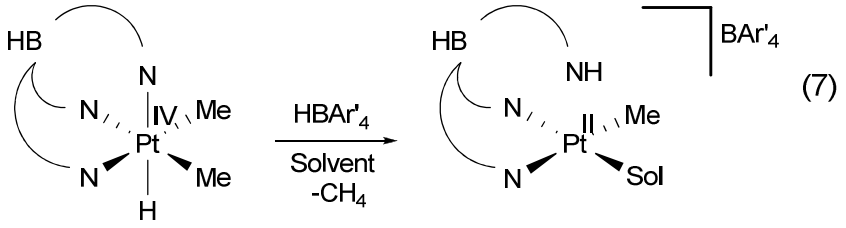

(7)

After addition of the desired ligand, deprotonation of the protonated Tp′ arm can be achieved using relatively mild bases, such as triethylamine. A similar route to reductive elimination has been achieved with Tp′PtMeH$_2$.[35] A variety of ligands can be introduced to the reactive three-coordinate Pt(II) hydride complex, producing Tp′Pt(H)(L) complexes analogous to the Tp′PtMeL complexes produced from Tp′PtMe$_2$H starting material.[26,34] However, the hydride complexes have often shown increased reactivity relative to the platinum methyl complexes. Many of the hydride products are difficult to isolate cleanly.

Tp′PtH$_3$ was first synthesized by our lab in 2000.[36] Protonation of this complex under an atmosphere of CO at low temperatures produces the cationic platinum (IV) complex, κ^2-HTp′PtH$_3$(CO).[37] This complex goes on to eliminate an equivalent of dihydrogen, producing the cationic Pt(II) complex, κ^2-HTp′PtH(CO) (Eq. 8).

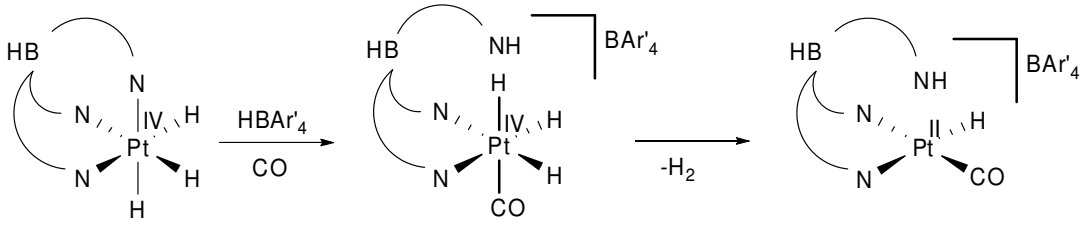

(8)

As highlighted by this reaction, platinum has the potential to act as a dihydrogen storage unit which is particularly striking as the world searches for alternative fuel sources. However, perhaps the greatest hindrance to the use of Tp′Pt for alternative fuels is that most eliminations from the system come from an intermediate in which the Tp′

ligand is protonated by acid. Regeneration of the starting material requires base to deprotonate the apical nitrogen of the Tp′ ligand. This need for the simultaneous presence of both acid and base to complete a catalytic cycle is one of the fundamental reasons why there are few reactions in which a Tp′Pt complex acts as a catalyst.

Slightly different reactivity has been observed with the Tp′PtPh$_2$H complex. Addition of acid dechelates one of the arms of the Tp′ ligand. Reductive coupling produces an η^2-bound benzene adduct (Eq. 9). However, this adduct does not readily eliminate benzene from the coordination sphere, rather it must be displaced with an incoming ligand. Thus, the viability of reactions with Tp′PtPh$_2$H is dependent on the nature of the incoming ligand.[38-40]

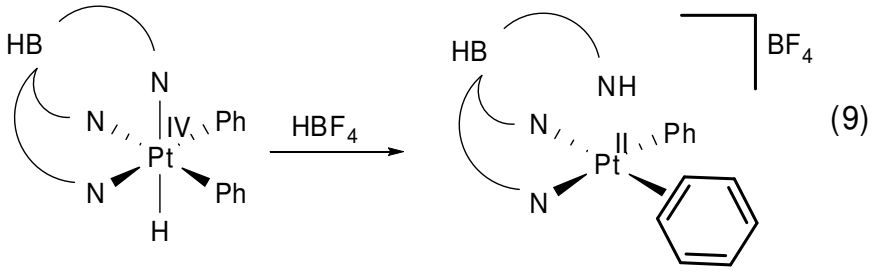

(9)

Transformations Between Pt(II) and Pt(IV) using the Tp′PtR Fragment – C-H Bond Activations and Oxidative Additions: As shown in the Shilov catalytic cycle for the oxidation of methane to methanol, controlled C-H bond activation is a highly desirable reaction that can be achieved by use of a metal center. There are multiple pathways for C-H bond activation (Table 1.1).[41,42]

The oxidative addition pathway (1) is viable for Tp′Pt complexes due to the availability of the M^{n+2} oxidation state when starting from either Pt(0) or Pt(II).[41,43] There are numerous proposed mechanisms for oxidative addition to an organoplatinum fragment, and in reality the exact mechanism is system and substrate dependent.

Table 1.1. C-H bond activation pathways

(1) oxidative addition

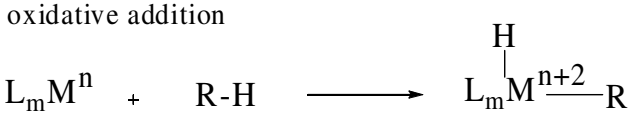

(2) σ bond metathesis

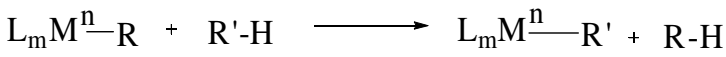

(3) electrophilic substitution

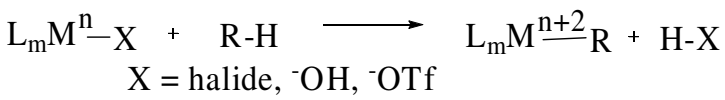

(4) 1,2-addition

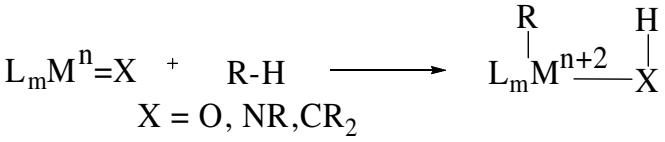

(5) metalloradical activation

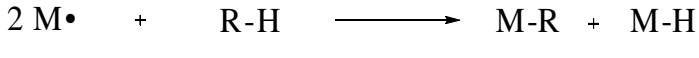

Goldberg has performed extensive research on the C-H bond activation of alkanes with the Tp′PtR fragment.[44] A vacant coordination site is generated by abstraction of CH_3^- from $[Tp'PtMe_2]^-$ by borane. Introduction of an alkane results in C-H bond activation, producing products of the form Tp′Pt(Me)(R)H (Eq. 10). This reaction is especially important because it highlights the ability of the Tp′PtR fragment to activate otherwise inactive sp^3 hybridized carbon centers.

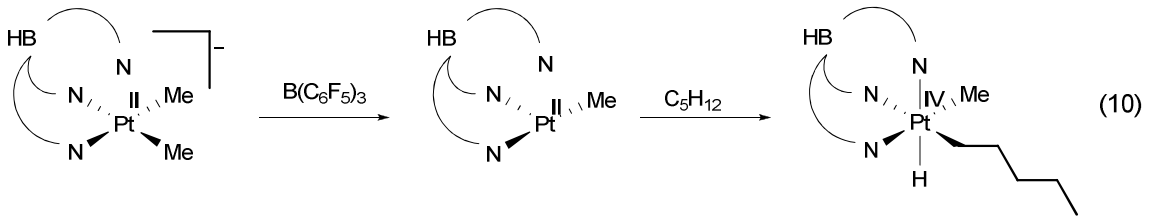

(10)

We have seen similar reactivity starting from Tp′PtMe$_2$H. Reductive elimination of methane facilitated by borane in alkane solvents results in C-H bond activation of the solvent producing the platinum (IV) complex, Tp′Pt(Me)(R)H. Reductive elimination of methane from this complex followed by a second C-H bond activation generates a platinum (II) complex with an η^2-bound alkene adduct (Eq. 11).[45]

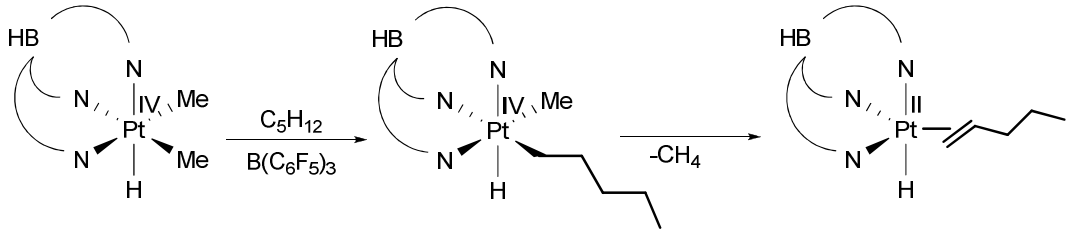

(11)

As we try to achieve transformations between Pt(II) and Pt(IV) our attention has been focused not only on the use of the Tp′ ligand system, which we propose plays a more sophisticated role in reactions than previously speculated, but also on an additional target ligand in the coordination sphere. All the research presented in this thesis uses ligands with an sp hybridized carbon atom. These are of particular interest because they can bind to metal centers as neutral two electron donors through either the π system or lone pair donation. However, altering the ligand by processes like C-H bond activation or reduction can transform them into monoanionic ligands. We will focus on three types of ligands with sp hybridized carbon atoms: alkynes, carbon monoxide, and isonitriles.

Reactivity of Platinum with sp Hybridized Carbon Centers - Alkynes: Alkynes bind to platinum through their π system. Platinum complexes with alkyne ligands have demonstrated an array of reactions including alkyne dimerization, C-H bond activation, and C-C bond cleavage.[46-50] For example, Jones determined the energy barrier for C-C bond formation to form coordinated internal alkynes by photolytically promoting C-C

bond cleavage from platinum(0) η^2-bound alkyne complexes.[51] The reverse reaction to reform the C-C bond can be thermally induced and the activation barriers measured (Eq. 12).

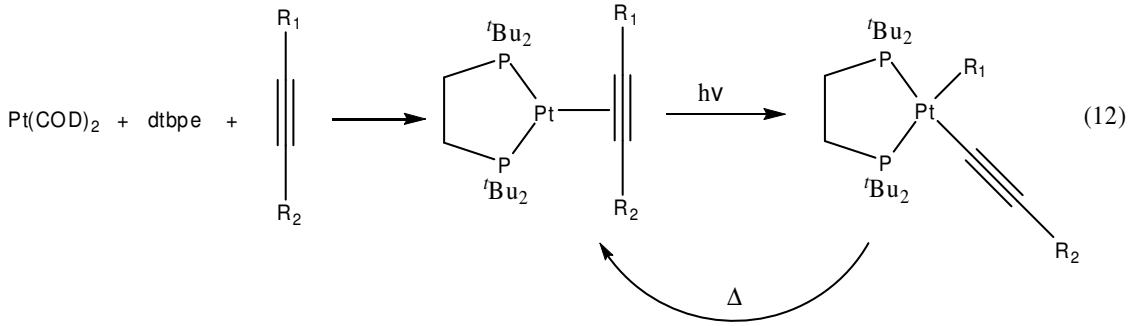

(12)

Chapter 2 will be devoted to a study of the binding of terminal alkynes to the Tp′PtMe fragment and subsequent C-H bond activation. An array of η^2-bound terminal alkyne complexes has been synthesized. Kinetics analysis of the thermal C-H bond activation of the alkyne provided insight into the approach to the transition state and the influence of the ligand system on the rate of the reaction.

In addition to the reactivity of terminal alkynes with the Tp′PtMe fragment, the reaction of alkynes with the Tp′PtPh and Tp′PtH fragment has been studied and will be discussed in Chapter 3. We previously reported the reactivity of a series of alkenes with the Tp′PtPh fragment. As mentioned earlier, reaction of Tp′PtPh$_2$H with acid produces an η^2-bound benzene adduct. Displacement of benzene with ethylene produces the η^2-bound ethylene adduct. Addition of borane as a promoter results in a platinum metallocycle. The proposed mechanism of this reaction involves phenyl migration to ethylene followed by ortho C-H bond activation of ethylbenzene (Eq. 13).[52]

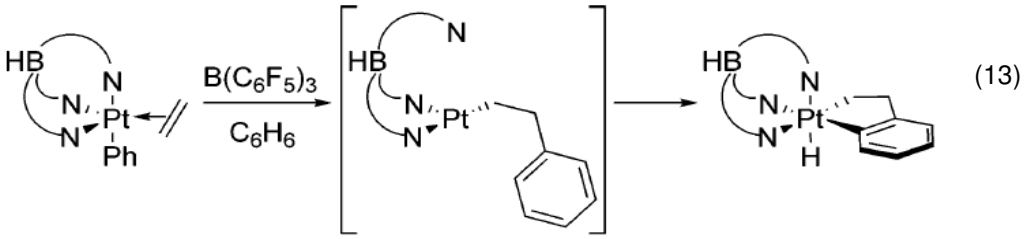

(13)

A number of platinum metallocycles have been reported, generally resulting from an elegant balance between reagents and reaction conditions.[53,54] Platinum metallocycles often have different chemical properties than their alkyl or aryl analogs. Reaction of Tp′PtPh$_2$H with a series of both internal and terminal alkyne compounds produces a metallocycle, this time with an additional degree of unsaturation relative to the olefin insertion products, as will be shown in Chapter 3. We propose a similar mechanism for the reaction of alkynes as for the reaction with olefins. Migration of the phenyl ring to the alkyne followed by *ortho* C-H bond activation produces the unsaturated metallocycle.

Addition of Tp′PtMeH$_2$ to an alkyne in solution produces neither metallocycles nor η^2-bound alkyne adducts. Indeed, there is no apparent reaction with the alkyne. This indicates the sensitivity of the reaction coordinate to the identity of the migratory ligand.

Reactivity of Platinum with sp Hybridized Carbon Centers – Carbon Monoxide:

The water gas shift reaction (WGSR) is an extremely valuable reaction in which water and carbon monoxide are converted to hydrogen and carbon dioxide.[55,56] The reaction has been advertised as a potential hydrogen source for a hydrogen fuel economy. The exact mechanism of metal catalyzed WGSR is debatable, but it follows a general pathway in which a carbonyl ligand binds to the metal center after ligand loss. Nucleophilic attack of hydroxide or water follows. From this complex, carbon dioxide is eliminated resulting

in a metal hydride. The addition of H^+ to the metal complex followed by elimination of dihydrogen produces the starting catalyst (Scheme 1.2).

Scheme 1.2. General Mechanism of Water Gas Shift Reaction

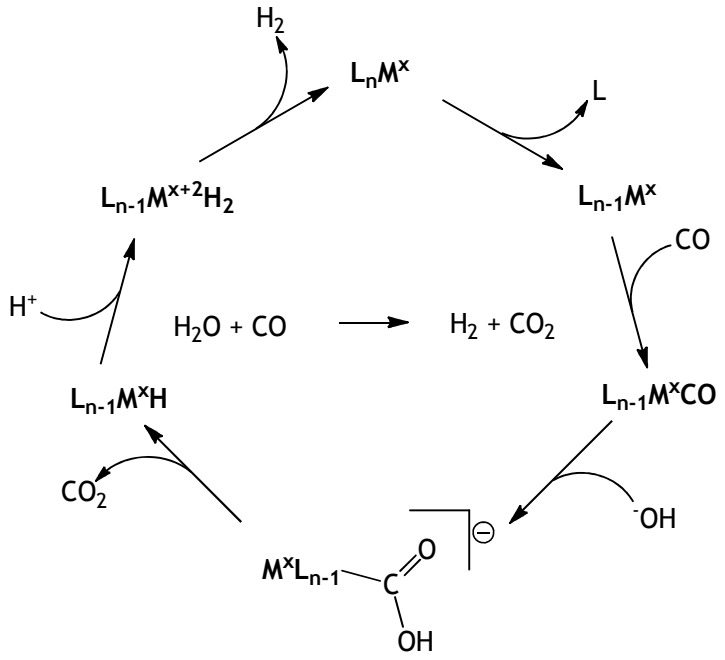

Catalytic Water Gas Shift Reactions are often performed using heterogeneous catalyst systems. The majority of platinum WGS reactions fall into this category, often using a mixture of elements such at Pt/Se or Pt/Si to realize catalytic hydrogen formation. Homogeneous platinum systems for WGSR are less common.[55,57-61] We postulate that Tp′PtH(CO) may give insight into optimization of homogeneous WGSR, due to the increased reactivity of a metal bound carbonyl. However, as previously mentioned, platinum hydride complexes are sometimes difficult to isolate cleanly, so Tp′PtMe(CO) will be used as a model system. We have attempted to perform WGSR using the metal carbonyl starting material. These results will be discussed in Chapter 4.

In addition to WGSR chemistry of Tp′Pt(Me)(CO), other reactions of this starting material have been studied. For instance, carboxamido ligands have been synthesized by

nucleophilic attack of an amide ion at the carbon of a platinum bound carbonyl. A variety of nucleophilic anions has been explored, and these will be discussed in greater detail in Chapter 4.

Reactivity of Platinum with sp Hybridized Carbon Centers – Isonitriles: The binding of isonitriles to metal centers is of interest since isonitriles are isoelectronic with the carbonyl ligand. The carbonyl ligand is integral to water gas shift reaction chemistry, so understanding the reactivity of isoelectronic ligands can provide insight to WGSR mechanisms. Binding of isonitriles to a metal center is facile,[62-64] but desired isonitrile derivatives have proven difficult to synthesize. One major area of success in the reactivity of metal bound isonitriles has been the reduction of the isonitrile using a protic nucleophile to produce an aminocarbene complex, such as N-heterocyclic carbenes (Eq. 14).[65]

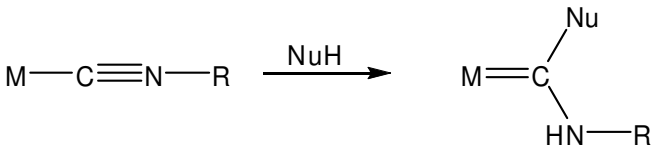

(14)

Conversions of platinum isonitrile complexes to iminoacyl complexes remain rare. More often, iminoacyl complexes are synthesized by either reaction of an isonitrile with a metal alkyl complex or reaction of a metal complex with an imidoyl halide.[66]

Chapter 5 will discuss the reduction of bound isonitriles resulting in the formation of aminocarbene and iminoacyl complexes. A series of rare six-coordinate Pt(IV) aminocarbene and iminoacyl complexes has been generated. We postulate that both the nature of the electrophile and the availability of the third arm of the Tp′ ligand determines whether four-coordinate Pt(II) or six-coordinate Pt(IV) products will be formed.

The flexible binding of the Tp′ ligand provides access to a variety of chemical transformations. In Chapter 2, dechelation occurs on the pathway to the transition state for oxidative addition of alkynes and chelation of the third arm provides access to a five-coordinate Pt(II) species. In Chapter 3, chelation of the third arm promotes phenyl migration and *ortho* C-H bond activation. In Chapter 4, proposed intermediates in the water gas shift reaction hinge upon the low energy barrier for dechelation/chelation of the third arm of Tp′. In Chapter 5, the availability of the lone pair at nitrogen of the third arm is the proposed reason why otherwise rare six-coordinate aminocarbene and iminoacyl complexes can be synthesized.

References

(1) Puddephatt, R. J. *Comprehensive Organometallic Chemisty II: Volume 9: Nickel, Palladium, and Platinum*; Elsevier: Tarrytown, New York, 1995.

(2) Hartley, F. R. *Chemistry of the Platinum Group Metals: Recent Developments, Volume 11*; Elsevier: Tarrytown, New York, 1991.

(3) Jain, V. K.; Rao, G. S.; Jain, L. *Adv. Organomet. Chem.* **1987**, *27*, 113.

(4) Byers, P. K. *Coord. Chem. Rev.* **1995**, *142*, 123.

(5) Gol'dshleger, N. F.; Shteinman, A. A.; Shilov, A. E.; Es'kova, V. V. *Russ. J. Phys. Chem.* **1972**, *46*, 785.

(6) Arakawa, H.; Aresta, M.; Armor, J. N.; Barteau, M. A.; Beckman, E. J.; Bell, A. T.; Bercaw, J. E.; Creutz, C.; Dinjus, E.; Dixon, D. A.; Domen, K.; DuBois, D. L.; Eckert, J.; Fujita, E.; Gibson, D. H.; Goddard, W. A.; Goodman, D. W.; Keller, J.; Kubas, G. J.; Kung, H. H.; Lyons, J. E.; Manzer, L. E.; Marks, T. J.; Morokuma, K.; Nicholas, K. M.; Periana, R.; Que, L.; Rostrup-Nielson, J.; Sachtler, W. M. H.; Schmidt, L. D.; Sen, A.; Somorjai, G. A.; Stair, P. C.; Stults, B. R.; Tumas, W. *Chem. Rev.* **2001**, *101*, 953.

(7) Crabtree, R. H. *J. Chem. Soc., Dalton Trans.* **2001**, 2437.

(8) Dyker, G. *Angew. Chem. Int. Ed.* **1999**, *38*, 1699.

(9) Guari, Y.; Sabo-Etienne, S.; Chaudret, B. *Eur. J. Inorg. Chem.* **1999**, 1047.

(10) Jia, C. G.; Kitamura, T.; Fujiwara, Y. *Acct. Chem. Res.* **2001**, *34*, 844.

(11) Labinger, J. A. *J. Mol. Catal. A.-Chem.* **2004**, *220*, 27.

(12) Periana, R. A.; Mironov, O.; Taube, D.; Bhalla, G.; Jones, C. J. *Science* **2003**, *301*, 814.

(13) Periana, R. A.; Taube, D. J.; Gamble, S.; Taube, H.; Satoh, T.; Fujii, H. *Science* **1998**, *280*, 560.

(14) Sen, A. *Acct. Chem. Res.* **1998**, *31*, 550.

(15) Shilov, A. E.; Shul'pin, G. B. *Chem. Rev.* **1997**, *97*, 2879.

(16) Labinger, J. A.; Bercaw, J. E. *Nature* **2002**, *417*, 507.

(17) Baratta, W.; Stoccoro, S.; Doppiu, A.; Herdtweck, E.; Zucca, A.; Rigo, P. *Angew. Chem. Int. Ed.* **2003**, *42*, 105.

(18) Goel, R. G.; Srivastava, R. C. *Can. J. Chem.* **1983**, *61*, 1352.

(19) Carr, N.; Dunne, B. J.; Orpen, A. G.; Spencer, J. L. *J. Chem. Soc., Chem. Comm.* **1988**, 926.

(20) Carr, N.; Mole, L.; Orpen, A. G.; Spencer, J. L. *J. Chem. Soc., Dalton Trans.* **1992**, 2653.

(21) Mole, L.; Spencer, J. L.; Carr, N.; Orpen, A. G. *Organometallics* **1991**, *10*, 49.

(22) Cramer, R. D.; Lindsey, R. V.; Prewitt, C. T.; Stolberg, U. G. *J. Am. Chem. Soc.* **1965**, *87*, 658.

(23) Gund, A.; Keppler, B. K.; Nuber, B. *Inorg. Chem.* **1995**, *34*, 2788.

(24) Fekl, U.; Kaminsky, W.; Goldberg, K. I. *J. Am. Chem. Soc.* **2001**, *123*, 6423.

(25) Fekl, U.; Goldberg, K. I. *J. Am. Chem. Soc.* **2002**, *124*, 6804.

(26) Reinartz, S.; White, P. S.; Brookhart, M.; Templeton, J. L. *J. Am. Chem. Soc.* **2001**, *123*, 6425.

(27) West, N. M.; White, P. S.; Templeton, J. L.; Nixon, J. F. *Organometallics* **2009**, *28*, 1425.

(28) McBee, J. L.; Tilley, T. D. *Organometallics* **2009**, *28*, 3947.

(29) Collman, J. P.; Hegedus, L. S.; Norton, J. R.; Finke, R. G. *Principles and Applications of Organotransition Metal Chemistry*; University Science Books: Mill Valley, CA, 1987.

(30) Trofimenko, S. *J. Am. Chem. Soc.* **1967**, *89*, 6288.

(31) Trofimenko, S. *J. Am. Chem. Soc.* **1967**, *89*, 3170.

(32) Trofimenko, S. *Scorpionates: Polypyrazolylborate Ligands and Their Coordination Chemistry*; Imperial College Press: London, 1999.

(33) O'Reilly, S. A.; White, P. S.; Templeton, J. L. *J. Am. Chem. Soc.* **1996**, *118*, 5684.

(34) Reinartz, S.; White, P. S.; Brookhart, M.; Templeton, J. L. *Organometallics* **2000**, *19*, 3854.

(35) Reinartz, S.; White, P. S.; Brookhart, M.; Templeton, J. L. *Organometallics* **2001**, *20*, 1709.

(36) Reinartz, S.; White, P. S.; Brookhart, M.; Templeton, J. L. *Organometallics* **2000**, *19*, 3748.

(37) West, N. M.; Reinartz, S.; White, P. S.; Templeton, J. L. *J. Am. Chem. Soc.* **2006**, *128*, 2059.

(38) Norris, C. M.; Reinartz, S.; White, P. S.; Templeton, J. L. *Organometallics* **2002**, *21*, 5649.

(39) Norris, C. M.; Templeton, J. L. *Organometallics* **2004**, *23*, 3101.

(40) Reinartz, S.; White, P. S.; Brookhart, M.; Templeton, J. L. *J. Am. Chem. Soc.* **2001**, *123*, 12724.

(41) Lersch, M.; Tilset, M. *Chem. Rev.* **2005**, *105*, 2471.

(42) Stahl, S. S.; Labinger, J. A.; Bercaw, J. E. *Angew. Chem. Int. Ed.* **1998**, *37*, 2181.

(43) Rendina, L. M.; Puddephatt, R. J. *Chem. Rev.* **1997**, *97*, 1735.

(44) Wick, D. D.; Goldberg, K. I. *J. Am. Chem. Soc.* **1997**, *119*, 10235.

(45) Kostelansky, C. N.; MacDonald, M. G.; White, P. S.; Templeton, J. L. *Organometallics* **2006**, *25*, 2993.

(46) Das, A.; Liao, H. H.; Liu, R. S. *J. Org. Chem.* **2007**, *72*, 9214.

(47) Berenguer, J. R.; Bernechea, M.; Fornies, J.; Lalinde, E.; Torroba, J. *Organometallics* **2005**, *24*, 431.

(48) Yamazaki, S. *Polyhedron* **1992**, *11*, 1983.

(49) Ananikov, V. P.; Mitchenko, S. A.; Beletskaya, I. P. *Russ. J. Organ. Chem.* **2002**, *38*, 636.

(50) Defelice, V.; Cucciolito, M. E.; Derenzi, A.; Ruffo, F.; Tesauro, D. *J. Organomet. Chem.* **1995**, *493*, 1.

(51) Gunay, A.; Jones, W. D. *J. Am. Chem. Soc.* **2007**, *129*, 8729.

(52) MacDonald, M. G.; Kostelansky, C. N.; White, P. S.; Templeton, J. L. *Organometallics* **2006**, *25*, 4560.

(53) Campora, J.; Palma, P.; Carmona, E. *Coord. Chem. Rev.* **1999**, *193-5*, 207.

(54) Newkome, G. R.; Evans, D. W.; Kiefer, G. E.; Theriot, K. J. *Organometallics* **1988**, *7*, 2537.

(55) Khan, M. M. T.; Halligudi, S. B.; Shukla, S. *Angew. Chem. Int. Ed.* **1988**, *27*, 1735.

(56) Spessard, G. O.; Miessler, G. L. *Organometallic Chemistry*; Prentice Hall: New Jersey, 1996.

(57) Laine, R. M.; Crawford, E. J. *J. Mol. Cat.* **1988**, *44*, 357.

(58) Yoshida, T.; Ueda, Y.; Otsuka, S. *J. Am. Chem. Soc.* **1978**, *100*, 3941.

(59) Ziessel, R. *Angew. Chem. Int. Ed.* **1991**, *30*, 844.

(60) Kubiak, C. P.; Eisenberg, R. *J. Am. Chem. Soc.* **1980**, *102*, 3637.

(61) Mhadeshwar, A. B.; Vlachos, D. G. *Catal. Today* **2005**, *105*, 162.

(62) Jovanovi.B; Manojlov.L; Muir, K. W. *J. Organomet. Chem.* **1971**, *33*, C75.

(63) Clark, H. C.; Manzer, L. E. *Inorg. Chem.* **1972**, *11*, 503.

(64) Treichel, P. M.; Knebel, W. J. *Inorg. Chem.* **1972**, *11*, 1289.

(65) Michelin, R. A.; Pombeiro, A. J. L.; Fatima, M.; da Silva, C. G. *Coord. Chem. Rev.* **2001**, *218*, 75.

(66) Durfee, L. D.; Rothwell, I. P. *Chem. Rev.* **1988**, *88*, 1059.

Chapter 2

Sequential Coordination and Oxidative Addition of Terminal Alkynes to the Tp'PtR Fragment

Introduction

Reactions of terminal alkynes with organometallic complexes have been extensively studied. These reactions generally result in one of three products: η^2-alkyne adducts (**a**), alkynyl-hydride oxidative addition products (**b**), or η^1-vinylidene rearrangement products (**c**) (Figure 2.1).[1] The formation of an η^1-vinylidene species from the reaction of a metal complex with a terminal alkyne is generally believed to result from η^2-binding of the alkyne followed by isomerization to the vinylidene complex by either a 1,2 hydrogen shift or a 1,3 hydrogen shift after oxidative addition of the terminal alkyne; the detailed mechanism is system dependent.[2-6]

Figure 2.1. Organometallic complexes accessible from terminal alkyne reagents.

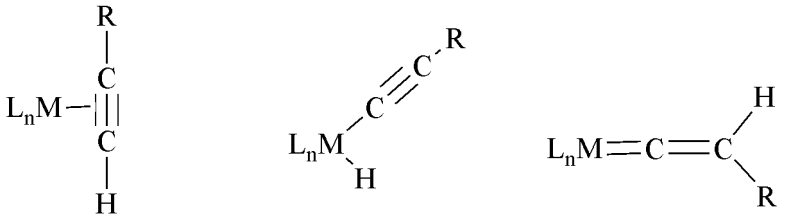

a **b** **c**

Intuitively and as theoretically determined, isomerization from free terminal alkyne to a vinylidene carbene is highly endothermic; however, metal promoted isomerization from a terminal alkyne η^2-adduct to an η^1-vinylidene complex is often energetically favorable, especially in d^6 metal complexes.[7-10] Conversion of an η^2-terminal alkyne complex to a vinylidene complex is often rapid, and neither an η^2-bound alkyne adduct nor an alkynyl-hydride complex is observed as an intermediate.[11]

There are numerous examples in which the η^2-bound terminal alkyne complex is the final product. These products are particularly prominent with Group 6 metals, and there are also examples in Groups 8, 9 and 10.[2,12-14] We have synthesized tungsten η^2-

terminal alkyne adducts in which the alkyne is a two electron donor to W(0).[12] Recently, Szymanska-Buzar reported three η^2-alkyne adducts of W(0) that were thermally unstable, synthesized by photosubstitution of CO. [13] Pörschke synthesized an array of η^2-terminal alkyne adducts bound to the $(R_2PC_2H_4PR_2)Pt(0)$ fragment that decompose after oxidative addition of the alkyne.[15] While platinum (II) complexes with η^2-bound internal alkynes are well known, [16,17] the analogous complexes with terminal alkynes were not reported until 1995. Steinborn utilized an analog of Zeise's salt to synthesize the first platinum (II) complex with η^2-bound terminal alkyne (eq 1).[18] Examples of η^2-bound terminal alkyne complexes of Pt(II) remain rare.[19]

$$[K(18\text{-cr-}6)][PtCl_3(MeC{\equiv}CMe)] \xrightarrow[-\ MeC{\equiv}CMe]{+\ RC{\equiv}CH} [K(18\text{-cr-}6)][PtCl_3(RC{\equiv}CH)] \qquad (1)$$

R = *n*-Pr
n-Bu
t-Bu
Ph
Ph(D)

Alkynyl-hydride metal complexes formed from the oxidative addition of terminal alkynes often isomerize to more stable vinylidene analogs.[2,11,14] Bianchini has studied the mechanism of isomerization of η^2-bound terminal alkyne ligands to the alkynyl-hydride products, followed by conversion to the vinylidene species.[1,14,20,21] In cationic $(P(CH_2CH_2PPh_2)_3)Rh$ systems, he found that conversion to the vinylidene species does not occur, whereas in cationic $(P(CH_2CH_2PPh_2)_3)Co$ systems the vinylidene complex is the thermodynamic product (Scheme 2.1).

Scheme 2.1. Bianchini's Transformations of η^2-bound Terminal Alkynes

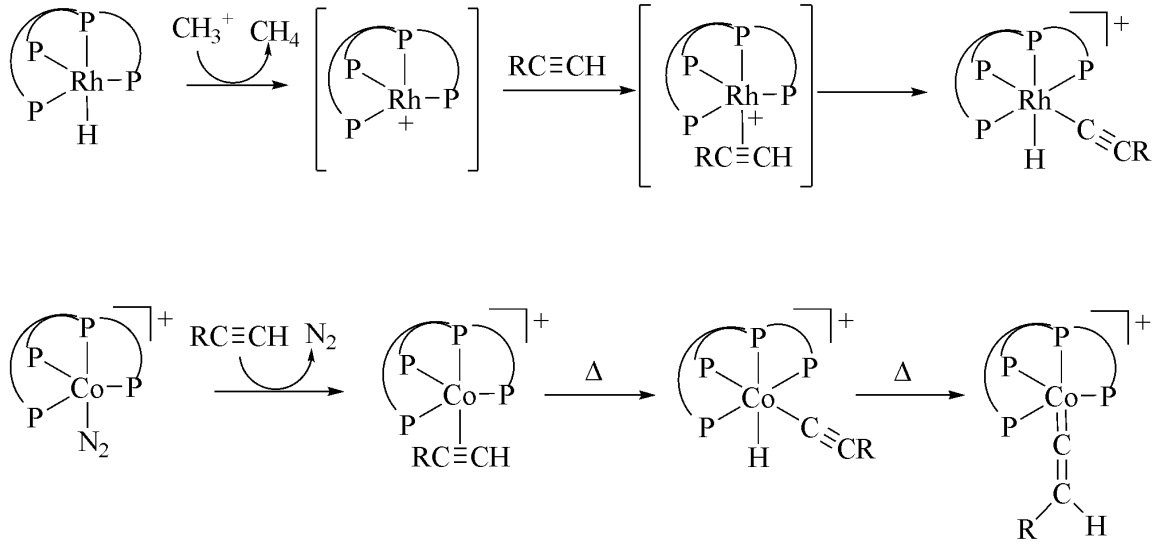

It is postulated that the rate of both oxidative addition and isomerization to the vinylidene complex are heavily influenced by the metal-hydride bond strength and the electron density of the R group on the terminal alkyne.[14,20] Electron density at the metal is also an important variable. Theoretical studies of the two systems indicate that in the cationic Co system, the vinylidene complex is lower in energy than the η^2 alkyne adduct; however, this is reversed for the cationic Rh system.[9] Density functional theory studies on the mechanism of isomerization of the η^2-alkyne adduct in the neutral Rh(I) system indicated that oxidative addition was only weakly exothermic and reversible, and the vinylidene complex is the heavily favored thermodynamic product.[22] Lynam synthesized a Rh(I) system that behaves in accord with these theoretical studies.[2] He observed, by NMR, an equilibrium between the η^2-alkyne adduct and the alkynyl-hydride complex. In both Bianchini's and Lynam's systems, the substituent on the terminal alkyne has a pronounced influence on the rate of oxidative addition and isomerization. Recently, Bassetti studied the rate of the reverse reaction, in which a terminal alkyne is eliminated

from Ru(0) vinylidene complexes, and found that electron donating substituents enhanced the rate reductive elimination of terminal alkynes.[23]

In this paper, we report a series of isolable η^2-bound terminal alkyne Pt(II) complexes and their isomeric alkynyl-hydride Pt(IV) oxidative addition products. We have studied the kinetics of the oxidative addition reaction to probe the influence of the 1-alkyne substituent on the rate of oxidative addition.

Results

The synthesis of η^2-terminal alkyne adducts of Pt(II) was achieved by exploitation of the unique characteristics of the Tp′ ligand. Protonation of one arm of the Tp′ ligand in Tp′PtMe$_2$H, **1**, using HBF_4 leads to loss of methane, resulting in a vacant coordination site.[24] Addition of the terminal alkyne followed by a short delay before addition of base to deprotonate the Tp′ ligand produces a Tp′Pt(η^2-HC≡CR)Me complex (R =, ^{t}Bu, *n*-Pr, CH_3, CH_2Ph, Ph) (eq. 2). The η^2-alkyne adducts were purified by flash column chromatography on alumina with methylene chloride.

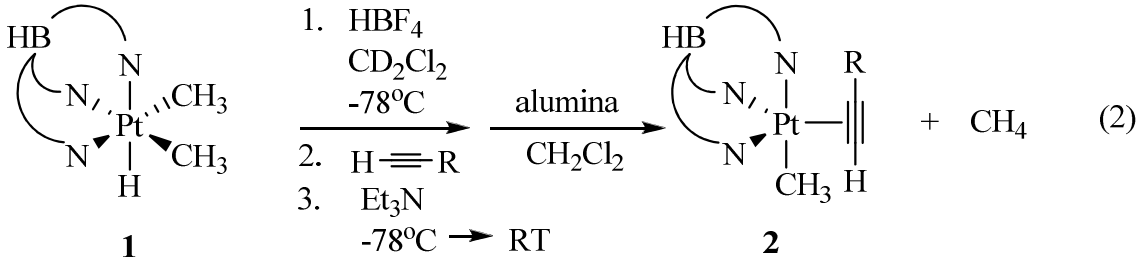

These η^2-bound alkyne complexes were isolated as beige powders that decomposed after several weeks when stored under argon at -32°C. ^{1}H NMR spectroscopy reflects two bond platinum coupling to the terminal proton with $^2J_{Pt\text{-}H}$

between 65 and 70 Hz . ^{13}C NMR spectroscopy reveals one bond platinum coupling to the coordinated α and β alkyne carbons, as shown in Table 1. Due to the thermal instability of these complexes, some of the ^{13}C NMR data were collected at 0 °C and the platinum satellites were too broad to be observed due to spin relaxation by chemical shift anisotropy.[25-27] The platinum (II) methyl signals are shifted significantly upfield from the starting Tp′PtMe$_2$H complex. We have generally observed in Tp′Pt chemistry that Pt(II) methyl signals are upfield of Pt(IV) methyl signals.[28-30] The upfield shift of the methyl group signal in the η^2-terminal alkyne adduct is consistent with a Pt(II) formulation. The IR spectrum of complex **2a** has a strong absorbance at 2533 cm^{-1} which is assigned to a κ^3 bound Tp′ ligand. A weak absorbance at 1761 cm^{-1} is assigned to the C≡C stretching frequency. This relatively weak and low stretching frequency is indicative of strong back bonding to the metal center.

Recrystallization of complex **2e** from CH_2Cl_2/pentane at -30°C yielded beige crystals suitable for x-ray crystallography (Figure 2.2). The alkyne binds equatorially and exhibits a loss of linearity upon coordination, with the C2-C3-C4 bond angle distorting to 151.5(9)°. The Pt1-C2 and Pt1-C3 bond distances are similar to one another, 2.032(9) and 2.061(8) Å, respectively, with the terminal carbon slightly closer to the metal. The alkyne C2-C3 bond distance is 1.263(13) Å, which is 0.05 Å elongated from the free alkyne C≡C bond distance of 1.214 Å.[18] The two equatorial nitrogens have Pt1-N25 and Pt1-N18 bond lengths of 2.175(6) and 2.181(6) Å, respectively, while the axial nitrogen trans to the methyl group has a slightly longer Pt1-N bond length of 2.227(8) Å.

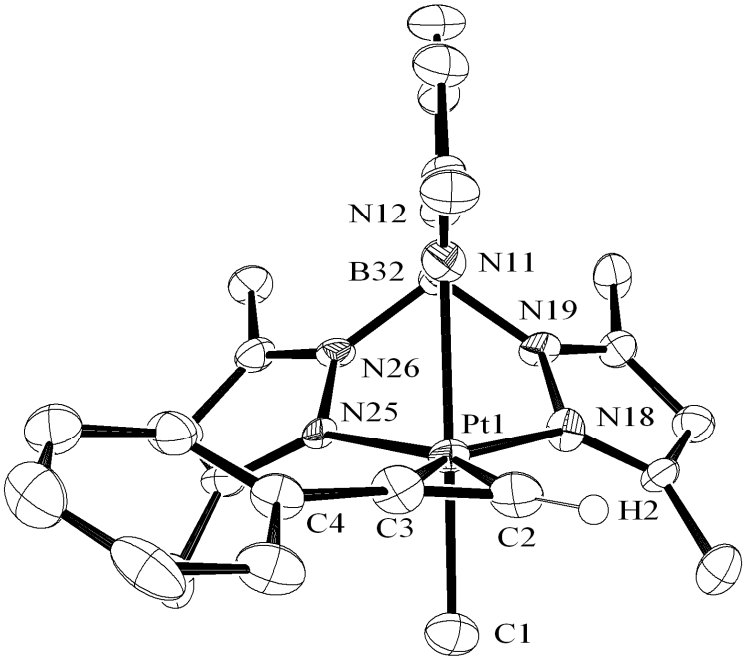

Figure 2.2 ORTEP diagram of Tp′Pt(HC≡CPh)Me, **2e**. Hydrogen atoms, with the exception of the acetylenic hydrogen, have been omitted for clarity. See Table 3 for crystal data and structure refinement. Selected bond lengths and angles: Pt1-C1 = 2.062(10) Å; Pt1-C2 = 2.032(9) Å; Pt1-C3 = 2.061 (8)Å; Pt1-N25 = 2.175(6) Å; Pt-1-N18 = 2.181(6) Å; Pt1-N11 = 2.227(8) Å; C2-C3 = 1.263(13) Å; N25-Pt1-N18 = 85.3(3)°; N25-Pt1-N11 = 84.8(3)°; N25-Pt1-C3 = 91.9(3)°; C3-Pt1-C2 = 36.0(4)°; C2-Pt1-C1 = 86.1(4); C3-Pt1-C1 = 88.6(4)°; C2-Pt1-N18 = 119.5(3); C1-Pt1-N18 = 91.2(3)°; C2-Pt1-N11 = 97.9(3)°; C3-Pt1-N11 = 95.1(3)°; C1-Pt1-N11 = 175.9(3)°; N18-Pt1-N11 = 86.1(3)°; C2-C3-C4 = 151.5(9)°.

Gentle heating of Tp′Pt(η^2-H≡CR)Me (R = Me, *n*-Pr, ^{t}Bu, CH_2Ph) at 40 °C resulted in oxidative addition of the alkyne, (eq. 3). ^{1}H NMR spectroscopy revealed that the new platinum complex has a downfield shifted Pt(IV) methyl and a new upfield Pt hydride (Table 1). These ^{1}H NMR signals are diagnostic for the alkynyl-hydride

complex formed by oxidative addition of the terminal alkyne. In addition, there is a small decrease of 2-3 Hz in the $^2J_{Pt\text{-}H}$ values for the methyl group upon oxidation from Pt(II) to Pt(IV). This may be a result of the complex going from pseudotrigonal bipyramidal geometry to octahedral geometry, in which there is an increase in the number of ligands *cis* to the methyl group and a higher *cis* influence on the coupling constant.[31,32]

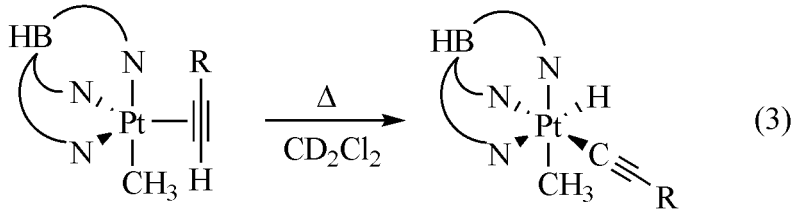

(3)

2 **3**

a R = ^{t}Bu
b *n*-Pr
c CH_3
d CH_2Ph

The IR spectrum of **3a** has a strong absorbance at 2533 cm^{-1}, which is indicative of a κ^3 binding mode for the Tp′ ligand. In addition, we have tentatively assigned a strong absorbance at 2279 cm-1 to the Pt-H and a weaker absorbance at 2173 cm-1 to the C≡C of the alkynyl ligand. The frequency of the Pt-H bond is comparable to previous systems we have studied, in which we find that the Pt-H absorbance is greater than 2200 cm^{-1}.[29,33,34] In addition, a KBr IR spectrum of the parent Tp′$PtMe_2H$ exhibits a Pt-H stretching frequency of 2271 cm^{-1}, which is in accordance with our expected $\nu_{Pt\text{-}H}$ of greater than 2200 cm^{-1}. Note that the phenyl acetylene adduct, **2e**, did not undergo oxidative addition, even when heated to 100 °C in toluene. The formation of the alkynyl-hydride complex at 40 °C was monitored via ^{1}H NMR spectroscopy. Rates for the oxidative addition were calculated based on decay of the terminal alkyne proton and the Pt(II) methyl signals utilizing either a ferrocene or mesitylene standard, as shown in Table 2.2. These kinetic studies indicate that the η^2-^{t}BuC≡CH adduct, **3a**, underwent

oxidative addition the fastest, while the oxidative addition of the η^2-$PhCH_2C{\equiv}CH$ adduct, **3d**, was the slowest. Prolonged heating of the alkynyl-hydride complex led to decomposition. No vinylidene species were detected. Although the alkynyl-hydride complexes are more thermodynamically stable than their η^2-alkyne isomers, they decompose into unidentified species after only a few days when stored under vacuum at -32°C.

Table 2.1. ^{1}H NMR spectroscopy and ^{13}C NMR spectroscopy chemical shifts (δ) with coupling constants (Hz) for Pt(II) η^2-alkyne adducts and Pt(IV) alkynyl-hydride complexes.

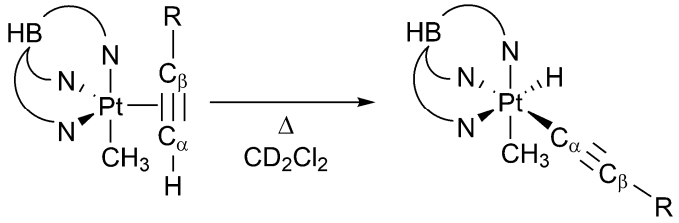

	η^2-alkyne adduct			alkynyl-hydride complex		
R	C_α (δ)	C_β (δ)	H (δ)	C_α (δ)	C_β (δ)	Pt-H (δ)
^{t}Bu	55 $^1J_{Pt\text{-}C}$ = 350	90	3.1 $^2J_{Pt\text{-}H}$ = 71	47	104	-20.0 $^1J_{Pt\text{-}H}$ = 1208
n-Pr	57 $^1J_{Pt\text{-}C}$ = 372	81 $^1J_{Pt\text{-}C}$ = 397	3.1 $^2J_{Pt\text{-}H}$ = 70	48	95	-20.1 $^1J_{Pt\text{-}H}$ = 1212
CH_3	55 $^1J_{Pt\text{-}C}$ = 372	77 $^1J_{Pt\text{-}C}$ = 391	3.2 $^2J_{Pt\text{-}H}$ = 69	47	89	-20.0 $^1J_{Pt\text{-}H}$ = 1210
CH_2Ph	58 $^1J_{Pt\text{-}C}$ = 369	79 $^1J_{Pt\text{-}C}$ = 408	3.3 $^2J_{Pt\text{-}H}$ = 67	51	92	-19.6 $^1J_{Pt\text{-}H}$ = 1198
Ph	65 $^1J_{Pt\text{-}C}$ = 378	81	4.2 $^2J_{Pt\text{-}H}$ = 66	N/A	N/A	N/A

Kinetic data were obtained over a temperature range of 30°C to 60°C for four complexes that undergo oxidative addition. Eyring plots were constructed, and activation parameters were derived from the Eyring plots. The $\Delta H^{\ddagger}$ values for this conversion range from 31 to 33 kcal/mol. The $\Delta S^{\ddagger}$ values were surprisingly large and positive, ranging from 21 to 28 cal/mol K. Values of $\Delta G^{\ddagger}$ at 298 K ranged between 24 and 26 kcal/mol (Table 2).

Table 2.2. Rate Constants at 313 K and Activation Parameters

R	$k_{(313)}$ (sec^{-1})	$\Delta H^{\ddagger}$ (kcal/mol)	$\Delta S^{\ddagger}$ (cal/mol K)	$\Delta G^{\ddagger}_{(298)}$ (kcal/mol)
^{t}Bu	$20 \pm 0.6 \times 10^{-5}$	33(4)	28(12)	24.3(0.2)
n-Pr	$6.7 \pm 1.3 \times 10^{-5}$	31(1)	21(2)	25.0(0.1)
CH_3	$1.4 \pm 5 \times 10^{-5}$	32(4)	22(12)	25.6(0.2)
CH_2Ph	$1.1 \pm 0.1 \times 10^{-5}$	32(3)	21(9)	26.7(0.1)

Discussion

The crystal structure of the η^2-phenyl acetylene complex **2e** indicates that there is only a minor increase in the alkyne bond length (0.05 Å), denoting a limited amount of back bonding to the alkyne. The Pt-C2 and Pt-C3 bond distances are similar, reflecting nearly equal bonding to both *sp* hybridized carbons. Two distinct formalisms can be used to describe this platinum coordination geometry. The first formulation is to view this as a five-coordinate platinum (II) complex; the second is to consider it as a platinum (IV) octahedral complex, (Figure 2.3).

Figure 2.3. Representations of the alkyne binding as a neutral η^2-bound adduct, **a**, or as a dianionic ligand, **b**.

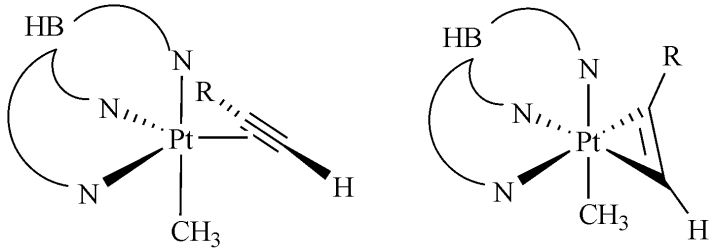

a **b**

In complex **a**, the neutral alkyne binds through the π system and the triple bond loses *sp* character, hence the deviation from linearity. The Tp′ ligand acts as a tridentate, facially coordinating ligand and binds two sites in the equatorial plane containing the alkyne and one site along the Pt-Me bond axis. There are many examples of five-coordinate Tp′ Pt complexes with unsaturated ligands, in which the complex assumes a pseudotrigonal bipyramidal geometry.[35] The presence of a π-acid ligand in the Pt(II) coordination sphere invariably promotes coordination of the third Tp′ arm. Thus, viewing this structure as a five coordinate Pt(II) species has precedent.

In the d^6 Pt(IV) formulation, complex **b**, the alkyne binds at both the C2 and C3 positions, and is viewed as a metallocyclopropene, thus acting as a dianionic ligand and occupying two coordination sites in the xy plane. The Tp′ ligand, commonly referred to as a tetrahedral enforcer in first row transition metals, can act as an octahedral enforcer in second and third row transition metals, which, in this complex, results in a Pt(IV) complex that assumes a distorted octahedral geometry.[35,36] Although either description is satisfactory, it may be more informative to view the structure as a six coordinate Pt(IV) complex, since the orientation of the C≡C carbons in the crystal structure is in agreement

with the simple Pt(IV) octahedral formalism. In contrast, there is an ambiguity associated with the alkyne orientation in a Pt(II) description since only the midpoint of the alkyne triple bond is riveted to the metal center.

Although the η^2-alkyne adduct is stable at low temperatures for several weeks, its thermal instability and slow isomerization indicate that it is a kinetic product; the thermodynamic product is the alkynyl-hydride complex. Since oxidative addition of η^2-bound terminal alkynes occurs slowly at room temperature, the formation of the alkynyl-hydride complex was amenable to kinetic analysis. The relative rates of the kinetics data indicate that the more acidic the terminal alkyne proton the slower the formation of the alkynyl-hydride complex. The alkynyl-hydride complex can be formed by C-H bond activation by numerous pathways, but two pathways are of particular interest. Either the terminal alkyne can undergo a true oxidative addition pathway via C-H bond activation or the metal can deprotonate the terminal alkyne.[24,37] In our system, less acidic protons undergo faster conversion to hydrides, suggesting that our complex does indeed form as a result of oxidative addition. This conclusion is supported by the fact that phenyl acetylene, which has the most acidic proton, did not undergo C-H bond activation.

The high $\Delta S^{\ddagger}$ values derived from the Eyring plots indicate that, in addition to the oxidative addition, another process is occurring along the reaction coordinate to the transition state. Goldberg has postulated that the third arm of the Tp′ ligand can be dechelated during reductive elimination reactions of Pt(IV) complexes, resulting in a reactive κ^2-transition state.[38-40] Formation of the κ^2-Pt(II) intermediate in the alkyne system here may facilitate oxidative addition via a pseudo square pyramidal transition state. The relative rates of oxidative addition further substantiate the possibility of

dechelation during the transition. Electron withdrawing groups on the alkyne make the alkyne a better π-acid, decreasing electron density at the metal center and binding the three arms of the Tp′ ligand more tightly. This results in stabilization of the pseudotrigonal bipyramidal complex. An electron donating group on the alkyne increases electron donation from the alkyne to the metal center. The increase in electron density at the metal center decreases how tightly bound the Tp′ ligand is and facilitates dechelation of one of the arms of the Tp′ ligand, providing easier acess to the κ^2-Pt(II) transition state. In our studies, the η^2-PhC≡CH adduct, a terminal alkyne with the least electron rich substituent we employed, did not undergo oxidative addition. Of those complexes that did undergo oxidative addition, the η^2-^{t}BuC≡CH adduct, the terminal alkyne with the most electron rich substituent, isomerized the fastest, while the η^2-$PhCH_2C$≡CH adduct, the terminal alkyne with the least electron donating group, underwent oxidative addition the slowest.

A pathway involving κ^3 to κ^2 conversion is attractive in the oxidative addition of terminal alkynes and is supported by the high $\Delta S^{\ddagger}$ value. If the process were merely oxidative addition, one would expect the $\Delta S^{\ddagger}$ to be small and possibly negative due to careful positioning of the alkyne ligand. The κ^3 to κ^2 pathway is also supported by the principle of microscopic reversibility. Formation of the η^2-terminal alkyne adduct from the alkynyl-hydride complex, the reverse of what we observe, would presumably involve the 5-coordinate κ^2-Tp′Pt intermediate. From the κ^2-Tp′Pt alkynyl-hydride complex, C-H bond formation can occur, producing a four coordinate Pt(IV) species. Chelation of the third arm would produce the five coordinate η^2-alkyne adduct.

Conclusions

We have generated a series of isolable η^2-terminal alkyne adducts bound to the Tp′PtMe fragment. Thermolysis of these complexes results in oxidative addition to form Pt(IV) alkynyl-hydride complexes. Activation parameters for oxidative addition indicate dechelation is occurring on the path to the transition state. Kinetics studies indicate that the nature of the R group on the terminal alkyne influences the rate of oxidative addition. Electron donating groups result in faster oxidative addition. We postulate that electron withdrawing groups on the alkyne make the alkyne a better π-acid, thus binding the Tp′ ligand more tightly and hindering dechelation; subsequently, access to the transition state is also hindered.

Acknowledgements

We thank the National Science Foundation (CHE-0717086) for financial support, David Harris for NMR assistance, and Sohrab Habibi for MS.

Experimental

General Information. Reactions were performed under a dry nitrogen atmosphere using standard Schlenk techniques. Methylene chloride-d_2 was dried over CaH_2 and degassed. All other reagents were purchased from commercial sources and were used without further purification. Tp′PtMe$_2$H (**1**) was synthesized according to a known procedure.[41]

NMR spectra were recorded on Bruker DRX500, DRX400, AMX400, or AMX300 spectrometers. Infrared spectra were recorded on an ASI Applied Systems React IR 1000 FT-IR spectrometer. Elemental analysis was performed by Robertson Microlit. High resolution mass spectra were recorded on a Bruker apex-Qe equipped

with an Apollo electrospray ionization (ESI) source. Mass spectral data are reported for the most abundant platinum isotope.

Tp′PtMe(η^2-HC≡CR): Tetrafluoroboric acid (12 μL, 0.10 mmol, 54% wt in Et_2O) was added to a solution of Tp′$PtMe_2H$ (**1**) (45 mg, 0.086 mmol) in CD_2Cl_2 (0.5 mL) in an NMR tube at -78°C. Alkyne (0.10 mmol) was added. The solution sat for 1 minute. Triethylamine (14 μL, 0.10 mmol) was added, and the solution was allowed to warm to room temperature. The product was chromatographed on alumina with methylene chloride.

Tp′PtMe(η^2-HC≡C^{t}Bu), 2a: (yield: 18 mg, 0.031 mmol, 36%). NMR: ^{1}H (300 MHz, CD_2Cl_2, 298 K), δ 5.92, 5.87, 5.54 (s, 1 H each, Tp′ CH), 3.09 (s, 1 H, C≡CH, $^2J_{Pt\text{-}H}$ = 71 Hz), 2.49, 2.41, 2.36, 2.32, 2.28, 2.08 (s, 3 H each, Tp′ CH_3), 1.33 (s, 9 H, ^{t}Bu), 0.63 (s, 3 H, Pt-Me, $^2J_{Pt\text{-}H}$ = 69 Hz); ^{13}C (125 MHz, CD_2Cl_2, 273 K) δ 150.4, 149.6, 149.5, 144.5, 144.4, 143.9 (Tp′ *C*CH_3), 107.6, 106.4, 106.1 (Tp′ CH), 89.6 (*C*≡CH), 55.4 (C≡*C*H, $^1J_{Pt\text{-}C}$ = 350 Hz), 30.3 (^{t}Bu), 15.3, 15.2, 13.8, 13.2, 13.0, 12.4 (Tp′ CH_3), -20.6 (Pt-Me). Anal. Calc for $C_{22}H_{35}BN_6Pt$: C 44.83, H 5.98, N 14.26. Found: C 44.65, H 5.72, N 13.95. HRMS (ESI) *m/z* Calc: 590.27 ($M + H^+$), 574.24 (M - Me). Found: 590.27, 574.25. IR (KBr): $\nu_{B\text{-}H}$ = 2533 cm^{-1}, $\nu_{C\equiv C}$ = 1761 cm^{-1}.

Tp′PtMe(η^2-HC≡C$(CH_2)_2CH_3$), 2b: (yield: 17 mg, 0.029 mmol, 34%). NMR: ^{1}H (300 MHz, CD_2Cl_2, 298 K), δ 5.89 (s, 2 H, Tp′ CH), 5.54 (s, 1 H, Tp′ CH), 3.17 (s, 1 H, C≡CH, $^2J_{Pt\text{-}H}$ = 70 Hz), 2.57 (m, 2 H, ≡C-CH_2) 2.36, 2.34 (s, 6 H each, Tp′ CH_3), 2.28, 2.05 (s, 3 H each, Tp′ CH_3), 1.82 (m, 2 H C$H_2$$CH_3$), 1.10 (t, 3 H, CH_2CH_3, J = 7 Hz) 0.53 (s, 3 H, Pt-Me, $^2J_{Pt\text{-}H}$ = 69 Hz); ^{13}C (125 MHz, CD_2Cl_2, 273 K) δ 150.3, 143.5 (Tp′

CCH_3), 107.3, 105.9 (Tp′ CH), 81.2 (*C*≡CH, $^1J_{Pt\text{-}C}$ = 397 Hz), 55.5 (C≡*C*H, $^1J_{Pt\text{-}C}$ = 372 Hz), 26.8 (*C*H_2CH_3), 22.36 (≡C*C*H2, $^2J_{Pt\text{-}C}$ = 58 Hz), 14.2, 13.9, 12.9 (Tp′ CH_3), -19.9 (Pt-Me, $^1J_{Pt\text{-}C}$ = 622 Hz). Anal. Calc for $C_{21}H_{33}BN_6Pt \cdot ½\ C_5H_{12}$: C 46.16, H 6.43, N 13.75. Found: C 45.95, H 6.11, N 13.33. HRMS (ESI) *m/z* Calc: 576.26 ($M + H^+$), 560.23 (M - Me). Found: 576.26, 560.23. IR (KBr): $\nu_{B\text{-}H}$ = 2526 cm^{-1}, $\nu_{C\equiv C}$ = 1776 cm^{-1}.

Tp′PtMe(η^2-HC≡CCH_3), 2c: (yield: 24 mg, 0.043 mmol, 50%). NMR: ^1H (400 MHz, CD_2Cl_2, 298 K), δ 5.90 (s, 2 H, Tp′ CH), 5.55 (s, 1 H, Tp′ CH), 3.3 (s, 1 H, C≡CH, *J* = 2 Hz, $^2J_{Pt\text{-}H}$ = 67 Hz), 2.39, 2.36 (s, 6 H each, Tp′ CH_3), 2.28, 2.05 (s, 3 H each, Tp′ CH_3), 0.53 (s, 3 H, Pt-Me, $^2J_{Pt\text{-}H}$ = 68 Hz); ^{13}C (125 MHz, CD_2Cl_2, 273 K) δ 150.3, 149.6, 149.3, 144.5, 144.1, 143.8 (Tp′ *C*CH_3), 107.5, 106.1, 105.9 (Tp′ CH), 76.6 (*C*≡CH, $^1J_{Pt\text{-}C}$ = 391 Hz), 55.1 (C≡*C*H, $^1J_{Pt\text{-}C}$ = 372 Hz), 14.2, 14.1, 14.0, 13.1, 12.8, 12.5 (Tp′ CH_3), 9.0 (≡C*C*H_3) -19.8 (Pt-Me, $^1J_{Pt\text{-}C}$ = 621 Hz). Anal. Calc for $C_{19}H_{29}BN_6Pt \cdot ½\ C_5H_{12}$: C 44.30, H 6.10, N 14.40. Found: C 43.94, H 5.78, N 14.05. HRMS (ESI) *m/z* Calc: 548.23 ($M + H^+$), 532.20 (M - Me). Found: 548.23, 532.20. IR (KBr): $\nu_{B\text{-}H}$ = 2526 cm^{-1}, $\nu_{C\equiv C}$ = 1784 cm^{-1}.

Tp′PtMe(η^2-HC≡CCH_2Ph), 2d: (yield: 20 mg, 0.032 mmol, 37%). NMR: ^1H (400 MHz, CD_2Cl_2, 298 K), δ 7.46 (d, 2 H, *o*-Ph, *J* = 7 Hz), 7.33 (t, 2 H, *m*-Ph, 6 Hz), 7.26 (d, 1 H, *p*-Ph, 7 Hz) 5.92 (s, 2 H, Tp′ CH) 5.51 (s, 1 H, Tp′ CH), 4.02 (s, 2 H, CH_2), 3.34 (s, 1 H, C≡CH, $^2J_{Pt\text{-}H}$ = 67 Hz), 2.41, 2.38 (s, 6 H each, Tp′ CH_3), 2.29, 2.02 (s, 3 H each, Tp′ CH_3), 0.62 (s, 3 H, Pt-Me, $^2J_{Pt\text{-}H}$ = 68 Hz); ^{13}C (125 MHz, CD_2Cl_2, 298 K) δ 150.7, 143.9, 140.0 (Tp′ *C*CH_3), 128.7, 126.6 (Ph) 107.6, 106.4 (Tp′ CH), 79.3 (*C*≡CH, $^1J_{Pt\text{-}C}$ = 408 Hz), 58.2 (C≡*C*H, $^1J_{Pt\text{-}C}$ = 369 Hz), 31.1 (CH_2), 14.4, 14.2, 13.1 (Tp′ CH_3), -

19.1 (Pt-Me, $^1J_{Pt\text{-}C}$ = 615 Hz). Anal. Calc for $C_{25}H_{33}BN_6Pt \cdot ½\ CH_2Cl_2 \cdot ½$ HC≡C(CH_2)Ph: C 49.78, H 5.30, N 11.61. Found: C 50.31, H 5.29, N 11.98. HRMS (ESI) *m/z* Calc: 624.25 ($M + H^+$), 608.23 (M - Me). Found: 624.26, 608.23. IR (KBr): $\nu_{B\text{-}H}$ = 2526 cm^{-1}, $\nu_{C\equiv C}$ = 1776 cm^{-1}.

Tp′PtMe(η^2-HC≡CPh), 2e: (yield: 22 mg, 0.036 mmol, 41%). NMR: ^{1}H (400 MHz, CD_2Cl_2, 298 K), δ 7.60 (3 H, *o,p*-Ph), 7.26 (t, 2 H, *m*-Ph, 4 Hz), 5.92, 5.90, 5.49 (s, 1 H each, Tp′ CH), 4.16 (s, 1 H, C≡CH, $^2J_{Pt\text{-}H}$ = 66 Hz), 2.39 (s, 6 H, Tp′ CH_3), 2.42, 2.29, 2.22, 1.79 (s, 3 H each, Tp′ CH_3), 0.60 (s, 3 H, Pt-Me, $^2J_{Pt\text{-}H}$ = 68 Hz); ^{13}C (100 MHz, CD_2Cl_2, 298 K) δ 150.9, 150.3, 144.8, 144.4, 144.0 (Tp′ *C*CH_3), 130.7, 128.6, 127.1 (Ph) 107.7, 106.7, 106.6 (Tp′ CH), 80.6 (*C*≡CH), 65.5 (C≡*C*H, $^1J_{Pt\text{-}C}$ = 378 Hz), 15.0, 14.8, 14.2, 13.2, 13.0, 12.6 (Tp′ CH_3), -17.8 (Pt-Me). Anal. Calc for $C_{24}H_{31}BN_6Pt \cdot ½\ CH_2Cl_2 \cdot ½\ C_5H_{12}$: C 47.14, H 5.58, N 12.22. Found: C 46.83, H 5.17, N 12.45. HRMS (ESI) *m/z* Calc: 610.25 ($M + H^+$), 594.21 (M - Me). Found: 610.24, 594.21. IR (KBr): $\nu_{B\text{-}H}$ = 2526 cm^{-1}, $\nu_{C\equiv C}$ = 1761 cm^{-1}.

Tp′PtMe(-C≡CR)H: A solution of Tp′PtMe(η^2-HC≡CR) in 0.5 mL CD_2Cl_2 was heated at 40°C and monitored by NMR until complete conversion to the oxidative addition product was obtained.

Tp′PtMe(-C≡C^{t}Bu)H, 3a: (yield: 0.041 mmol, 89 %). NMR: ^{1}H (400 MHz, CD_2Cl_2, 298 K), δ 5.85, 5.84, 5.80(s, 1 H each, Tp′ CH), 2.55, 2.40, 2.38, 2.36, 2.34, 2.23 (s, 3 H each, Tp′ CH_3), 1.20 (s, 9 H, ^{t}Bu), 1.42 (s, 3 H, Pt-Me, $^2J_{Pt\text{-}H}$ = 66 Hz), -20.00 (s, 1 H, Pt-H, $^1J_{Pt\text{-}H}$ = 1208 Hz); ^{13}C (100 MHz, CD_2Cl_2, 298 K) δ 151.5, 150.8, 150.4, 145.1, 144.6, 144.3 (Tp′ *C*CH_3), 107.5, 106.9, 106.4 (Tp′ CH), 104.3 (*C*≡CH), 46.6 (C≡*C*H), 32.6 (^{t}Bu), 15.0, 14.9, 13.4, 13.3, 12.9, 12.7 (Tp′ CH_3), -19.5 (Pt-Me, $^1J_{Pt\text{-}C}$ =

664 Hz). Anal. Calc for $C_{22}H_{35}BN_6Pt$: C 44.83, H 5.98, N 14.26. Found: C 44.81, H 5.62, N 13.37. HRMS (ESI) *m/z* Calc: 590.27 ($M + H^+$). Found: 590.27. IR (KBr): $\nu_{B\text{-}H}$ = 2533 cm^{-1}, $\nu_{Pt\text{-}H}$ = 2279 cm^{-1}, $\nu_{C\equiv C}$ = 2173 cm^{-1}.

Tp′PtMe(-C≡C(CH$_2$)$_2$CH$_3$)H, 3b: (yield: 0.041 mmol, 89 %). NMR: ^{1}H (400 MHz, CD_2Cl_2, 298 K), δ 5.86 (s, 2 H, Tp′ CH), 5.81 (s, 1 H, Tp′ CH), 2.55, 2.41, 2.35, 2.24 (s, 3 H, Tp′ CH_3), 2.38 (s, 6 H, Tp′ CH_3), 2.36 (m, 2 H, ≡C-CH_2), 1.50 (m, 2 H CH_2CH$_3$), 1.46 (s, 3 H, Pt-Me, $^2J_{Pt\text{-}H}$ = 66 Hz), 0.98 (t, 3 H, CH_2CH_3, J = 7 Hz), -20.1(s, 1H, $^1J_{Pt\text{-}H}$ = 1212 Hz, Pt-H); ^{13}C (100 MHz, CD_2Cl_2, 298 K) δ 150.9, 150.2, 149.9, 144.8, 144.1, 143.9 (Tp′ *C*CH$_3$), 107.0, 106.4, 105.9 (Tp′ CH), 94.9 (*C*≡CH, $^1J_{Pt\text{-}C}$ = 290 Hz), 47.6 (C≡*C*H), 23.7 (*C*H$_2$CH$_3$, $^3J_{Pt\text{-}C}$ = 11 Hz), 22.36 (≡C*C*H2, $^2J_{Pt\text{-}C}$ = 22 Hz), 14.6, 14.5, 13.5, 12.9, 12.4, 12.2 (Tp′ CH_3), -20.5 (Pt-Me, $^1J_{Pt\text{-}C}$ = 526 Hz). Anal. Calc for $C_{21}H_{33}BN_6Pt \cdot ½\ CH_2Cl_2 \cdot ½\ C_5H_{12}$: C 44.08, H 6.17, N 12.82. Found: C 44.45, H 5.64, N 12.82. HRMS (ESI) *m/z* Calc: 574.24 ($M - H^+$). Found: 574.24. IR (KBr): $\nu_{B\text{-}H}$ = 2541 cm^{-1}, $\nu_{Pt\text{-}H}$ = 2271 cm^{-1}, $\nu_{C\equiv C}$ = 2170 cm^{-1}.

Tp′PtMe(-C≡CCH$_3$)H, 3c: (yield: 0.039 mmol, 76 %). NMR: ^{1}H (400 MHz, CD_2Cl_2, 298 K), δ 5.89 (s, 1 H, Tp′ CH), 5.86 (s, 2 H, Tp′ CH), 2.51, 2.39, 2.38, 2.37, 2.36, 2.34 (s, 3 H each, Tp′ CH_3), 2.14 (s, 3H, $^2J_{Pt\text{-}H}$ = 14 Hz, ≡CCH_3), 1.43 (s, 3 H, Pt-Me, $^2J_{Pt\text{-}H}$ = 65 Hz), -19.99 (s, 1H, $^1J_{Pt\text{-}H}$ = 1210 Hz, Pt-H); ^{13}C (100 MHz, CD_2Cl_2, 298 K) δ 150.7, 150.0, 149.9, 144.7, 144.0, 143.8 (Tp′ *C*CH$_3$), 106.9, 106.3, 105.8 (Tp′ CH), 89.1 (*C*≡CH), 46.6 (C≡*C*H), 14.2, 12.6, 12.3, 12.01 (Tp′ CH_3), 4.92 (≡C*C*H$_3$) -20.9 (Pt-Me, $^1J_{Pt\text{-}C}$ = 526 Hz). Anal. Calc for $C_{19}H_{29}BN_6Pt \cdot ½\ C_5H_{12} \cdot ½\ C_5H_{12}$: C 42.20, H 5.81, N 13.40. Found: C 42.98, H 5.46, N 13.07. HRMS (ESI) *m/z* Calc: 548.22 ($M + H^+$). Found: 548.23. IR (KBr): $\nu_{B\text{-}H}$ = 2533 cm^{-1}, $\nu_{Pt\text{-}H}$ = 2271 cm^{-1}, $\nu_{C\equiv C}$ = 2178 cm^{-1}.

Tp′PtMe(-C≡CCH$_2$Ph)H, 3d: (yield: 0.031 mmol, 86 %). NMR: ^{1}H (400 MHz, CD_2Cl_2, 298 K), δ 7.45 (d, 2 H, *o*-Ph, J = 7 Hz), 7.28 (t, 2 H, *m*-Ph, 8 Hz), 7.20 (d, 1 H, *p*-Ph, 7 Hz), 5.87(s, 1 H, Tp′ CH), 5.86 (s, 1 H, Tp′ CH), 5.75 (s, 1 H, Tp′ CH), 3.80 (s, 2 H, CH_2, $^3J_{Pt-H}$ = 17 Hz), 2.50, 2.40, 2.37, 2.34, 2.33, 2.20 (s, 3 H each, Tp′ CH_3), 1.49 (s, 3 H, Pt-Me, $^2J_{Pt-H}$ = 658 Hz), -19.84 (s, 1H, Pt-H, $^1J_{Pt-H}$ = 1198); ^{13}C (100 MHz, CD_2Cl_2, 298 K) δ 150.8, 150.0, 149.8, 144.9, 144.1, 143.8 (Tp′ *C*CH_3), 127.9, 127.8, 127.7 (Ph) 106.9, 106.3, 105.8 (Tp′ CH), 92.1 (*C*≡CH), 51.0 (C≡*C*H), 27.1 (CH_2), 14.4, 14.3, 14.2, 12.7, 12.3, 12.0 (Tp′ CH_3), -20.5 (Pt-Me, $^1J_{Pt-C}$ = 524 Hz). Anal. Calc for $C_{25}H_{33}BN_6Pt \cdot$ ½ $CH_2Cl_2 \cdot$ ½ HC≡C(CH_2)Ph: C 49.78, H 5.30, N 11.61. Found: C 49.43, H 5.26, N 12.30. HRMS (ESI) *m/z* Calc: 624.25 (M + H$^+$). Found: 624.26. IR (KBr): ν_{B-H} = 2533 cm^{-1}, ν_{Pt-H} = 2271 cm^{-1}, $\nu_{C\equiv C}$ = 2170 cm^{-1}.

Crystallographic Data for Complex 2e:

Table 2.3. Crystal data and structure refinement for 2e

Complex	**2e**
Empirical Formula	C26H35BC14N6Pt
Mol wt	779.30
Temperature	100(2) K
Wavelength	1.54178 Å
Cryst Syst	Monoclinic
Space Group	$P2_{1/c}$
a, Å	12.1135(8)
b, Å	34.882(2)
c, Å	7.7231(5)
α, deg	90
β, deg	105.135(5)
γ, deg	90
Vol. Å3	3150.2(4)
Z	4
Density (calculated)	1.643 Mg/m^3
μ, mm^{-1}	11.657
F(000)	1536
Crystal size	0.10 x 0.05 x 0.03 mm^3
2θ range	2.53 to 66.33°
Index Ranges	-14<=h<=14 -39<=k<=39 -8<=l<=9
Reflections Collected	14509
Independent reflections	5270 [R(int) = 0.0560]
Data/restraints/parameters	5270/12/350
Goodness-of-fit on F^2	1.185
Final R indices[I>2sigma(I)]	R1 = 0.0546 wR2 = 0.1194
R indices (all data)	R1 = 0.0755 wR2 = 0.1262
Largest diff. peak and hole	3.149 and -3.268 e $Å^{-3}$

References

(1) Bianchini, C.; Meli, A.; Peruzzini, M.; Zanobini, F.; Zanello, P. *Organometallics* **1990**, *9*, 241.

(2) Cowley, M. J.; Lynam, J. M.; Slattery, J. M. *Dalton Trans.* **2008**, *18*, 4552.

(3) de Los Rios, I.; Tenorio, M. J.; Puerta, M. C.; Valerga, P. *J. Am. Chem. Soc.* **1997**, *119*, 6529.

(4) Olivan, M.; Clot, E.; Eisenstein, O.; Caulton, K. G. *Organometallics* **1998**, *17*, 3091.

(5) Silvestre, J.; Hoffmann, R. *Helv. Chim. Acta* **1985**, *68*, 1461.

(6) Wakatsuki, Y.; Koga, N.; Yamazaki, H.; Morokuma, K. *J. Am. Chem. Soc.* **1994**, *116*, 8105.

(7) De Angelis, F.; Sgamellotti, A.; Re, N. *Organometallics* **2002**, *21*, 5944.

(8) De Angelis, F.; Sgamellotti, A.; Re, N. *Dalton Trans.* **2004**, 3225.

(9) Peréz-Carreño, E.; Paoli, P.; Ienco, A.; Mealli, C. *Eur. J. Inorg. Chem.* **1999**, 1315.

(10) Stegmann, R.; Frenking, G. *Organometallics* **1998**, *17*, 2089.

(11) Bustelo, E.; Carbó, J. J.; Lledós, A.; Mereiter, K.; Puerta, M. C.; Valerga, P. *J. Am. Chem. Soc.* **2003**, *125*, 3311.

(12) Birdwhistell, K. R.; Tonker, T. L.; Templeton, J. L. *J. Am. Chem. Soc.* **1987**, *109*, 1401.

(13) Szymańska-Buzar, T.; Kern, K. *J. Organomet. Chem.* **2001**, *622*, 74.

(14) Bianchini, C.; Peruzzini, M.; Vacca, A.; Zanobini, F. *Organometallics* **1991**, *10*, 3697.

(15) Schager, F.; Bonrath, W.; Pörschke, K. R.; Kessler, M.; Krüger, C.; Seevogel, K. *Organometallics* **1997**, *16*, 4276.

(16) Davies, B. W.; Payne, N. C. *Inorg. Chem.* **1974**, *13*, 1843.

(17) Davies, B. W.; Payne, N. C. *J. Organomet. Chem.* **1975**, *102*, 245.

(18) Steinborn, D.; Tschoerner, M.; Von Zweidorf, A.; Sieler, J.; Bögel, H. *Inorg. Chim. Acta* **1995**, *234*, 47.

(19) Belluco, U.; Bertani, R.; Michelin, R. A.; Mozzon, M. *J. Organomet. Chem.* **2000**, *600*, 37.

(20) Bianchini, C.; Masi, D.; Meli, A.; Peruzzini, M.; Ramirez, J. A.; Vacca, A.; Zanobini, F. *Organometallics* **1989**, *8*, 2179.

(21) Bianchini, C. P., M.; Zanobini, F. *Organometallics* **1991**, *10*, 3415.

(22) Vastine, B. A.; Hall, M. B. *Organometallics* **2008**, *27*, 4325.

(23) Bassetti, M.; Cadierno, V.; Gimeno, J.; Pasquini, C. *Organometallics* **2008**, *27*, 5009.

(24) Shilov, A. E.; Shul'pin, G. B. *Chem. Rev.* **1997**, *97*, 2879.

(25) Benn, R.; Buch, H. M.; Reinhardt, R. D. *Magn. Reson. Chem* **1985**, *23*, 559.

(26) Ghosh, P.; Desrosiers, P. J.; Parkin, G. *J. Am. Chem. Soc.* **1998**, *120*, 10416.

(27) Anklin, C. G.; Pregosin, P. S. *Magn. Reson. Chem* **1985**, *23*, 671.

(28) O'Reilly, S. A.; White, P. S.; Templeton, J. L. *J. Am. Chem. Soc.* **1996**, *118*, 5684.

(29) Reinartz, S.; Brookhart, M.; Templeton, J. L. *Organometallics* **2002**, *21*, 247.

(30) Reinartz, S.; White, P. S.; Brookhart, M.; Templeton, J. L. *Organometallics* **2000**, *19*, 3854.

(31) Clegg, D. E.; Swile, G. A.; Hall, J. R. *J. Organomet. Chem.* **1972**, *38*, 403.

(32) Kite, K.; Smith, J. A. S.; Wilkins, E. J. *J. Chem. Soc. (A)* **1966**, 1744.

(33) West, N. M.; Reinartz, S.; White, P. S.; Templeton, J. L. *J. Am. Chem. Soc.* **2006**, *128*, 2059.

(34) Kostelansky, C. N.; MacDonald, M. G.; White, P. S.; Templeton, J. L. *Organometallics* **2006**, *25*, 2993.

(35) Trofimenko, S. *Scorpionates: The coordination chemistry of polypyrazolborate ligands*; Imperial College Press: River Edge, NJ, 1999.

(36) Hall, A.; Fink, M. J. *Advances in Organometallic Chemistry*; Elsevier Inc: Oxford, 2008.

(37) Periana, R. A.; Bhalla, G.; Tenn, W. J.; Young, K. J. H.; Liu, X. Y.; Mironov, O.; Jones, C. J.; Ziatdinov, V. R. *J. Mol. Catal. A* **2004**, *220*, 7.

(38) Jensen, M. P.; Wick, D. D.; Reinartz, S.; White, P. S.; Templeton, J. L.; Goldberg, K. I. *J. Am. Chem. Soc.* **2003**, *125*, 8614.

(39) Wick, D. D.; Goldberg, K. I. *J. Am. Chem. Soc.* **1997**, *119*, 10235.

(40) Rendina, L. M.; Puddephatt, R. J. *Chem. Rev.* **1997**, *97*, 1735.

(41) O'Reilly, S. A.; White, P. S.; Templeton, J. L. *J. Am. Chem. Soc.* **1996**, *118*, 5684.

Chapter 3

Synthesis of Vinyl Metallacycles from Tp'PtPh$_2$H and Alkynes: Phenyl Migration Resulting in C-C Bond Formation and C-H Bond Activation

Introduction

Group 10 metallacycles have been known for decades.[1] Depending upon the nature of the metallacycle, they often are reactive and provide access to a wide variety of organic compounds. Group 10 metallacycles have been shown to be susceptible to electrophilic addition,[2-4] rearrangement,[5-7] and insertion reactions.[8-10] For instance, Carmona synthesized a nickel metallacycle that reacted with CO to produce a cyclic ketone, while reaction with CO_2 followed by CO produces an anhydride (Scheme 3.1).[11,12] This complex has also shown to form lactones, acyclic anhydrides, and dimetallic carbonates.[12]

Scheme 3.1: Reactivity of Carmona's Nickel Metallacycle

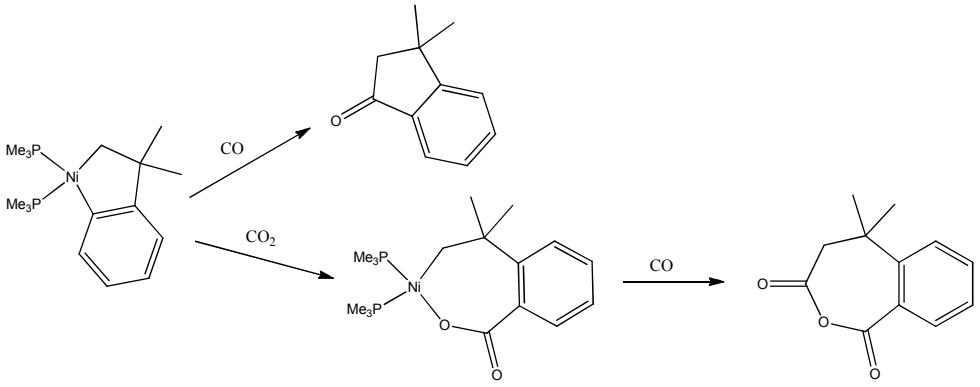

Common routes used to synthesize group 10 metallacycles, and more specifically platinum metallacycles, include transmetallation with dilithium, dimagnesium, or di-Grignard reagents;[13-15] cyclometallation via intramolecular C-H bond activation;[16-18] oxidative addition of C-C bonds;[6,19-21] and cycloaddition of unsaturated molecules.[22,23]

Previously, our lab reported the synthesis of a stable platinum(IV) *ortho*-metalated complex, Tp′Pt(CH_2CH_2-*o*-C_6H_4)(H).[24] The starting complex, Tp′Pt(Ph)(η^2-CH_2=CH_2), was synthesized from Tp′$PtPh_2H$ (eq.1). Protonation of Tp′$PtPh_2H$ using HBF_4 results in the formation of an η^2-benzene adduct, from which benzene is displaced

upon introduction of ethylene. Addition of borane to Tp′Pt(Ph)(η^2-CH_2=CH_2) promotes phenyl migration to ethylene and C-H bond activation of an *ortho*-aryl proton producing a Pt(IV) metallacycle.

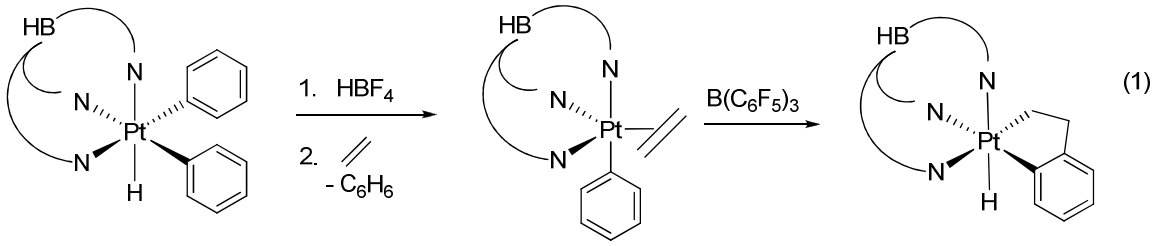

(1)

The formation of the η^2-benzene adduct has been studied by our group.[25-27] The reverse reaction in which Tp′$PtPh_2H$ is formed from the η^2-benzene adduct was shown to have an energy barrier of 12.7 kcal/mol. A crystal structure of the η^2-benzene adduct was obtained and the platinum carbon bond distances to the arene adduct were found to be 2.241(11) and 2.214(11) Å with the η^2-benzene adduct almost perpendicular to the plane of the metal center.

In this chapter, we report the synthesis of vinyl metallacycles from the reaction of alkynes with Tp′$PtPh_2H$. The metallacycles appear to be quite robust and resistant to most reagents. Reaction of Tp′$PtPh_2H$ with terminal alkynes demonstrated selectivity for the 2,1-insertion product, providing insight into the mechanism.

Results

Protonation of Tp′$PtPh_2H$, **1**, with HBF_4 results in the formation of an η^2-benzene adduct.[25-27] Addition of an internal alkyne followed by deprotonation with Et_3N produces the metallacyclic complex, **2**, instead of the expected η^2-alkyne adduct, Tp′Pt(Ph)(η^2-RC≡CR) (eq. 2). Chromatography on alumina with CH_2Cl_2 produced a white powder.

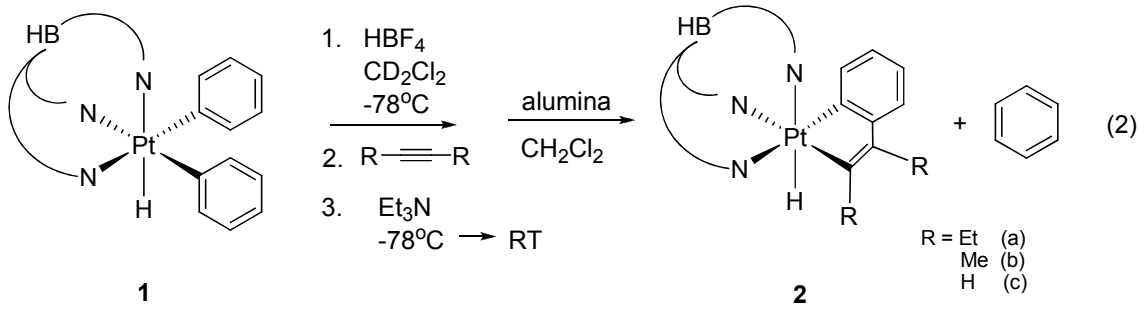

(2)

The ^{1}H NMR spectrum of **2a** indicates a C_1 symmetric species with a Pt-H resonance at -19.9 ppm with $^1J_{Pt\text{-}H}$ of 1326 Hz. The methylene protons of the two ethyl groups are diastereotopic, occurring as a multiplet around 2.5 ppm. The methyl groups appear as separate triplets at 1.13 ppm and 0.416 ppm. The ^{1}H NMR spectrum of **2b** also indicates a C_1 symmetric species with a new Pt-H resonance at -19.9 with $^1J_{Pt\text{-}H}$ of 1342 Hz. The methyl groups from the 2-butyne reagent resonate at 1.44 ppm for the distal methyl group and 2.26 ppm with $^3J_{Pt\text{-}H}$ of 28 Hz for the methyl group closest to the metal center. The ^{1}H NMR spectrum of **2c** also indicates a C_1 symmetric species with a Pt-H peak at -20.5 ppm with $^1J_{Pt\text{-}H}$ of 1309 Hz. The protons on the vinyl moiety were not identified. It is assumed that they are in the aromatic region, but initial 2D NMR analysis failed to provide conclusive data.

The reaction of Tp′PtPh$_2$H with terminal alkynes did not produce as clean a product as the reaction with internal alkynes. However, the results seem to indicate that one insertion product is formed preferentially. Insertion of an unsymmetrical alkyne into the phenyl platinum bond can either produce a metallacycle from a 1,2-insertion or a 2,1-insertion (Figure 3.1).

Figure 3.1: Products resulting from either 1,2-insertion or 2,1-insertion

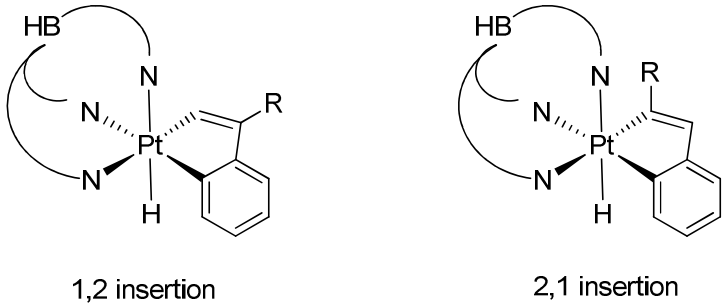

In a similar manner to the formation of **2**, protonation of the apical nitrogen with acid, followed by introduction of terminal unsymmetrical alkyne with a short delay before deprotonation of the apical nitrogen leads to formation of vinyl metallacyclic complexes. Chromatography on alumina with CH_2Cl_2 resulted in isolation of a mixture of products in which both insertion products are present. The ratio of insertion products after chromatography was nearly identical to the ratio in the crude mixture.

The reaction reflecting insertion of ^{t}BuC≡CH into the Pt-Ph linkage gave nearly exclusive formation of the 2,1-insertion product, **3a**. All of the starting Tp′PtPh$_2$H was consumed during the reaction, and the 2,1-insertion product was formed in a >10:1 ratio to the 1,2-insertion product, **3b** (eq. 3). Additional chromatography of this mixture with a 1:9 ratio of hexanes to CH_2Cl_2 resulted in isolation of only the 2,1-insertion product, **3a**. The ^{1}H NMR spectrum of **3a** indicates a C_1 symmetric species with a Pt-H resonance at -20.3 ppm with $^1J_{Pt\text{-}H}$ of 1336 Hz. The proton of the vinyl moiety is tentatively assigned to a singlet at 6.94 ppm. This singlet does not display measurable platinum coupling, leading us to believe that it is the 2,1-insertion product. The 1,2-insertion product would be likely to have visible 2-bond coupling to platinum.

The reaction of Tp′PtPh$_2$H with propyne gave a mixture of products tentatively assigned to be 5:1 with respect to the 2,1-insertion product, **4a,** and the 1,2-insertion

product, **4b** (eq. 3). Additional chromatography on alumina with a 1:9 ratio of hexanes to CH_2Cl_2 resulted in isolation of the 2,1-insertion product, **4a**. In the ^{1}H NMR spectrum, a resonance at -20.27 with $^1J_{Pt\text{-}H}$ of 1317 Hz corresponds to the hydride ligand. The methyl group of the vinyl moiety appeared at 2.22 ppm with $^3J_{Pt\text{-}H}$ of 29 Hz. In the ^{1}H NMR spectrum of the crude mixture, a resonance at -19.9 ppm with $^1J_{Pt\text{-}H}$ of 1314 Hz was assigned to the hydride ligand of the 1,2-insertion product, **4b**. The methyl group of the vinyl moiety was not identified due to signal overlap with the 2,1-insertion product, **4a**.

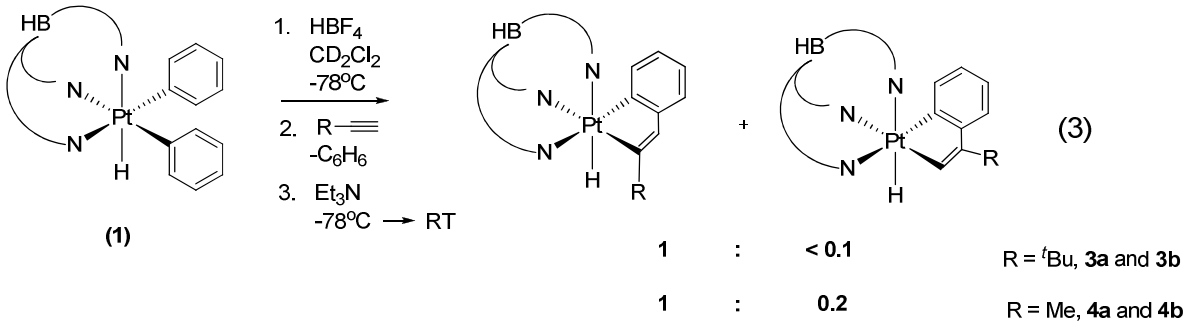

Discussion

As previously reported, η^2-alkyne adducts on the Tp′PtMe fragment can be readily isolated.[28] In contrast, η^2-alkyne adducts of the Tp′PtPh fragment cannot be isolated. Perhaps more important to note is that η^2-alkene adducts of the Tp′PtPh fragment can also be isolated.[24] Thus, by careful selection of the metal fragment and unsaturated species, we have decreased the stability of the alkyne adduct and favored C-C bond formation and C-H bond activation to achieve the metallacyclic complex.

To further demonstrate the importance of the other ligands in the coordination sphere on the properties of η^2-alkyne adducts, the reaction of Tp′PtMeH_2 with both hexyne and *tert*-butyl acetylene using a similar acid-assisted reductive elimination

pathway shows no apparent binding of the alkyne to the metal center. Instead, ^{1}H NMR suggests that a dimer is formed.

As the results from the reaction of terminal alkynes with Tp′PtPh$_2$H suggest, 2,1-insertion of the alkyne is favored. Our previous work demonstrated that 2,1-insertion was favored with alkenes. However, in our previous work, the 2,1-insertion product thermally isomerized to the 1,2-isomerization product (eq. 4). The vinyl complexes discussed in this chapter did not isomerize upon thermolysis.

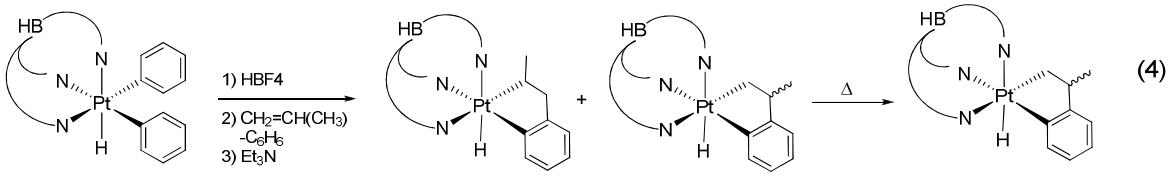

(4)

These results suggest that the sequence of steps includes migration of the phenyl ring to the unsaturated ligand (Scheme 3.2). Protonation of the apical nitrogen results in formation of an η^2-benzene adduct. The alkyne displaces the benzene ligand. The phenyl group migrates to the least sterically hindered carbon of the alkyne. Thus, Pt-C bond formation occurs at the more sterically hindered site. *Ortho* C-H bond activation produces the vinyl metallacycle complex.

Scheme 3.2: Mechanism of Formation of Metallacycle

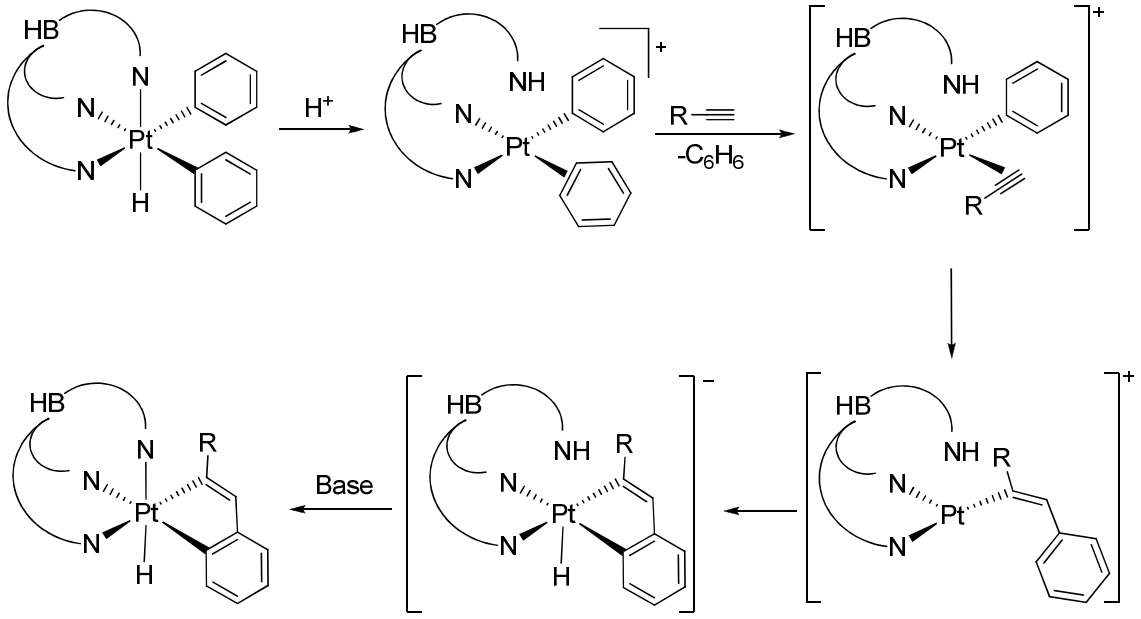

Conclusions

A series of vinyl metallacycles has been synthesized. Symmetrical internal alkynes react with Tp′Pt(Ph)(η^2-C_6H_6) to produce unsaturated metallacycles. The reaction of terminal alkynes produces a mixture of the 2,1-insertion product and the 1,2-insertion product with the 2,1-insertion product being favored. We propose a mechanism in which an η^2-benzene ligand is displaced by an incoming alkyne ligand to form an unobserved η^2-alkyne adduct. From this species, the phenyl ligand migrates to the least substituted carbon of the alkyne and a platinum-carbon bond is formed with the most substituted carbon of the alkyne. *Ortho* C-H bond activation leads to the formation of the metallacycle and a platinum-hydride bond. Deprotonation with base produces the neutral Pt(IV) metallacycle.

Experimental

General Information. Reactions were performed under a dry nitrogen atmosphere using standard Schlenk techniques. Methylene chloride and hexanes were

purified by passage through an activated alumina column under a dry argon atmosphere. Methylene chloride-d_2 was dried over CaH_2 and degassed. All other reagents were purchased from commercial sources and were used without further purification. Tp′$PtPh_2H$ was prepared according to a literature procedure.[29]

NMR spectra were recorded on Bruker DRX500, DRX400, AMX400, or AMX300 spectrometers. Infrared spectra were recorded on an ASI Applied Systems React IR 1000 FT-IR spectrometer.

Tp′Pt(RC=CR-*o*-C_6H_4)H, 2 – In an NMR tube, 10 mg Tp′$PtPh_2H$ (0.015 mmol) was combined with 5 μL HBF_4 (51% wt in Et_2O, 0.043 mmol) in 500 μL CD_2Cl_2 at -78°C. After 1 minute, 0.020 mmol alkyne was added and the NMR tube was shaken. After 5 minutes, 6 μL Et_3N (0.043 mmol) was added and the solution was brought up to room temperature. Chromatography on alumina with CH_2Cl_2 produced a white powder.

Tp′Pt(EtC=CEt-*o*-C_6H_4)H, 2a: NMR: ^{1}H (400 MHz, CD_2Cl_2, 298 K), δ 7.07 (d, 1H$_{ortho}$, Pt-EtC=CEt-*o*-C_6H_4, $J_{H\text{-}H}$ = 6 Hz, $^3J_{Pt\text{-}H}$ = 38 Hz), 6.98 (t, 1H, Pt-EtC=CEt-*o*-C_6H_4, $J_{H\text{-}H}$ = 7 Hz), 6.84 (d, 1H, Pt-EtC=CEt-*o*-C_6H_4), 6.63 (t, 1H, Pt-EtC=CEt-*o*-C_6H_4), 5.82, 5.78, 5.60 (s, 1H, Tp′ CH), 2.53 (m, 4H, CH_2CH$_3$), 2.40, 2.37, 2.32, 2.23, 2.16, 1.42 (s, 3H each, Tp′ CH_3), 1.09 (t, 3H, CH_2CH_3, $J_{H\text{-}H}$ = 7 Hz), 0.42 (t, 3H, CH_2CH_3, $J_{H\text{-}H}$ = 7 Hz), -19.86 (s, 1H, Pt-H, $^1J_{Pt\text{-}H}$ = 1326 Hz).

Tp′Pt(MeC=CMe-*o*-C_6H_4)H, 2b: NMR: ^{1}H (400 MHz, CD_2Cl_2, 298 K), δ 7.18 (d, 1H$_{ortho}$, Pt-MeC=CMe-*o*-C_6H_4), 6.98 (t, 1H, Pt-MeC=CMe-*o*-C_6H_4), 6.63 (d, 1H, Pt-MeC=CMe-*o*-C_6H_4), 6.53 (t, 1H, Pt-MeC=CMe-*o*-C_6H_4), 5.81, 5.80, 5.61 (s, 1H, Tp′ CH), 2.39, 2.35, 2.34 (s, 6H each, Tp′ CH_3), 2.21 (s, 3H, CH_3, $^3J_{Pt\text{-}H}$ = 37 Hz), 1.44 (s, 3H, CH_3), -19.97 (s, 1H, Pt-H, $^1J_{Pt\text{-}H}$ = 1342 Hz).

Tp′Pt(HC=CH-*o*-C_6H_4)H, 2c: NMR: ^{1}H (400 MHz, CD_2Cl_2, 298 K), δ **AROMATIC REGION CANNOT BE ASSIGNED DEFINITIVELY**, 5.86, 5.83, 5.58 (s, 1H, Tp′ CH), 2.38, 2.31, 2.22, 1.48 (s, 3H each, Tp′ CH_3), 2.37 (s, 6H, Tp′CH_3), -20.26 (s, 1H, Pt-H, $^1J_{Pt\text{-}H}$ = 1309 Hz).

Tp′Pt(RC=CH-*o*-C_6H_4)H, 3 and 4: In an NMR tube, 10 mg Tp′$PtPh_2H$ (0.015 mmol) was combined with 5 μL HBF_4 (51% wt in Et_2O, 0.043 mmol) in 500 μL CD_2Cl_2 at -78°C. After 1 minute, 0.020 mmol alkyne was added and the NMR tube was shaken. After 5 minutes, 6 μL Et_3N (0.043 mmol) was added and the solution was brought up to room temperature. Chromatography on alumina with CH_2Cl_2 followed by chromatography with a 1:9 ratio of hexanes toCH_2Cl_2 produced a white powder. NOTE: The 1,2-insertion products were not isolated cleanly and were only identified by their hydride resonance.

Tp′Pt(^{t}BuC=CH-*o*-C_6H_4)H, 3a: NMR: ^{1}H (400 MHz, CD_2Cl_2, 298 K), δ 7.16 (d, $1H_{ortho}$, Pt-^{t}BuC=CH-*o*-C_6H_4, $J_{H\text{-}H}$ = 7 Hz, $^3J_{Pt\text{-}H}$ = 27 Hz), 6.98 (t, 1H, Pt-^{t}BuC=CH-*o*-C_6H_4, 1H), 6.94 (s, 1H, Pt-^{t}BuC=C*H*-*o*-C_6H_4), 6.68 (t, 1H, Pt-MeC=CMe-*o*-C_6H_4), 5.85, 5.84, 5.58 (s, 1H, Tp′ CH), 2.37, 2.33, 2.33, 1.43 (s, 3H each, Tp′ CH_3), 2.35 (s, 6H each, Tp′ CH_3), 1.34 (s, 9H, ^{t}Bu), -20.31 (s, 1H, Pt-H, $^1J_{Pt\text{-}H}$ = 1336 Hz).

Tp′Pt(HC=C^{t}Bu-*o*-C_6H_4)H, 3b: NMR: ^{1}H (400 MHz, CD_2Cl_2, 298 K) -20.08 (s, 1H, Pt-H, $^1J_{Pt\text{-}H}$ = 1387 Hz)

Tp′Pt(MeC=CH-*o*-C_6H_4)H, 4a: NMR: ^{1}H (400 MHz, CD_2Cl_2, 298 K), δ 7.10 (d, $1H_{ortho}$, Pt-MeC=CH-*o*-C_6H_4, $J_{H\text{-}H}$ = 8 Hz), 7.03 (t, 1H, Pt-MeC=CH-*o*-C_6H_4, 1H), 6.85 (d, 1H, 6.94, Pt-MeC=CH-*o*-C_6H_4), 6.72 (t, 1H, Pt-MeC=CMe-*o*-C_6H_4), 6.70 (s, 1H, Pt-MeC=C*H*-*o*-C_6H_4), 5.89, 5.88, 5.60 (s, 1H, Tp′ CH), 2.52, 2.38, 2.11, 1.41 (s, 3H each,

Tp′ CH_3), 2.42 (s, 6H each, Tp′ CH_3), 2.30 (s, 3H, Me, $^3J_{Pt\text{-}H}$ = 40 Hz), -20.25 (s, 1H, Pt-H, $^1J_{Pt\text{-}H}$ = 1317 Hz).

Tp′Pt(HC=CMe-*o*-C_6H_4)H, 4b: NMR: ^{1}H (400 MHz, CD_2Cl_2, 298 K) -19.84 (s, 1H, Pt-H, $^1J_{Pt\text{-}H}$ = 1314 Hz)

References

(1) Campora, J.; Palma, P.; Carmona, E. *Coord. Chem. Rev.* **1999**, *193-5*, 207.

(2) Cheetham, A. K.; Puddephatt, R. J.; Zalkin, A.; Templeton, D. H.; Templeton, L. K. *Inorg. Chem.* **1976**, *15*, 2997.

(3) Rashidi, M.; Esmaeilbeig, A. R.; Shahabadi, N.; Tangestaninejad, S.; Puddephatt, R. J. *J. Organomet. Chem.* **1998**, *568*, 53.

(4) Tangestaninejad, S.; Rashidi, M.; Puddephatt, R. J. *J. Organomet. Chem.* **1991**, *412*, 445.

(5) Alessa, R. J.; Puddephatt, R. J.; Quyser, M. A.; Tipper, C. F. H. *J. Am. Chem. Soc.* **1979**, *101*, 364.

(6) Puddephatt, R. J. *Coord. Chem. Rev.* **1980**, *33*, 149.

(7) Miyashita, A.; Ohyoshi, M.; Shitara, H.; Nohira, H. *J. Organomet. Chem.* **1988**, *338*, 103.

(8) Klingler, R. J.; Huffman, J. C.; Kochi, J. K. *J. Am. Chem. Soc.* **1982**, *104*, 2147.

(9) Campora, J.; Llebaria, A.; Moreto, J. M.; Poveda, M. L.; Carmona, E. *Organometallics* **1993**, *12*, 4032.

(10) Bennett, M. A.; Hockless, D. C. R.; Humphrey, M. G.; Schultz, M.; Wenger, E. *Organometallics* **1996**, *15*, 928.

(11) Carmona, E.; Palma, P.; Paneque, M.; Poveda, M. L.; Gutierrezpuebla, E.; Monge, A. *J. Am. Chem. Soc.* **1986**, *108*, 6424.

(12) Carmona, E.; Gutierrezpuebla, E.; Marin, J. M.; Monge, A.; Paneque, M.; Poveda, M. L.; Ruiz, C. *J. Am. Chem. Soc.* **1989**, *111*, 2883.

(13) McDermot, J. X; White, J. F.; Whiteside, G. M. *J. Am. Chem. Soc.* **1973**, *95*, 4451.

(14) Grubbs, R. H.; Miyashita, A.; Liu, M. I. M.; Burk, P. L. *J. Am. Chem. Soc.* **1977**, *99*, 3863.

(15) Lappert, M. F.; Martin, T. R.; Raston, C. L.; Skelton, B. W.; White, A. H. *J. Chem. Soc.-Dalton Trans.* **1982**, 1959.

(16) Foley, P.; Whitesides, G. M. *J. Am. Chem. Soc.* **1979**, *101*, 2732.

(17) Griffiths, D. C.; Joy, L. G.; Skapski, A. C.; Wilkes, D. J.; Young, G. B. *Organometallics* **1986**, *5*, 1744.

(18) Griffiths, D. C.; Young, G. B. *Polyhedron* **1983**, *2*, 1095.

(19) Tipper, C. F. H. *J. Chem. Soc.* **1955**, 2045.

(20) Jennings, P. W.; Johnson, L. L. *Chem. Rev.* **1994**, *94*, 2241.

(21) Grabowski, N. A.; Hughes, R. P.; Jaynes, B. S.; Rheingold, A. L. *J. Chem. Soc.-Chem. Commun.* **1986**, 1694.

(22) Barker, G. K.; Green, M.; Howard, J. A. K.; Spencer, J. L.; Stone, F. G. A. *J. Am. Chem. Soc.* **1976**, *98*, 3373.

(23) Browning, J.; Cundy, C. S.; Green, M.; Stone, F. G. A. *J. Chem. Soc. (A)* **1971**, 448.

(24) MacDonald, M. G.; Kostelansky, C. N.; White, P. S.; Templeton, J. L. *Organometallics* **2006**, *25*, 4560.

(25) Norris, C. M.; Templeton, J. L. *Organometallics* **2004**, *23*, 3101.

(26) Reinartz, S.; White, P. S.; Brookhart, M.; Templeton, J. L. *J. Am. Chem. Soc.* **2001**, *123*, 12724.

(27) Norris, C. M.; Reinartz, S.; White, P. S.; Templeton, J. L. *Organometallics* **2002**, *21*, 5649.

(28) Engelman, K. L.; White, P. S.; Templeton, J. L. *Inorg. Chim. Acta* **2009**, *362*, 4461.

(29) O'Reilly, S. A.; White, P. S.; Templeton, J. L. *J. Am. Chem. Soc.* **1996**, *118*, 5684.

Chapter 4

Reactions of the Tp'PtMe(CO) Fragment: Insight Into Metal Catalyzed Water Gas Shift Reactions

Introduction

As sources of fossil fuels continue to diminish, alternative fuel sources become more important.[1-3] Extensive research has been focused on hydrogen production for a hydrogen fuel economy, including the formation of hydrogen from biomass, water, and other renewable sources.[4-9]

Metal catalyzed water gas shift reactions (WGSR) convert water and carbon monoxide to hydrogen and carbon dioxide (Scheme 4.1).[10-12] The portion of the proposed mechanism for the metal catalyzed WGSR cycle that we will be exploring in this chapter is the binding of CO to the metal center and elimination of carbon dioxide, which is made possible by nucleophilic attack at the carbon of the carbonyl moiety by hydroxide or water.

Scheme 4.1: General mechanism of the water gas shift reaction.

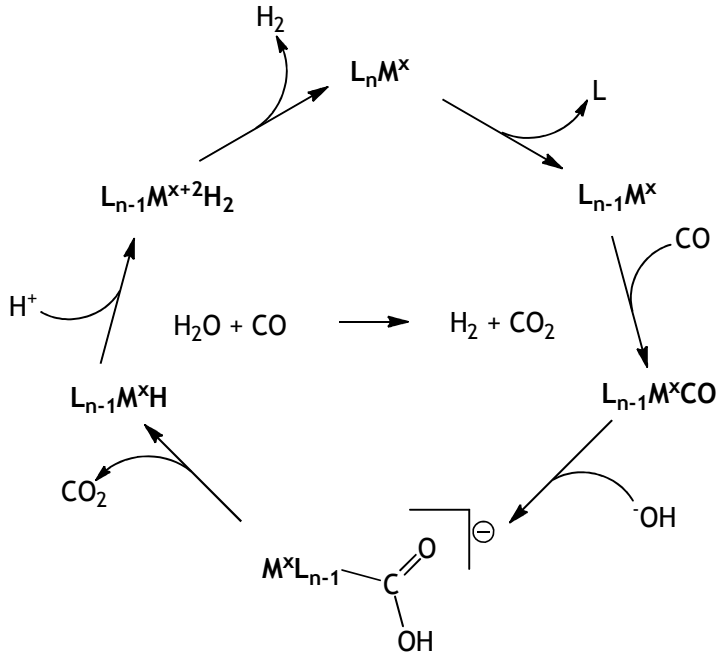

Heterogeneous platinum containing catalysts have been used to catalyze this reaction for decades.[10,11,13-15] In1977, Ford reported homogeneous catalysis of WGSR

using $Ru_3(CO)_{12}$ and KOH.[16] The reaction proceeds at 100°C, which is significantly lower than the temperature required for most heterogeneous systems. Since then, numerous homogeneous water gas shift reaction catalysts have been reported, but none of them have proven industrially feasible.[10,17-21]

We propose that a study of the reactions of the Tp′Pt(CO) fragment will give insight into the metal catalyzed WGSR mechanism and thus help clarify the requirements for a successful homogeneous WGSR catalyst.

[κ^2-HTp′Pt(II)Me(CO)][BAr′$_4$] was first reported by our lab in 2000, using an acid-assisted reductive elimination pathway to synthesize this compound from Tp′PtMe$_2$H (eq. 1).[22]

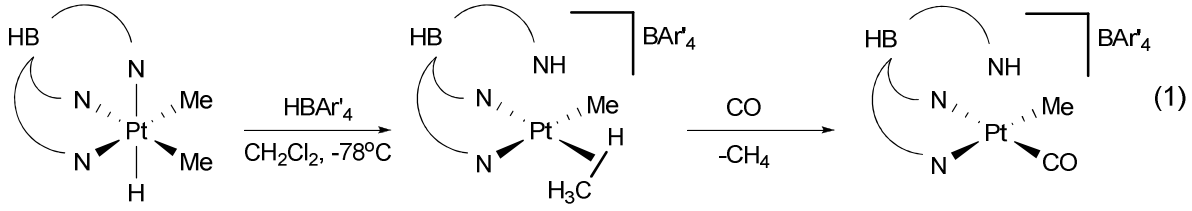

(1)

This complex adopts a square planar geometry and has a single C-O stretch in the IR of 2099 cm^{-1}. However, deprotonation of the apical nitrogen by base leads to an unusual pattern in the solution IR spectrum. Two B-H stretches are observed (2521, 2478 cm^{-1}) and two C-O stretches are observed (2081, 2065 cm^{-1}), indicating that the complex is in equilibrium between a κ^3 trigonal bipyramidal structure and a κ^2 square planar structure (Figure 4.1).[23]

Figure 4.1: Equilibrium between square planar Tp′PtMe(CO) and trigonal bipyramidal Tp′PtMe(CO).

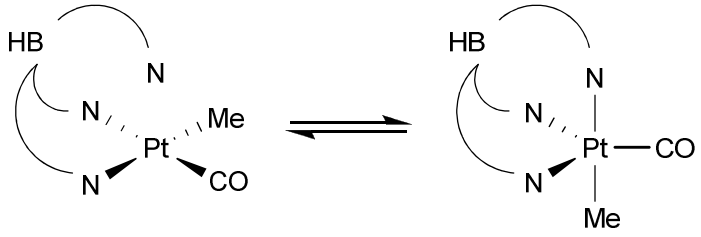

The ^{1}H NMR data is representative of only a single C_s symmetric species, and the ^{11}B NMR signal appears at -7.38 ppm. This is between the chemical shifts expected for square planar structures and trigonal bipyramidal structures, indicating an average of the two signals.[22] Clark and Keinan studied the analogous TpPtMe(CO) system and also observed fluxionality in solution.[24-26]

Recently, we reported carbon monoxide promoted reductive elimination of hydrogen from $Tp'PtH_3$.[27] $Tp'PtH_3$ is synthesized by refluxing Tp′Pt(CO)H in acetone/water under slightly basic conditions via a step that is proposed to be involved in the water gas shift mechanism. The formation of the trihydride complex using water instead of hydride sources or dihydrogen is significant.[28-30] Under an atmosphere of CO, protonation of $Tp'PtH_3$ results in the formation of a cationic trihydride carbonyl species on the way to a cationic monohydride species (eq. 2). Mechanistic studies suggest that the monohydride complex is formed by reversible reductive coupling to form dihydrogen and then irreversible elimination of dihydrogen. The electron withdrawing effect of the π-acid CO ligand facilitates elimination of dihydrogen by creating an electron poor metal center.

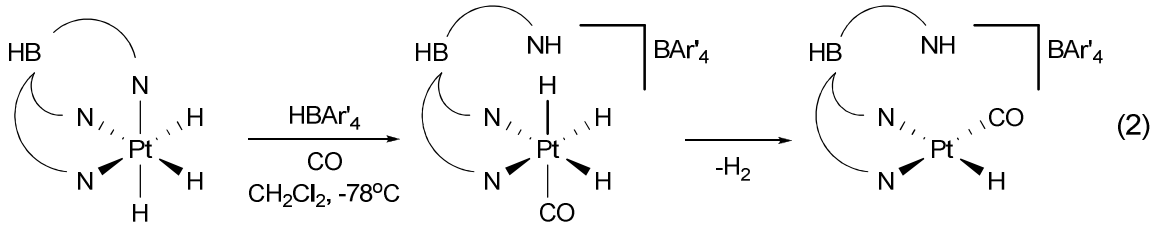

(2)

WGSR Results and Discussion

Using the neutral Tp′PtMe(CO) complex, **1**, as a starting material, an array of Pt(IV) complexes has been synthesized. Tp′Pt((C=O)Me)(Me)(H), **2**, has been previously reported by our lab, however the yield was only 36%.[31] Optimization of the reaction conditions by waiting longer after adding the nucleophilic MeLi reagent before addition of acid has increased the yield to 66% (eq. 3).

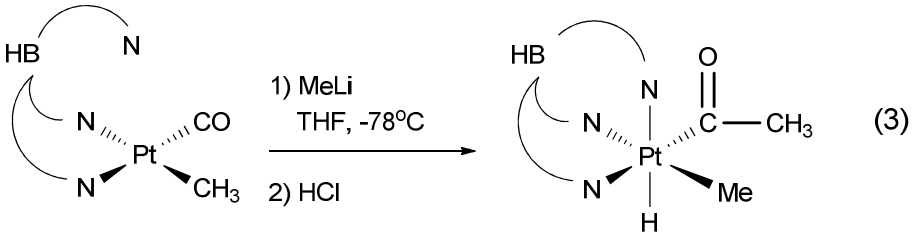

(3)

1 **2**

A resonance at 2.54 ppm with $^{3}J_{Pt\text{-}H}$ of 37 Hz in the ^{1}H NMR spectrum is assigned to the methyl group of the acyl. The Pt-CH_3 resonance appears at 1.29 ppm with $^{2}J_{Pt\text{-}H}$ of 70 Hz and the Pt-H resonance appears at -19.16 ppm with $^{1}J_{Pt\text{-}H}$ of 1427 Hz. The acyl C=O stretching frequency is 1667 cm^{-1}**,** supporting reduction of the C≡O moiety.

In an attempt to synthesize the four-coordinate Pt(II) acyl CO complex, acid was added to **2**. In accord with previous results, the outcome is protonation at the apical nitrogen and reductive elimination of methane.[22] Carbon monoxide gas was bubbled into the solution for 15 minutes. Triethylamine was then added to deprotonate the apical

nitrogen. Instead of isolating the desired Pt(II) acyl CO product, a Pt(IV) dihydride complex, **3**, was isolated (eq. 4).

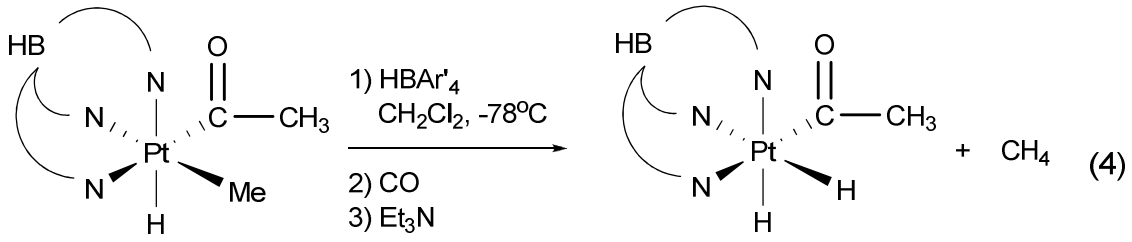

2 **3**

The ^{1}H NMR of **3** indicates a C_s symmetric complex. The resonance for the methyl group of the acyl appears at 2.68 ppm and has $^{3}J_{Pt\text{-}H}$ of 36 Hz. The Pt-H resonance is at -18.32 ppm and has $^{1}J_{Pt\text{-}H}$ of 1331 Hz. A stretch in the IR at 1687 cm^{-1} has been assigned to the C=O moiety.

In order to further study how the product, **3**, is formed, stepwise monitoring of the reaction was performed. To a solution of **2** in CH_2Cl_2, $HBAr'_4$ was added at -78°C. Immediately after addition of acid, CO was bubbled into the solution for 5 minutes (eq. 5). The solvent was removed *in vacuo* and the cationic acyl carbonyl complex was isolated, **4**.

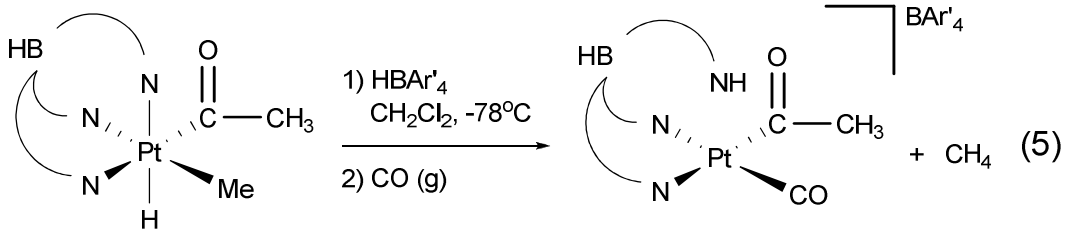

2 **4**

^{1}H NMR indicates a C_1 symmetric species with no hydride resonances present. Thus, elimination of methane from **2** is quantitative and the hydride signal in the

dihydride product **3** is not coming from the hydride originally present in **2**. The methyl resonance of the acyl moiety is at 2.61 ppm with $^{3}J_{Pt\text{-}H}$ of 22 Hz. In the IR spectrum, there are stretches at 2099 cm^{-1} for the C≡O and 1611 cm^{-1} for the C=O. We propose that this complex is formed by reductive elimination from a coordinatively unsaturated 5-coordinate methane complex, as is common for reductive elimination from a Pt(IV) species.[32-39] The carbon monoxide ligand then binds in the vacant coordination site. Dissolving this complex in methylene chloride followed by addition of base resulted in clean formation of the dihydride complex, **3**. These results indicate that adventitious water from the solvent is being activated by the Pt(II) carbonyl intermediate via a water gas shift reaction that takes carbon monoxide and water to carbon dioxide and a Pt(IV) dihydride complex.

In further support that **3** is formed by WGSR, the reaction of **2** with ethylene did not produce a dihydride complex. HBF_4 was added to a solution of **2** in CH_2Cl_2 at -78°C. After a short delay, ethylene gas was bubbled into the solution for 10 minutes. Chromatography on alumina with CH_2Cl_2 produced a white powder. Although the ^{1}H NMR is not definitive, a resonance around 3.5 ppm may be indicative of the formation of an η^{2}-bound ethylene complex. A stretch in the IR at 1632 cm^{-1} is tentatively assigned to the C=O of the acyl and the proposed structure is that of a Pt(II) ethylene acyl complex (eq. 6). The fact that **3** is not formed demonstrates that CO is necessary for the formation of the dihydride species.

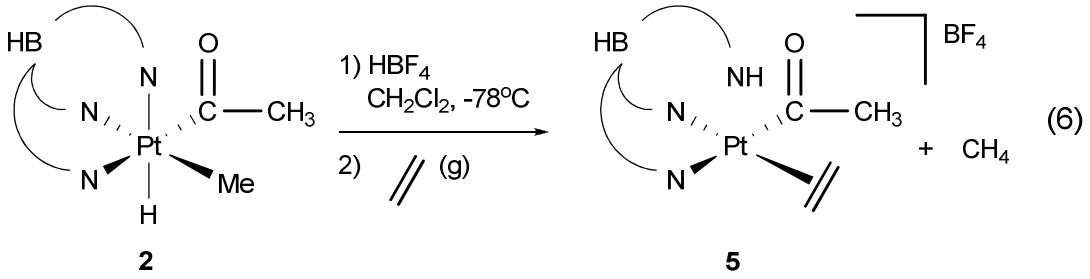

2 **5** (6)

To test the viability of the dihydride complex **3** as a WGSR catalyst, acid was added to **3** in the presence of carbon monoxide. Monitoring by variable temperature ^{1}H NMR indicated that there is immediate formation of a second Pt hydride complex upon addition of acid to **3** at 195 K. The complex is tentatively assigned as the cationic analogue of **3**, in which the Tp′ ligand is bound in a κ^2 fashion with the apical nitrogen protonated. Upon slow warming, free dihydrogen formation is observed at 255 K along with a decrease in the hydride signal. However, at room temperature, decomposition is observed and free Tp′ is formed. Performing this reaction in the absence of carbon monoxide gas leads to the same results, indicating that **3** does not in fact perform metal catalyzed WGSR. Instead, simple acid assisted reductive elimination of dihydrogen followed by decomposition may be occurring. Although **3** may be formed by a metal mediated WGSR, neither **2** nor **3** are viable WGSR catalysts using this protocol.

Additional CO Derived Complexes

The formation of **2** via MeLi addition to the carbon monoxide ligand generated interest in the synthesis of other carbonyl derived species via nucleophilic attack at the carbon of the CO ligand. In particular, the formation of amides is of interest since these can be viewed as precursors to isocyanates. Since isocyanates are monomers in the synthesis of valuable polyureas and pesticides, metal catalyzed reactions used for the

synthesis of isocyanates with a high functional group tolerance are desirable.[40,41] Also, the elimination of isocyanate from a metal center may provide insight into the elimination of carbon dioxide in the water gas shift reaction.

It is important to clarify the nomenclature used for the remainder of the paper. We will be using amides of the type NHR^- as nucleophiles to synthesize metal bound ligands of the type (C=O)NHR. We will refer to NHR^- species as amides and we will label metal bound (C=O)NHR fragments as carboxamido ligands.

Ethylamine was deprotonated by the addition of *n*BuLi to a solution of amine in THF at -78°C, to produce the ethylamide ion. This solution was cannula transferred to a solution of Tp′PtMe(CO) in THF at -78°C, resulting in nucleophilic attack of the amide at the carbon of the CO ligand. Addition of iodomethane resulted in the formation of the Pt(IV) carboxamido complex, **6** (eq. 7). Chromatography on alumina with 25:75 THF:CH_2Cl_2 produces an off white powder in 54% yield.

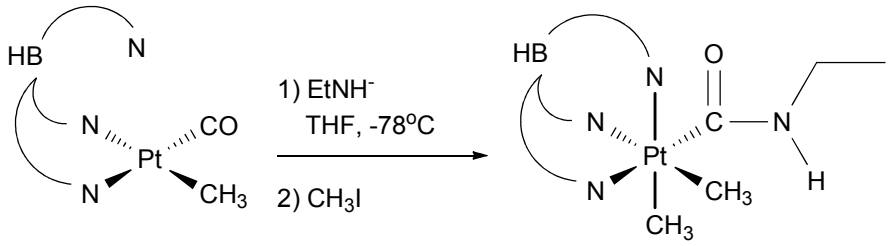

1 **6** (7)

^{1}H NMR spectroscopy indicates a C_s symmetric species. A broad resonance at 5.16 with shoulders can be assigned to the proton on the nitrogen of the amide. The platinum methyl groups appear as a singlet at 1.45 ppm with $^2J_{Pt\text{-}H}$ of 72 Hz. The C=O stretching frequency is 1638 cm^{-1}, which is approximately 50 cm^{-1} lower than in the acyl complex, **2**, consistent with donation to the CO group from the nitrogen lone pair as is common for carboxamido moieties.

As previously mentioned, the carboxamido complex **6** can serve as a precursor for the synthesis of free isocyanates. In an attempt to probe this reaction, LDA was added to **6** in THF at -78°C to deprotonate the nitrogen. After stirring for an hour at room temperature, the solution was acidified with a concentrated NH_4Cl solution (eq. 8). The solvent was removed *in vacuo* and the remaining residue was washed with water. Although the free isocyanate was not observed due to its low boiling point, ^1H NMR indicated the formation of some Tp′$PtMe_2H$, **7**, which is presumed to form after elimination of ethyl isocyanate. Significant decomposition was also observed.

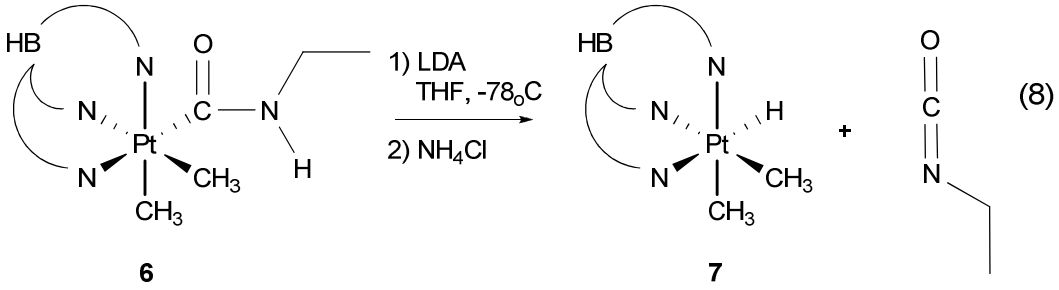

6 **7** (8)

In addition to the ethylamide ion, the reaction with phenylamide ion was also studied. A phenyl carboxamido complex analogous to **6** was synthesized. In the IR, a peak at 1605 cm^{-1} is indicative of a C=O bond and supports that the C≡O bond has been reduced. This stretching frequency is about 30 cm^{-1} lower than the ethylamido analogue, **6**, and about 80 cm^{-1} lower than the acyl complex, **2**. Although the scope of amide ions tested is limited, the results are promising for functional group tolerance and current research efforts are focused on expanding the scope of amide ions used.

In addition to using amide ions to synthesize isocyanates, derivatization of the carboxamido ligands was also explored. LDA was added to a solution of **6** in THF at -78°C. The solution was stirred at room temperature for 15 minutes. After cooling to -78°C, methyl triflate was added. Chromatography on alumina with 25:75 THF:CH_2Cl_2

did not produce the desired carboxamido complex with a tertiary nitrogen. Instead, a small amount of Tp′PtMe$_3$ was formed. This suggests that elimination of free isocyanate occurs after deprotonation of the carboxamido ligand and is not dependent upon the nature of the incoming ligand.

Alternatively, the use of secondary amide ions was investigated. However, the addition of dimethylamide ion to **1** did not result in formation of a tertiary carboxamido complex. Instead, multiple products were formed and no C=O stretch was observed in the IR spectrum of the product mixture.

Discussion

The reactions of the platinum acyl and platinum carboxamido complexes have provided insight into the reactivity of the starting platinum carbonyl complex. The synthesis of the dihydride acyl complex **3** is indicative that complex **2** can react with water via a proposed metal mediated WGSR mechanism. Protonation of **2** under an atmosphere of CO led to the formation of a complex with a C≡O stretch in the IR at 2099 cm^{-1} in addition to the acyl C=O stretch at 1611 cm^{-1}. This is evidence for the formation of the cationic acyl carbonyl complex, **4**, as the precursor to the dihydride complex. Deprotonation of the apical nitrogen facilitates formation of the dihydride complex **3** (eq. 9). Two processes occur at the ligand upon deprotonation. First, the charge on the ligand is changed from neutral to monoanionic. Second, the lone pair on the apical nitrogen becomes readily available to bind to the metal center. This second process has been shown to be exceptionally important in the isolation of six-coordinate platinum complexes (See Chapter 5).

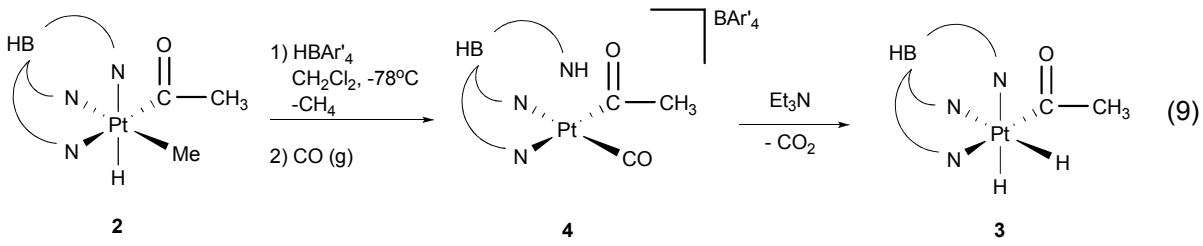

(9)

When the third arm is protonated, formation of the carbonyl complex **4** is favored. However, upon deprotonation, the second half of the water gas shift reaction (Scheme 4.1) can occur and the dihydride complex **3** is the favored product. Although **3** can undergo acid-assisted formation of dihydrogen, **2** is not reformed and thus the cycle is not catalytic. Complex **3** may be a dihydrogen storage unit, since it produces dihydrogen upon addition of acid. This work exhibits some improvement over our previous work in that the CO complex, **4**, and the dihydride complex, **3**, can be synthesized by a carefully selected one pot synthetic route. Previously, a similar acid catalyzed reductive elimination pathway was used to synthesize the Tp′Pt(CO)H complex and then a harsh basic reflux with copious amounts of water was necessary to form the trihydride complex. However, we have now developed a system that binds CO(g) and activates water at low temperatures with only adventitious amounts of water present. The downside to this system is that after formation of dihydrogen it does not appear to bind CO again to reform **4**.

In addition to the platinum WGSR chemistry studied, the platinum carboxamido chemistry has shown promise as a convenient precursor to small isocyanates. The scope of amide ions susceptible to reaction with **1** needs to be expanded. Deprotonation of the carboxamido complex followed by acidification appears to form a small amount of the dimethyl hydride complex, **7**. *In situ* studies need to be performed to confirm the

presence of free isocyanate. Since complex **7** is the precursor to the carbonyl complex **1**, this reaction can be viewed as a recyclable way to synthesize isocyanates.

Since deprotonation of the carboxamido complex **6** followed by addition of methyl triflate resulted in the formation of a trimethyl complex and addition of acid resulted in the formation of a dimethyl hydride complex, we propose that the reaction proceeds by elimination of the isocyanate upon deprotonation to form a reactive anionic intermediate (Scheme 4.2). This elimination is not dependent upon the nature of the incoming ligand.

Scheme 4.2: Elimination of isocyanate from carboxamide complex

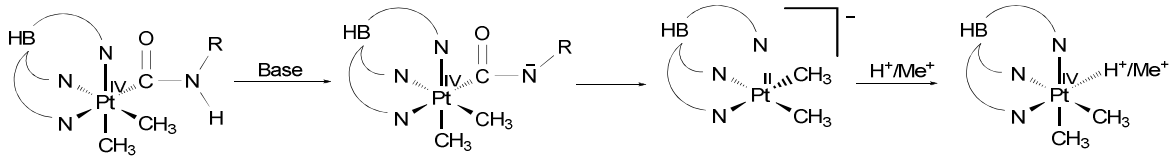

Current efforts are focused on monitoring the C=O stretch throughout the reaction. Observation of the free isocyanate in solution is necessary to confirm this mechanism. Further studies of this mechanism will also be beneficial in understanding of metal catalyzed WGSR chemistry, since the anionic intermediate on the path to carbon dioxide elimination is formed by nucleophilic attack at the carbonyl ligand in a manner similar to the formation of the carboxamido complex by nucleophilic attack of an amide ion. From this anionic intermediate, carbon dioxide is eliminated. Thus, better understanding of the elimination of isocyanate from the Pt(IV) center will lead to more knowledge about Tp′Pt water gas shift reaction chemistry.

Conclusion

The platinum (II) carbonyl complex, **1**, has lead to a diverse array of reactions. The acyl complex **2** reductively eliminates methane upon addition of acid under an atmosphere of CO to form the complex **4**, which we propose reacts with water via a metal mediated WGSR to form **3** upon deprotonation of the third arm of the Tp′ chelate. Reprotonation of the third arm of the chelate in **3** results in decomposition of the complex, but only after formation of dihydrogen. We postulate that the availability of the WSGR mechanism and reductive elimination of dihydrogen are heavily dependent upon the binding mode of the Tp′ ligand.

In addition to WGSR chemistry, the platinum (II) carbonyl complex has shown promise as a recyclable route to synthesizing small isocyanates. Nucleophilic attack of a primary amide ion at the carbon of the carbonyl moiety results in a platinum carboxamido complex. Deprotonation of the ethylamido complex **6** is a viable route to the elimination of ethyl isocyanate.

Experimental

General Information. Reactions were performed under a dry nitrogen atmosphere using standard Schlenk techniques. Methylene chloride, hexanes, and pentane were purified by passage through an activated alumina column under a dry argon atmosphere. THF was distilled from a sodium ketal suspension. Methylene chloride-d_2 was dried over CaH_2 and degassed. All other reagents were purchased from commercial sources and were used without further purification.

Tp′PtMe(CO) (**1**)[22] and $[H(OEt_2)_2][BAr'_4]$[42] were synthesized according to known procedures. NMR spectra were recorded on Bruker DRX500, DRX400, AMX400, or AMX300 spectrometers. Infrared spectra were recorded on an ASI Applied Systems React IR 1000 FT-IR spectrometer.

Tp′Pt((C=O)Me)MeH, 2: Methyl lithium (1.6 M in Et_2O, 145 μL, 0.232 mmol) was added to a solution of Tp′PtMe(CO) (103 mg, 0.193 mmol) in THF at -78°C. The solution was stirred at room temperature for 30 minutes. After cooling to -78°C, hydrochloric acid (1 M in Et_2O, 300 μL, 0.300 mmol) was added. The solution was brought up to room temperature and stirred for thirty minutes, after which the solvent removed *in vacuo*. Chromatography on alumina with CH_2Cl_2 produced a white powder (yield: 70 mg, 0.127 mmol, 66%). NMR: ^{1}H (400 MHz, CD_2Cl_2, 298 K), δ 5.87 (s, 1H, Tp′ CH), 5.83 (s, 2H, Tp′ CH), 2.54 (s, 3H, (C=O)CH_3, $^3J_{Pt\text{-}H}$ = 37 Hz), 2.41, 2.35, 2.34, 2.24, 2.07, 1.98 (s, 3H each, Tp′ CH_3), 1.29 (s, 3H, Pt-Me, $^2J_{Pt\text{-}H}$ = 70 Hz), -19.15 (s, 1H, Pt-H, $^1J_{Pt\text{-}H}$ = 1427 Hz); IR(THF): $\nu_{C=O}$ = 1667 cm^{-1}.

Tp′Pt((C=O)Me)H_2, 3: $[H(OEt_2)_2][BAr'_4]$ (221 mg, 0.218 mmol) was added to a solution of **2** (80 mg, 0.145 mmol) in 15 mL CH_2Cl_2 at -78°C. CO (g) was bubbled through the solution for 10 minutes. Triethylamine (50 μL, 0.359 mmol) was added and the solution was brought up to room temperature. The solvent was removed *in vacuo*. Chromatography on Et_3N treated silica with 2:3 CH_2Cl_2:hexanes produced a yellow powder (yield: 24 mg, 0.045 mmol, 31%). NMR: ^{1}H (400 MHz, CD_2Cl_2, 298 K), δ 5.87 (s, 2H, Tp′ CH), 5.80 (s, 1H, Tp′ CH), 2.68 (s, 3H, (C=O)CH_3, $^3J_{Pt\text{-}H}$ = 36 Hz), 2.39, 1.99 (s, 6H each, Tp′CH_3), 2.32, 2.20 (s, 3H each, Tp′ CH_3), -18.33 (s, 2H, Pt-H, $^1J_{Pt\text{-}H}$ = 1332 Hz); IR(CH_2Cl_2): $\nu_{C=O}$ = 1687 cm^{-1}.

[HTp′Pt((C=O)CH_3)(CO)][BAr′$_4$], 4: A Schlenk flask containing **2** (30 mg, 0.054 mmol) and [H(OEt_2)$_2$][BAr′$_4$] (83 mg, 0.082 mmol) was evacuated and filled with CO(g). CH_2Cl_2 was added to the flask and the solution was stirred at -78°C for 10 minutes. The solvent was then removed *in vacuo* for analysis. NMR: ^{1}H (300 MHz, CD_2Cl_2, 298 K), δ 11.17 (s, 1H, N-H), 7.73 (s, 12H, BAr$_4$′), 7.57 (s, 6H, BAr$_4$′) , 6.18, 6.09, 6.04 (s, 1H each, Tp′ CH), 2.61 (s, 3H, (C=O)CH_3, $^3J_{Pt\text{-}H}$ = 22 Hz), 2.42, 2.31, 2.16, 2.05 (s, 3H each, Tp′CH_3), 2.35 (s, 6H, Tp′ CH_3); IR(CH_2Cl_2): $\nu_{C\equiv O}$ = 2099 cm^{-1}, $\nu_{C=O}$ = 1611 cm^{-1}.

[HTp′Pt((C=O)CH_3)(η^2-CH_2=CH_2)][BAr′$_4$], 5: A Schlenk flask containing **2** (30 mg, 0.054 mmol) and [H(OEt_2)$_2$][BAr′$_4$] (83 mg, 0.082 mmol) was evacuated and filled with ethylene(g). CH_2Cl_2 was added to the flask and the solution was stirred at -78°C for 10 minutes. The solvent was then removed *in vacuo* for analysis. NMR: ^{1}H - **Current NMR data is inconclusive.**

Tp′Pt((C=O)NHCH_2CH_3)(CH_3)$_2$, 6: Ethylamine (2 M in THF, 70 µL, 0.14 mmol) was deprotonated using *n*BuLi (2.5 M in hexanes, 65µL, 0.163 mmol) in 10 mL THF at -78°C. The amide solution was cannula transferred to a separate flask containing **1** (50 mg, 0.093 mmol) in 10 mL THF at -78°C. The solution was stirred at room temperature for 25 minutes. After cooling the solution to -78°C, CH_3I (15µL, 0.236 mmol) was added. The solution was stirred at room temperature for 30 minutes. The solvent was removed *in vacuo*. Chromatography on alumina with 1:3 THF:CH_2Cl_2 produced a white powder (29 mg, 0.05 mmol, 54%). %). NMR: ^{1}H (400 MHz, CD_2Cl_2, 298 K), δ 5.85 (s, 2H, Tp′ CH), 5.81 (s, 1H, Tp′ CH), 5.16 (s, 1H, NH), 3.21 (m, 2H, C$H_2$$CH_3$), 2.39, 2.18 (s, 6H each, Tp′ CH_3), 2.34, 2.29 (s, 3H each, Tp′ CH_3), 1.42 (s, 6H, Pt-Me, $^2J_{Pt\text{-}H}$ = 72 Hz), 0.99 (t, 3H, CH_2CH_3); IR(THF): $\nu_{C=O}$ = 1638 cm^{-1}.

Tp′PtMe$_2$H, 7: A solution of LDA (5 mg, 0.048 mmol) in 5 mL THF at -78°C was cannula transferred to a flask containing **6** (20 mg, 0.034 mmol) in 5 mL THF also at -78°C. The solution was brought up to room temperature and stirred for 1 hour. The solution was cooled to -78°C and acidified with a 3 mL of concentrated NH_4Cl solution. The solvent was removed *in vacuo*. The residual powder was washed with 3 x 10 mL H_2O. NMR: ^{1}H (300 MHz, CD_2Cl_2, 298 K), δ 5.78 (s, 3H, Tp′ CH), 2.40. 2.34 (s, 3H each, Tp′ CH_3), 2.35, 2.14 (s, 6H each, Tp′ CH_3), 1.26 (s, 6H, Pt-Me, $^2J_{Pt\text{-}H}$ = 68 Hz), -20.87 (s, 1H, Pt-H, $^1J_{Pt\text{-}H}$ = 1355 Hz).

References

(1) Okkerse, C.; van Bekkum, H. *Green Chem.* **1999**, *1*, 107.

(2) Olah, G. A. *Angew. Chem.-Int. Edit.* **2005**, *44*, 2636.

(3) Periana, R. A.; Bhalla, G.; Tenn, W. J.; Young, K. J. H.; Liu, X. Y.; Mironov, O.; Jones, C. J.; Ziatdinov, V. R. *J. Mol. Catal. A-Chem.* **2004**, *220*, 7.

(4) Cortright, R. D.; Davda, R. R.; Dumesic, J. A. *Nature* **2002**, *418*, 964.

(5) Forsberg, C. W. *Int. J. Hydrog. Energy* **2003**, *28*, 1073.

(6) Huber, G. W.; Shabaker, J. W.; Dumesic, J. A. *Science* **2003**, *300*, 2075.

(7) Sayama, K.; Nomura, A.; Zou, Z. G.; Abe, R.; Abe, Y.; Arakawa, H. *Chem. Commun.* **2003**, 2908.

(8) Deluga, G. A.; Salge, J. R.; Schmidt, L. D.; Verykios, X. E. *Science* **2004**, *303*, 993.

(9) Huber, G. W.; Iborra, S.; Corma, A. *Chem. Rev.* **2006**, *106*, 4044.

(10) Khan, M. M. T.; Halligudi, S. B.; Shukla, S. *Angew. Chem.-Int. Edit. Engl.* **1988**, *27*, 1735.

(11) Spessard, G. O.; Miessler, G. L. *Organometallic Chemistry*; Prentice Hall: New Jersey, 1996.

(12) Rhodes, C.; Hutchings, G. J.; Ward, A. M. *Catal. Today* **1995**, *23*, 43.

(13) Chen, C. S.; Lin, J. H.; Lai, T. W. *Chem. Commun.* **2008**, 4983.

(14) Opalka, S. M.; Vanderspurt, T. H.; Radhakrishnan, R.; She, Y.; Willigan, R. R. *J. Phys.-Condes. Matter* **2008**, *20*.

(15) Radhakrishnan, R.; Willigan, R. R.; Dardas, Z.; Vanderspurt, T. H. *Appl. Catal. B-Environ.* **2006**, *66*, 23.

(16) Laine, R. M.; Rinker, R. G.; Ford, P. C. *J. Am. Chem. Soc.* **1977**, *99*, 252.

(17) Kubiak, C. P.; Eisenberg, R. *J. Am. Chem. Soc.* **1980**, *102*, 3637.

(18) Laine, R. M.; Crawford, E. J. *J. Mol. Catal.* **1988**, *44*, 357.

(19) Yoshida, T.; Ueda, Y.; Otsuka, S. *J. Am. Chem. Soc.* **1978**, *100*, 3941.

(20) Ziessel, R. *Angew. Chem.-Int. Edit. Engl.* **1991**, *30*, 844.

(21) King, R. B. *J. Organomet. Chem.* **1999**, *586*, 2.

(22) Reinartz, S.; White, P. S.; Brookhart, M.; Templeton, J. L. *Organometallics* **2000**, *19*, 3854.

(23) Akita, M.; Ohta, K.; Takahashi, Y.; Hikichi, S.; Morooka, Y. *Organometallics* **1997**, *16*, 4121.

(24) Clark, H. C.; Manzer, L. E. *J. Am. Chem. Soc.* **1973**, *95*, 3812.

(25) Clark, H. C.; Manzer, L. E. *Inorg. Chem.* **1974**, *13*, 1996.

(26) Haskel, A.; Keinan, E. *Organometallics* **1999**, *18*, 4677.

(27) West, N. M.; Reinartz, S.; White, P. S.; Templeton, J. L. *J. Am. Chem. Soc.* **2006**, *128*, 2059.

(28) Ingleson, M. J.; Brayshaw, S. K.; Mahon, M. F.; Ruggiero, G. D.; Weller, A. S. *Inorg. Chem.* **2005**, *44*, 3162.

(29) Packett, D. L.; Jensen, C. M.; Cowan, R. L.; Strouse, C. E.; Trogler, W. C. *Inorg. Chem.* **1985**, *24*, 3578.

(30) Vaska, L. *Acc. Chem. Res.* **1968**, *1*, 335.

(31) Reinartz, S.; Brookhart, M.; Templeton, J. L. *Organometallics* **2002**, *21*, 247.

(32) Bartlett, K. L.; Goldberg, K. I.; Borden, W. T. *J. Am. Chem. Soc.* **2000**, *122*, 1456.

(33) Bartlett, K. L.; Goldberg, K. I.; Borden, W. T. *Organometallics* **2001**, *20*, 2669.

(34) Brown, M. P.; Puddephatt, R. J.; Upton, C. E. E. *J. Chem. Soc.-Dalton Trans.* **1974**, 2457.

(35) Crumpton-Bregel, D. M.; Goldberg, K. I. *J. Am. Chem. Soc.* **2003**, *125*, 9442.

(36) Edelbach, B. L.; Lachicotte, R. J.; Jones, W. D. *J. Am. Chem. Soc.* **1998**, *120*, 2843.

(37) Hill, G. S.; Yap, G. P. A.; Puddephatt, R. J. *Organometallics* **1999**, *18*, 1408.

(38) Jensen, M. P.; Wick, D. D.; Reinartz, S.; White, P. S.; Templeton, J. L.; Goldberg, K. I. *J. Am. Chem. Soc.* **2003**, *125*, 8614.

(39) Roy, S.; Puddephatt, R. J.; Scott, J. D. *J. Chem. Soc.-Dalton Trans.* **1989**, 2121.

(40) Dhar, D. N. *The Chemistry of Chlorosulfonyl Isocyanate*; World Scientific: River Edge, N.J., 2002.

(41) Ulrich, H. *Chemistry and Technology of Isocyanates*; J. Wiley & Sons: New York, 1996.

(42) Brookhart, M.; Grant, B.; Volpe, A. F. *Organometallics* **1992**, *11*, 3920.

Chapter 5

Synthesis of Isonitrile, Iminoacyl and Aminocarbene Tp'Pt Complexes

Abstract

Generation of a reactive Tp′PtR fragment (Tp′ = hydridotris(3,5-dimethylpyrazolyl)borate) in the presence of free isonitrile leads to a σ-isonitrile Pt(II) complex. Related Pt(II) aminocarbene complexes can be synthesized by nucleophilic attack at the isonitrile carbon followed by addition of acid. Protonation at nitrogen produces the observed aminocarbene product. Nucleophilic attack at the carbon of the coordinated isonitrile by metal alkyl reagents followed by addition of iodomethane as an electrophilic reagent results in Pt(IV) iminoacyl complexes of the type Tp′Pt(RC=N(2,6-$C_6Me_2H_3$))Me_2 where R = Me or Et. Alternatively, the Pt(II) aminocarbene complexes can be converted to these same Pt(IV) iminoacyl products by deprotonation of the N-H site followed by addition of iodomethane, with the outcome reflecting methylation at platinum. Addition of acid to the Pt(IV) iminoacyl complex generates a rare cationic Pt(IV) aminocarbene complex via protonation at the iminoacyl nitrogen as {Tp′Pt(C(R)NH(2,6-$C_6Me_2H_3$))Me_2}{BF_4} forms.

Introduction

Coordination of isonitrile to a metal center often activates the isonitrile ligand toward nucleophilic attack.[1-5] Platinum (II) isonitrile complexes have been known for decades, and their reactivity has been thoroughly studied.[6-11] In the past twenty years, nucleophilic attack at the carbon of a coordinated isonitrile has provided the first step toward the subsequent formation of a carbene, most commonly an N-heterocyclic carbene.[1] Non-heterocyclic carbenes can be synthesized by the reaction of a coordinated isonitrile with a nucleophile of the type Nu-H in which proton transfer from the

nucleophile to the nitrogen of the isonitrile occurs (Eq. 1). Platinum carbene complexes derived from platinum isonitrile complexes are dominated by Pt(0) and Pt(II) compounds, while platinum (IV) carbene complexes remain rare.[11-15]

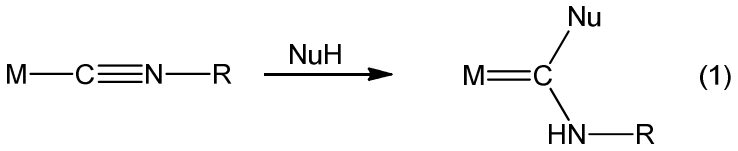

(1)

The formation of non-heterocyclic carbenes by the reaction of a bound isonitrile with a monoanionic nucleophile followed by addition of an electrophile have been less thoroughly studied. This reaction generally results in the formation of an imino containing moiety, such as an iminoacyl complex.[16] However, most metal iminoacyl complexes are formed by migratory insertion of a bound isonitrile ligand into a metal alkyl bond or by reaction of a metal complex with an imidoyl halide rather than by reduction of a bound isonitrile.[16-19] Kukushkin has recently reported a series of reactions using a Pt(IV) nitrile complex in which Pt(IV) products are formed, but these products are bound through the nitrogen of the imine to the metal center (Eq. 2).[20-24]

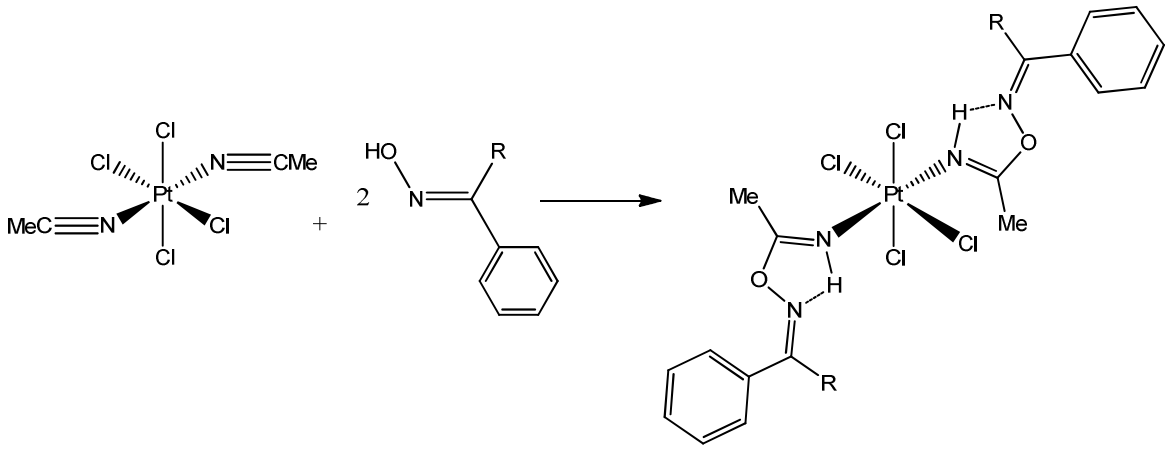

(2)

Transformations among isonitrile, iminoacyl, and aminocarbene ligands often hinge upon the nitrogen's ability to carry a lone pair. We previously reported a series of

reactions in which molybdenum bound isonitrile ligands were converted to aminocarbyne, η^2-iminoacyl, and η^2-vinyl ligands.[25] In 1990, Carmona reported conversion from an η^2-iminoacyl nickel complex to an aminocarbene complex utilizing diprotic acids (Eq. 3).[26]

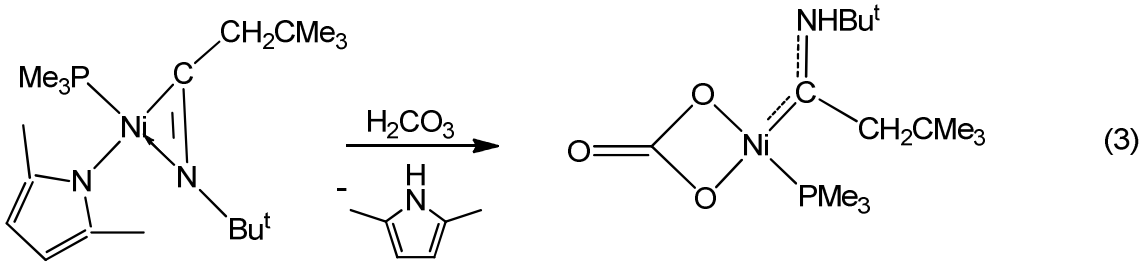

(3)

Bianchini demonstrated that carbene complexes can be precursors to isonitrile complexes via simple thermolysis in wet solvent.[27] However, conversions of Pt(II) isonitrile complexes to Pt(IV) iminoacyl or Pt(IV) aminocarbene complexes remain rare.

In this chapter, we report the synthesis of a Tp′Pt(II) isonitrile complex and subsequent transformations that result in Pt(II) aminocarbene complexes, Pt(IV) iminoacyl complexes, and a cationic Pt(IV) aminocarbene complex.

Results

Protonation of one arm of the Tp′ ligand (Tp′ = hydridotris(3,5-dimethylpyrazolyl) borate) of Tp′PtMe$_2$H, **1,** with HBF_4 leads to loss of methane.[28] Coordination of 2,6-dimethylphenyl isonitrile at the vacant coordination site, followed by a short delay before deprotonation of the Tp′ ligand, produces Tp′Pt(CNR)Me (R= 2,6-$C_6Me_2H_3$) (Eq. 4). This σ-bound isonitrile Pt(II) complex was purified by chromatography on alumina with 25:75 THF:CH_2Cl_2.

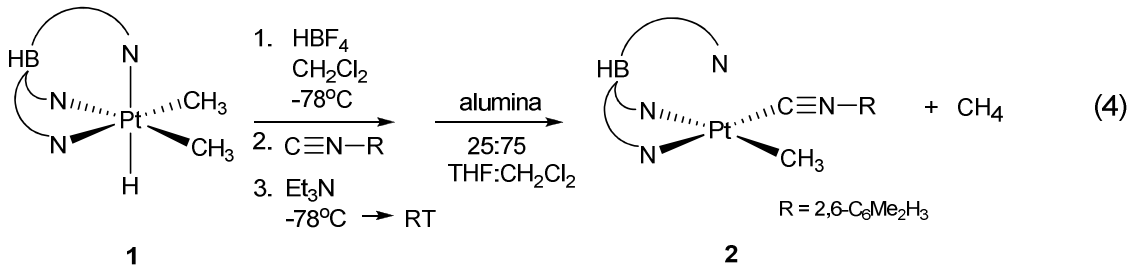

(4)

Tp′Pt(CNR)Me, **2**, was isolated as a beige powder that was stable at room temperature. ^{1}H NMR spectroscopy indicated a Pt-Me resonance at 0.62 ppm with satellites reflecting a $^{2}J_{Pt\text{-}H}$ value of 77 Hz. The platinum (II) methyl signal is shifted significantly upfield from the starting Tp′PtMe$_2$H complex methyl singlet (1.3 ppm). We have generally observed that Pt(II) methyl signals appear upfield relative to Pt(IV) methyl signals in Tp′Pt chemistry.[29-31] C-13 spectroscopy revealed a broad resonance at 132.9 ppm for the carbon of the isonitrile and a resonance at -23.2 ppm with $^{1}J_{Pt\text{-}C}$ of 591 Hz for the Pt(II)-Me. The IR spectrum of **2** has a strong absorbance at 2163 cm^{-1} for the C≡N stretch and a weaker absorbance at 2472 cm^{-1} for the B-H stretch. Literature reports indicate that B-H stretches below 2500 cm^{-1} are indicative of a κ^2 binding mode for the Tp′ ligand and stretches above 2500 cm^{-1} reflect a κ^3 binding mode.[29,32,33]

Recrystallization of complex **2** from CH_2Cl_2/pentane at -30°C yielded colorless blocks suitable for x-ray crystallography (Figure 5.1). One arm of the Tp′ ligand is dechelated producing a four-coordinate Pt(II) complex. The C≡N bond distance is 1.150(4) Å, and the Pt1-C2-N3 bond angle is 176.4(3)°, close to linear.

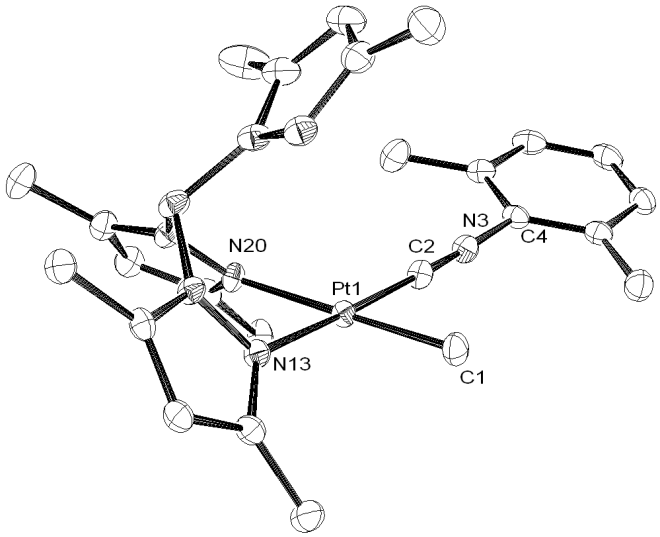

Figure 5.1: ORTEP diagram of Tp′Pt(C≡N(2,6-$C_6Me_2H_3$))Me, **2**. Hydrogen atoms have been omitted for clarity. See Table 5.2 for crystal data and structure refinement. Selected bond lengths and angles: Pt1-C1 = 2.041(3) Å, Pt1-C2 = 1.891(3) Å, Pt1-N20 = 2.097(3)Å, Pt1-N13 = 2.065(3) Å, C2-N3 = 1.150(4) Å, N3-C4 = 1.399(4) Å, C1-Pt1-C2 = 86.29°, C2-Pt1-N20 = 96.57°, N20-Pt1-N13 = 85.25(11)°, N13-Pt1-C1 = 91.73°, Pt1-C2-N3 = 176.4(3)°, C2-N3-C4 = 177.8(3)°.

Reaction of complex **2** with methyl lithium at -78°C in an NMR tube in diethyl ether results in nucleophilic attack at the carbon of the isonitrile. A delay of one minute before addition of 1.2 equivalents of HBF_4 to the presumed anionic species produces a four-coordinate Pt(II) aminocarbene complex (Eq. 5). Chromatography on alumina with CH_2Cl_2 results in an isolable white powder.

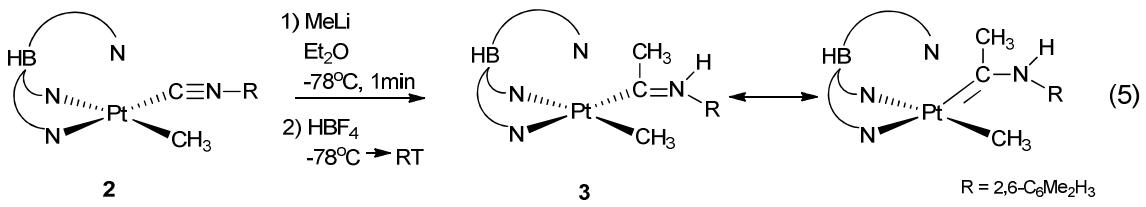

^{1}H NMR spectroscopy indicated a characteristic N-H resonance at 11.1 ppm with $^{3}J_{Pt\text{-}H}$ of 44 Hz. This large vicinal platinum coupling constant may indicate that the hydrogen lies trans to the metal center. The Pt-Me resonance at 0.26 ppm is unusually far upfield for a Tp′Pt(II) methyl resonance and exhibits a large $^{2}J_{Pt\text{-}H}$ of 86 Hz. ^{13}C NMR spectroscopy demonstrated a significantly downfield resonance at 224.5 ppm for the carbon of the aminocarbene. This downfield resonance reveals the carbene character of this carbon compared to the isonitrile. The resonance for the methyl group on the aminocarbene is at 30.0 ppm with $^{2}J_{Pt\text{-}C}$ coupling of 135 Hz and the platinum methyl signal is at -23.3 ppm with $^{1}J_{Pt\text{-}C}$ coupling of 756 Hz.

However, reaction of complex **2** with methyl lithium at -78°C in an NMR tube in ether followed by a five minute delay before addition of ten equivalents of HBF_4 produces a Pt(II) aminocarbene chloride complex (Eq. 6). Chromatography on alumina with 25:75 THF:CH_2Cl_2 produces a white powder.

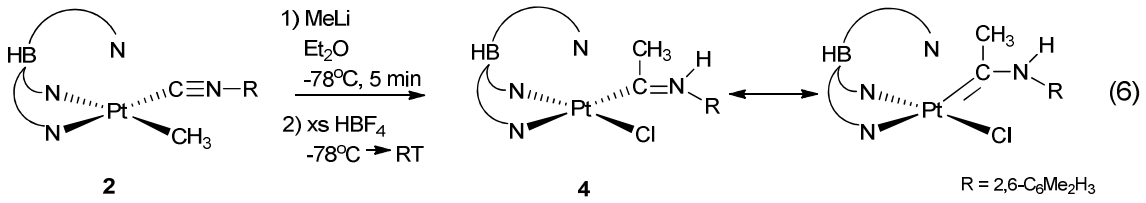

2 **4** R = 2,6-$C_6Me_2H_3$

^{1}H NMR spectroscopy indicated a C_1 symmetric species, and no Pt-Me signal was observed. The N-H resonance differs from the other aminocarbene complexes in that it is broad at room temperature and satellites cannot be detected. ^{13}C NMR spectroscopy revealed a downfield resonance for the carbon of the aminocarbene at 215.6 ppm with $^{1}J_{Pt\text{-}C}$ of 1040 Hz.

Slow diffusion of pentanes into a solution of **4** in CH_2Cl_2 at 0°C produced colorless blocks suitable for X-ray crystallography (Figure 5.2). The Pt1-C2 bond distance is 1.952(6) Å and the C2-N12 bond distance is 1.307(7) Å.

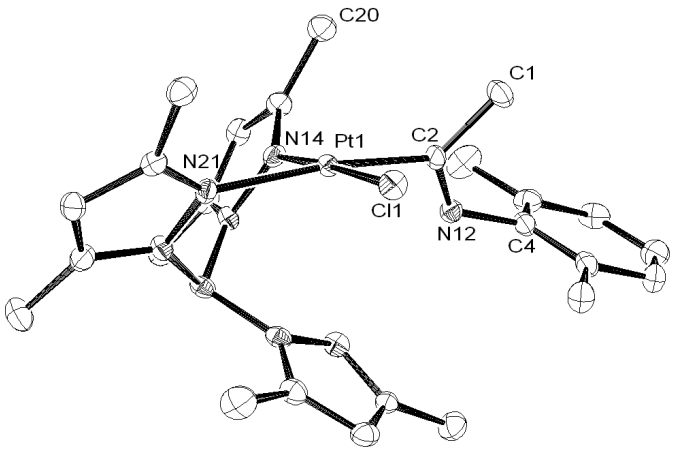

Figure 5.2: ORTEP diagram of Tp′Pt[C(Me)N(2,6-$C_6Me_2H_3$)H]Cl, **4**. Hydrogen atoms have been omitted for clarity. See Table 5.2 for crystal data and structure refinement. Selected bond lengths and angles: Pt1-Cl1 = 2.3011(11) Å, Pt1-C2 = 1.952(6) Å, Pt1-N14 = 2.014(5) Å, Pt1-N21 = 2.090(5) Å, C2-N12 = 1.307(7) Å, Cl1-Pt1-C2 = 90.12°, C2-Pt1-N14 = 91.2(2)°, N14-Pt1-N21 = 86.3(2)°, N21-Pt1-Cl1 = 92.12(15)°, Pt1-C2-C1 = 123.3(4)°, Pt1-C2-N12 = 117.4(4)°, C1-C2-N12 = 119.3°.

Note that reaction of complex **4** with acid followed by MeLi produces complex **3** (Eq. 7).

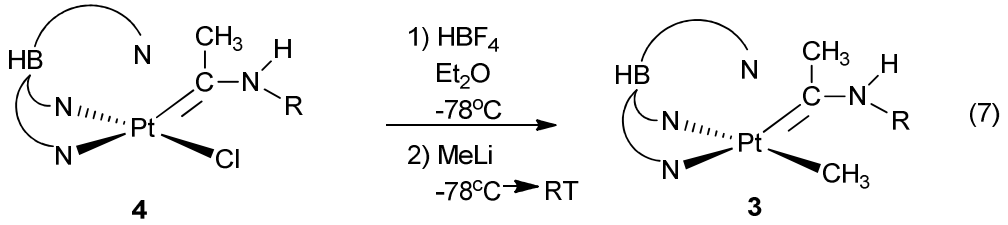

(7)

Reaction of isonitrile complex **2** with alkyl lithium reagents in ether at -78°C followed by addition of iodomethane to the putative anionic iminoacyl complex produces six coordinate complexes of the type Tp′Pt(R′C=NR)Me_2 (R′ = Me, Et) (Eq. 8). These complexes were chromatographed on alumina with 25:75 THF:CH_2Cl_2.

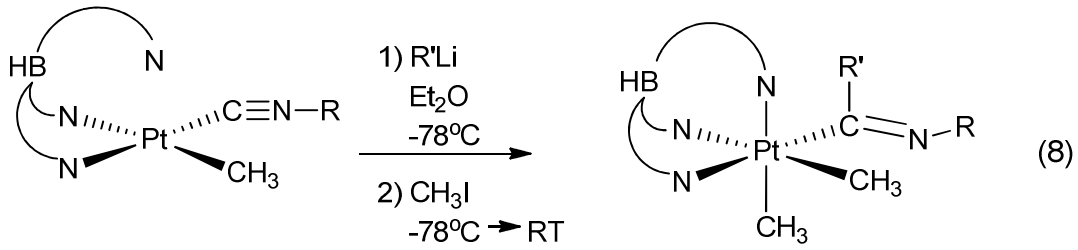

(8)

2 **5**

R = 2,6-$C_6Me_2H_3$

a R' = Me

b Et

Tp′Pt(MeC=NR)Me_2, **5a**, was isolated as a yellow powder. ^{1}H NMR spectroscopy indicated a Pt-Me resonance at 1.80 ppm with $^2J_{Pt-H}$ of 73 Hz. This downfield chemical shift is consistent with an oxidation of the metal center from Pt(II) to Pt(IV). The methyl group in the iminoacyl moiety resonates at 1.71 ppm with $^3J_{Pt-H}$ of 17 Hz. ^{13}C spectroscopy revealed a resonance shifted downfield for the carbon of the iminoacyl at 158.2 ppm relative to the starting isonitrile complex, **2** (132.9 ppm), but upfield of the Pt(II) aminocarbene complex, **3** (224.5 ppm). This carbon signal reflects a large $^1J_{Pt-C}$ coupling of 1045 Hz, indicating that the iminoacyl is tightly bound to the metal center. The Pt-Me C-13 resonance is upfield at -3.0 ppm with $^1J_{Pt-C}$ coupling of 693 Hz.

Recrystallization of complex **5a** from CH_2Cl_2/pentane at room temperature yielded yellow needles suitable for x-ray crystallography (Figure 5.3). The C3-N5 bond distance is 1.279(10) Å which is 0.129 Å longer than the bound isonitrile bond distance.

The increased C-N bond distance is consistent with reduction of the isonitrile C-N triple bond to a double bond in the iminoacyl ligand product. In addition, the Pt1-C3-C4, Pt1-C3-N5, and C4-C3-N5 bond angles are 116.8(5)°, 121.1(7)°, and 122.1(8)° respectively, indicative of an sp^2 hybridized carbon at the C3 position.

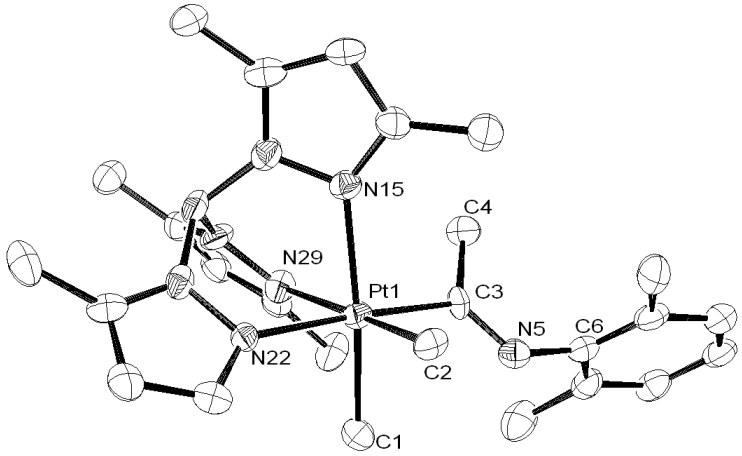

Figure 5.3: ORTEP diagram of Tp′Pt(MeC=N(2,6-$C_6Me_2H_3$))Me_2, **5a**. Hydrogen atoms have been omitted for clarity. See Table 5.2 for crystal data and structure refinement. Selected bond lengths and angles: Pt1-C1 = 2.049(8) Å, Pt1-C2 = 2.060(7) Å, Pt1-C3 = 2.030(8) Å, Pt1-N15 = 2.203(6) Å, Pt1-N22 = 2.179(6) Å, Pt1-N29 = 2.186(7) Å, C3-N5 = 1.279(10)°, N5-C6 = 1.403(11)°, C1-Pt1-C2 = 89.2(3)°, C2-Pt1-C3 = 88.0(4)°, C4-C3-N5 = 122.1(8)°, Pt1-C3-C4 = 116.8(5)°, Pt1-C3-N5 = 121.1(7)°, C3-N5-C6 = 125.6(8)°.

Surprisingly, reaction of **2** with methyl lithium in tetrahydrofuran at -78°C followed by addition of iodomethane results in the six coordinate complex Tp′Pt(MeC=NR)MeI, **6,** rather than complex **5a** (Eq. 9). This iodo complex was purified by chromatography on alumina with 25:75 THF:CH_2Cl_2. The two different products, **6**

and **5a**, result from the same reaction conditions but in different solvents. Formation of **6** in THF and **5a** in ether is an unusual solvent dependence on whether CH_3 or I occupies the sixth coordination site.

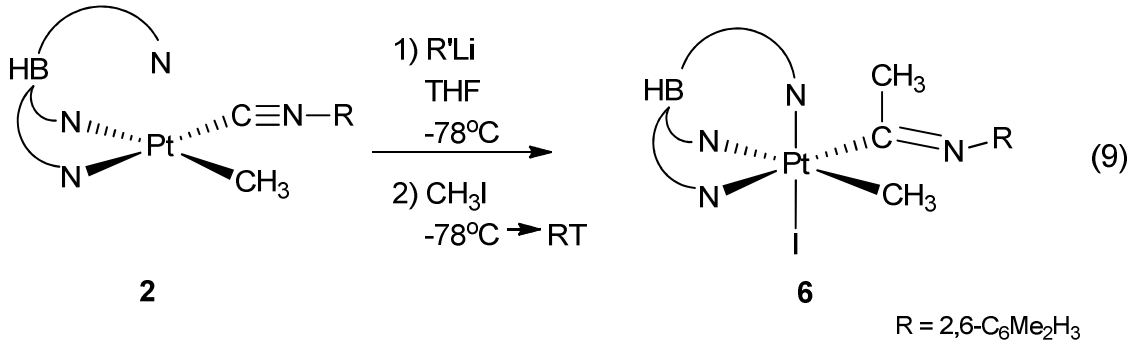

^{1}H NMR spectroscopy of **6** indicated a C_1 symmetric species. The Pt-Me resonance appears downfield at 2.73 ppm with $^2J_{Pt\text{-}H}$ = 73 Hz. This significant downfield shift from the Pt-Me of **2** (0.62 ppm) is presumably due to the presence of an iodide ligand in the coordination sphere and by oxidation of the metal center from Pt(II) to Pt(IV). The resonance for the methyl group of the iminoacyl moiety appears at 1.64 ppm with $^3J_{Pt\text{-}H}$ = 14 Hz. ^{13}C NMR spectroscopy revealed a broad signal at 145.9 ppm with $^1J_{Pt\text{-}C}$ = 813 Hz for the carbon of the iminoacyl ligand, which is consistent with **5a** in chemical shift for a carbon that is part of an iminoacyl moiety and not an aminocarbene moiety.

Slow diffusion of pentanes into a solution of **6** in CH_2Cl_2 at 0°C yielded yellow blocks suitable for X-ray crystallography (Figure 5.4). The CN bond distance is 1.247(12) Å, which is about 0.09 Å longer than bound isonitrile. The C-N-C angle at the nitrogen of the iminoacyl is 125.0(9)°, indicative of an sp^2 hybridized center.

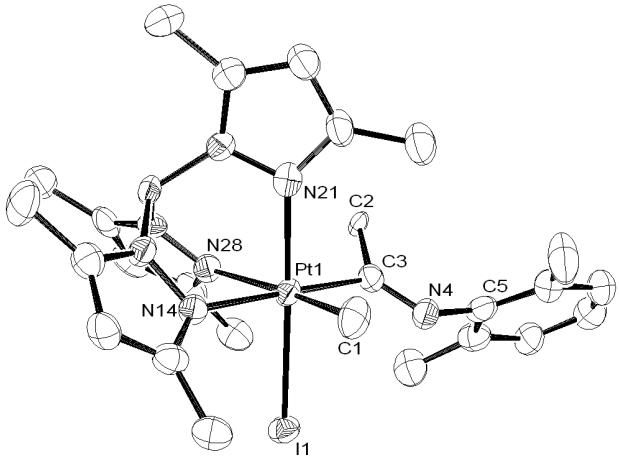

Figure 5.4: ORTEP diagram of Tp′Pt(MeC=N(2,6-$C_6Me_2H_3$))MeI, **6**. Hydrogen atoms have been omitted for clarity. See Table 5.2 for crystal data and structure refinement. Selected bond lengths and angles: Pt1-C1 = 1.951(15) Å, Pt1-C3 = 2.048(10) Å, Pt1-I1 = 2.6480(9) Å, Pt1-N14 = 2.217(8) Å, Pt1-N28 = 2.166(7) Å, Pt1-N21 = 2.114(8) Å, C3-N4 = 1.247(12), C1-Pt1-C3 = 92.3(6)°, Pt1-C3-C2 = 115.4(6)°, Pt1-C3-N4 = 120.3(8)°, C2-C3-N4 = 124.3(9)°, C3-N4-C5 = 125.0(9)°.

Reaction of complex **5a** with HBF_4 in CD_2Cl_2 at -78°C results in protonation of the nitrogen of the iminoacyl generating a cationic Pt(IV) aminocarbene complex (Eq. 10). Recrystallization at -30°C in CH_2Cl_2/pentanes produced a white powder.

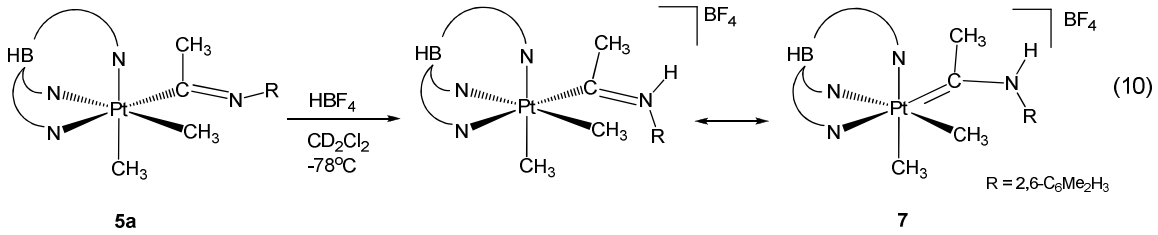

(10)

The cationic aminocarbene complex {Tp′Pt[C(Me)NHR]Me_2}{BF_4}, **7**, displayed characteristic resonances in ^{1}H NMR and ^{13}C NMR spectroscopy. A broad resonance at 11.62 ppm with $^3J_{Pt\text{-}H}$ of 52 Hz is attributed to the N-H. This large three

bond Pt-H coupling suggests that the hydrogen is trans to the metal center. The methyl of the aminocarbene moiety resonance is at 2.09 ppm with $^{3}J_{Pt\text{-}H}$ of 18 Hz and the Pt-Me resonance is at 2.01 ppm with $^{2}J_{Pt\text{-}H}$ of 65 Hz. ^{13}C NMR spectroscopy revealed a significantly downfield shifted resonance at 203.8 ppm with $^{1}J_{Pt\text{-}C}$ of 1039 Hz for the carbon of the carbene. The Pt-Me resonance is upfield at -3.67 ppm with $^{1}J_{Pt\text{-}c}$ of 577 Hz.

Discussion

Reaction of the isonitrile complex **1** with alkyl lithium reagents demonstrates the ease with which the triple bond can be reduced. The ^{13}C shifts of the carbon of the aminocarbene complexes are shifted significantly downfield from the starting isonitrile complex indicative of the carbene character of those complexes, while the iminoacyl complexes only exhibit a modest downfield shift (Table 5.1).

Table 5.1: ^{13}C spectroscopic data for complexes **2** through **7**.

		Pt-*C*N (δ)
ISONITRILE	Tp′Pt(C≡NR)Me, **2**	132.3
AMINOCARBENE	Tp′Pt[C(Me)NHR]Me, **3**	224.5
	Tp′Pt[C(Me)NHR]Cl, **4**	215.6 $^{1}J_{Pt\text{-}C}$ = 1040 Hz
	{Tp′Pt[C(Me)NHR]Me$_2$}{BF$_4$}, **7**	203.8 $^{1}J_{Pt\text{-}C}$ = 1039 Hz
IMINOACYL	Tp′Pt(MeC=NR)Me$_2$, **5a**	158.2 $^{1}J_{Pt\text{-}C}$ = 1050 Hz
	Tp′Pt(MeC=NR)MeI, **6**	145.9 $^{1}J_{Pt\text{-}C}$ = 813 Hz

In addition, X-ray diffraction gives insight into the bonding difference between Pt(II) the starting isonitrile complex, **2**, the Pt(IV) aminocarbene complex, **7**, and the

Pt(IV) iminoacyl complexes, **5** and **6**. The bond distance between the platinum and the carbon of the isonitrile in complex **2** is 1.891(3) Å and the C≡N bond distance is 1.150(4) Å. The aminocarbene complex **7** has a platinum carbon bond distance of 1.952(6) Å and a C-N bond distance of 1.307 Å. The increase in C-N bond distance clearly indicates reduction of the isonitrile, however the platinum carbon bond distance is intermediate between the isonitrile and the iminoacyl, which is representative of its carbene nature. In the iminoacyl complexes **5** and **6**, the platinum carbon bond distance is increased to 2.030(8) Å and 2.048(10) Å respectively, which is a significant increase of around 0.15 Å from the starting isonitrile in both cases. The C=N bond distances for complexes **5** and **6** are 1.279(10) Å and 1.247(12) Å respectively. This increase in bond distance is expected for the reduction of the CN bond from a triple bond to a double bond. The iminoacyl bond lengths are shorter than the aminocarbene C-N bond length.

These isonitrile, iminoacyl, and aminocarbene complex are robust; all are stable to chromatography. Conversion from aminocarbene to iminoacyl can be achieved by the addition of *n*BuLi to **3**, which results in deprotonation of the hydrogen at the nitrogen of the aminocarbene moiety. Addition of iodomethane to the putative anionic complex results in formation of the Pt(IV) iminoacyl complex, **5a** (Eq. 11).

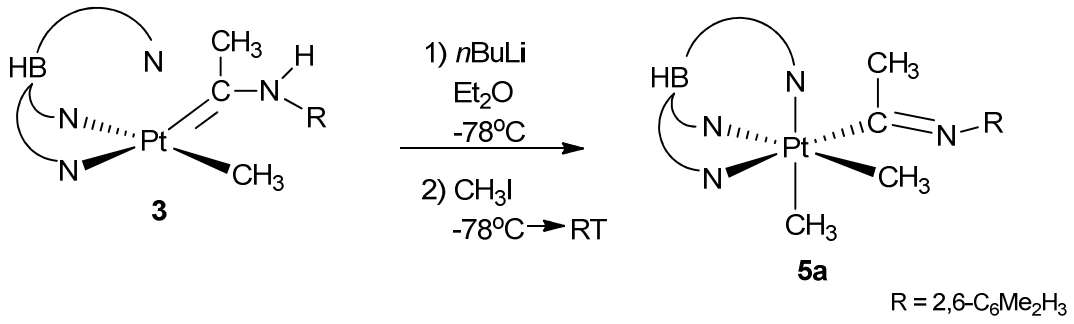

(11)

Similar synthetic routes are used to prepare both the four-coordinate Pt(II) aminocarbene complex and the six-coordinate Pt(IV) iminoacyl complex, with the

difference being the electrophile used, either H^+ or Me^+. After nucleophilic attack of Me^- at the carbon of the isonitrile of the Pt(II) isonitrile complex, the presumed anionic complex can either undergo electrophilic addition at the nitrogen to form an aminocarbene Pt(II) complex, or an electrophile can bind to the metal center and oxidize platinum to Pt(IV). The availability of the third arm of the Tp′ ligand surely facilitates synthesis of the six-coordinate Pt(IV) iminoacyl complex. In order to saturate the valence shell of the Pt(IV) complex, after the electrophile has been added, another ligand is needed. Due to the flexibility of the Tp′ ligand, which has a low energy barrier to both chelation and dechelation of the apical nitrogen, the third arm of the Tp′ ligand is readily available to bind to the metal center and complete the coordination sphere, producing a neutral Pt(IV) complex. The scarcity of Pt(IV) aminocarbene and Pt(IV) iminoacyl complexes may reflect the balance required to add an electrophile to Pt(II) in the presence of a readily available donor ligand. Without a ligand system with a lone pair of electrons that can rapidly bind to the metal center, an additional ligand must be brought in to fill the vacant site of a five-coordinate Pt(IV) intermediate. Here the unique reactivity of Tp′, with its lone pair of electrons at the free pyrazole nitrogen, provides access to rare Pt(IV) products.

Conclusion

A four-coordinate Pt(II) isonitrile complex has been synthesized. Reaction of this complex with methyl lithium followed by addition of acid produces a neutral Pt(II) aminocarbene complex. However, reaction of **2** with methyl lithium followed by addition of methyl iodide results in a six-coordinate Pt(IV) iminoacyl complex. We

postulate that the availability of the third arm of the Tp′ ligand to bind to the metal center along with the nature of the electrophile are the features that provide access to rare Pt(IV) iminoacyl complexes here. More importantly, the Pt(IV) iminoacyl complex is susceptible to protonation at the nitrogen to generate a rare Pt(IV) aminocarbene complex.

Acknowledgements

We thank the National Science Foundation (CHE-0717086) for financial support, David Harris for NMR assistance, and Sohrab Habibi for MS.

Experimental

General Information. Reactions were performed under a dry nitrogen atmosphere using standard Schlenk techniques. Methylene chloride, diethyl ether, hexanes, and pentane were purified by passage through an activated alumina column under a dry argon atmosphere. THF was distilled from a sodium ketal suspension. Methylene chloride-d_2 was dried over CaH_2 and degassed. All other reagents were purchased from commercial sources and were used without further purification.

Tp′$PtMe_2H$ (**1**) was synthesized according to a known procedure.[30] NMR spectra were recorded on Bruker DRX500, DRX400, AMX400, or AMX300 spectrometers. Infrared spectra were recorded on an ASI Applied Systems React IR 1000 FT-IR spectrometer. Elemental analysis was performed by Robertson Microlit. High resolution mass spectra were recorded on a Bruker apex-Qe equipped with an Apollo electrospray

ionization (ESI) source. Mass spectral data are reported for the most abundant platinum isotope.

Synthesis of Tp′Pt(C≡NR)Me, 2: Fluoroboric acid (60 μL, 0.51 mmol) was added to a solution of Tp′PtMe$_2$H (200 mg, 0.38 mmol) in 20 mL CH_2Cl_2 at -78°C in a 100 mL Schlenk flask. The solution was allowed to stir for 1 minute and then cannula transferred into a flask containing 2,6-dimethylphenyl isonitrile (68 mg, 0.52 mmol). The solution was allowed to warm up to room temperature and then stirred for 30 minutes. The solution was cooled to -78°C and triethylamine (70 μL, 0.50 mmol) was added. The solution was brought up to room temperature and the solvent was removed *in vacuo*. Chromatography on alumina with 1:3 THF:CH_2Cl_2 resulted in an off white powder (yield: 156 mg, 0.24 mmol, 64%). NMR: ^{1}H (400 MHz, CD_2Cl_2, 298 K), δ 7.21 (t, 1H, *p*-Ph, 8 Hz), 7.12 (d, 2H, *m*-Ph, 8 Hz), 5.90 (s, 1H, Tp′ CH), 5.81 (s, 2H, Tp′ CH), 2.39, 2.30 (s, 3H each, Tp′ CH_3), 2.32, 2.22 (s, 6H each, Tp′ CH_3), 2.01 (s, 6H, Ph-CH_3), 0.62 (s, 3H, Pt-Me, $^2J_{Pt\text{-}H}$ = 77 Hz); ^{13}C (125 MHz, $CDCl_3$, 298 K) δ 148.2, 148.1, 145.5, 144.3 (Tp′ *C*CH_3), 134.8 (N-Ph), 132.9 (*C*≡N), 128.5, 128.0 (Ph), 106.2, 105.7 (Tp′ CH), 18.7 (Ph-*C*H_3), 15.0, 14.2, 13.3, 12.5 (Tp′ CH_3), -23.3 (Pt-Me, $^1J_{Pt\text{-}C}$ = 591 Hz); Anal. Calc for $C_{25}H_{34}BN_7Pt$: C 47.03, H 5.37, N 15.36. Found: C 47.31, H 5.37, N 15.09.

Synthesis of Tp′Pt[C(CH$_3$)NHR]Me, 3: In an NMR tube, methyl lithium (40 μL, 0.06 mmol) was added to a solution of Tp′Pt(C≡NR)Me (30 mg, 0.047 mmol), **2**, in 500 μL diethyl ether at -78°C. After a 1 minute delay, HBF_4 (8 μL, 0.068 mmol) was added. Chromatography on alumina with CH_2Cl_2 yielded a white powder (yield: 20 mg, 0.031 mmol, 60%). NMR: ^{1}H (400 MHz, $CDCl_3$, 298 K), δ 11.11 (s, 1H, N*H*, $^3J_{Pt\text{-}H}$ = 44 Hz), 7.14 (t, 1H, *p*-Ph, 8 Hz), 7.04 (m, 2H, *m*-Ph, 8 Hz), 5.86 (s, 2H, Tp′CH), 5.76 (s, 1H, Tp′

CH), 2.41, 2.40, 2.38, 1.98 (s, 3H each, Tp′ CH_3), 2.02 (s, 6H, Tp′CH_3), 2.11 (s, 3H, CH_3C=N, $^3J_{Pt-H}$ = 13 Hz), 1.65, 1.63 (s, 3H each, Ph-CH_3), 0.26 (s, 3H, Pt-Me, $^2J_{Pt-H}$ = 86 Hz). ^{13}C (125 MHz, $CDCl_3$, 298 K) δ 224.5 (*C*=N), 149.8, 147.9, 147.6, 145.9, 144.8, 144.5 (Tp′ *C*CH_3), 137.6, 133.8, 133.7, 128.4, 128.3, 128.2, 128.1 (Ph), 106.4, 105.9, 104.9 (Tp′ CH), 30.0 (*C*H_3C=N, $^2J_{Pt-H}$ = 135 Hz), 17.9, 17.3 (Ph-*C*H_3), 15.2, 13.6, 13.4, 12.9, 12.8, 11.3 (Tp′ CH_3), -23.3 (Pt-Me, $^1J_{Pt-C}$ = 756 Hz); Anal. Calc for $C_{27}H_{40}BN_7Pt$: C 48.51, H 6.03, N 14.67. Found: C 48.37, H 5.81, N 14.04.

Synthesis of Tp′Pt[C(CH$_3$)NHR]Cl, 4: In an NMR tube, methyl lithium (40 μL, 0.064 mmol) was added to a solution of Tp′Pt(C≡NR)Me (30 mg, 0.047 mmol), in 500 μL diethyl ether at -78°C. After a 5 minute delay, HBF_4 (50 μL, 0.43 mmol) was added. Chromatography on alumina with 1:3 THF:CH_2Cl_2 yielded a white powder (yield: 15 mg, 0.022 mmol, 44%). NMR: ^{1}H (400 MHz, $CDCl_3$, 298 K), δ 11.61 (s, 1H, N*H*,), 7.16 (t, 1H, *p*-Ph, 8 Hz), 7.05 (m, 2H, *m*-Ph, 8 Hz), 5.89 (s, 1H, Tp′ CH), 5.83 (s, 2H, Tp′CH), 2.51, 2.33, 1.98, 1.94, 1.75, 1.63 (s, 3H each, Tp′ CH_3, Ph-CH_3), 2.41 (s, 6H, Tp′CH_3), 2.12 (s, 3H, CH_3C=N,). ^{13}C (125 MHz, $CDCl_3$, 298 K) δ 215.6 (*C*=N, $^1J_{Pt-C}$ = 1040 Hz), 151.2, 148.9, 148.7, 146.2, 145.9, 145.6 (Tp′ *C*CH_3), 136.5, 134.1, 133.4, 128.7, 128.6, 128.5, 128.4 (Ph), 106.9, 106.5, 105.7 (Tp′ CH), 29.7 (*C*H_3C=N), 17.8, 17.1 (Ph-*C*H_3), 15.2, 13.9, 13.4, 13.2, 13.0, 12.8, 11.6 (Tp′CH_3). HRMS (ESI) *m/z* Calc: 675.25 (M + H^+), 639.26 (M - Cl^-). Anal. Calc for $C_{25}H_{35}BN_7PtCl \bullet C_5H_{12}$: C 48.23, H 6.35, N 13.12. Found: C 48.00, H 5.93, N 14.05.

Synthesis of Tp′Pt(C(CH$_3$)=NR)Me$_2$, 5a: Methyl lithium (40 μL, 0.064mmol) was added to a solution of Tp′Pt(C≡NR)Me (30 mg, 0.047 mmol), **2**, in 10 mL diethyl ether at -78°C. The solution was brought up to room temperature and stirred for 5 minutes. The

solution was cooled to -78°C and iodomethane (5 μL, 0.079 mmol) was added. The solvent was removed *in vacuo*. Chromatography on alumina with 1:3 THF:CH_2Cl_2 yielded a white powder (yield: 19 mg, 0.028 mmo, 47%). NMR: ^{1}H (300 MHz, $CDCl_3$, 298 K), δ 6.98 (d, 2H, *m*-Ph, 7 Hz), 6.83 (t, 1H, *o*-Ph, 7 Hz), 5.85 (s, 2H, Tp′ CH), 5.78 (s, 1H, Tp′ CH), 2.45, 2.33 (s, 6H each, Tp′ CH_3), 2.43, 2.39 (s, 3H each, Tp′ CH_3), 2.29 (s, 6H, Ph-CH_3), 1.80 (s, 6H, Pt-Me, $^2J_{Pt\text{-}H}$ = 73 Hz), 1.71 (s, 3H, CH_3C=N, $^3J_{Pt\text{-}H}$ = 17 Hz); ^{13}C (125 MHz, $CDCl_3$, 298 K) δ 158.2 (*C*=N, $^1J_{Pt\text{-}C}$ = 1044 Hz), 150.4, 148.7, 143.9, 143.5 (Tp′ *C*CH_3), 128.1, 126.5, 121.7 (Ph), 108.1, 107.7 (Tp′ CH), 28.0 (*C*H_3C=N, $^2J_{Pt\text{-}H}$ = 61 Hz), 19.1 (Ph-*C*H_3), 14.9, 13.3, 13.1, 12.7 (Tp′ CH_3), -3.0 (Pt-Me, $^1J_{Pt\text{-}C}$ = 693 Hz); Anal. Calc for $C_{27}H_{40}BN_7Pt$ • ½ C_5H_{12} • ½ CH_2Cl_2: C 48.22, H 6.35, N 13.13. Found: C 48.14, H 5.92, N 13.35.

Synthesis of Tp′Pt(C(CH_2CH_3)=NR)Me_2, 5b: Ethyl lithium (35 μL, 0.056mmol) was added to a solution of Tp′Pt(C≡NR)Me (30 mg, 0.047 mmol), **2**, in 500 μL diethyl ether at -78°C in an NMR tube. The solution was brought up to room temperature and stirred for 5 minutes. The solution was cooled to -78°C and iodomethane (5 μL, 0.079 mmol) was added. The solvent was removed *in vacuo*. Chromatography on alumina with CH_2Cl_2 yielded a white powder (13 mg, 0.019 mmol, 33%). NMR: ^{1}H (300 MHz, $CDCl_3$, 298 K), δ 6.91 (d, 2H, *m*-Ph, 8 Hz), 6.72 (t, 1H, *p*-Ph, 7 Hz), 5.89 (s, 2H, Tp′ CH), 5.79 (s, 1H, Tp′ CH), 2.43, (s, 6H, Tp′ CH_3), 2.36 (s, 9H, Tp′ CH_3), 2.28 (s, 3H, Tp′ CH_3), 2.24 (s, 6H, Ph-CH_3), 1.71 (s, 6H, Pt-Me, $^2J_{Pt\text{-}H}$ = 74 Hz), 0.34 (t, 3H, CH_2CH_3, 8 Hz); Anal. Calc for $C_{28}H_{42}BN_7Pt$ • C_5H_{12} • ½ CH_2Cl_2: C 50.47, H 6.97, N 12.29. Found: C 50.22, H 6.25, N 12.69.

Synthesis of Tp′Pt(C(CH_3)=NR)MeI, 6: Methyl lithium (40 μL, 0.064 mmol) was added to a solution of Tp′Pt(C≡NR)Me (30 mg, 0.047 mmol), **2**, in 500 μL THF at -78°C in an NMR tube. The solution was allowed to warm to room temperature and stirred for 5 minutes. The solution was cooled to -78°C and iodomethane (5 μL, 0.079 mmol) was added. The solvent was removed *in vacuo*. Chromatography on alumina with CH_2Cl_2 yielded a yellow powder (yield: 14 mg, 0.018 mmol, 30%). NMR: ^{1}H (300 MHz, $CDCl_3$, 298 K), δ 6.95 (m, 2H, *m*-Ph), 6.80 (t, 1H, *p*-Ph, 7 Hz), 5.89, 5.83, 5.80 (s, 1H each, Tp′ CH), 2.73 (s, 3H, Pt-Me, $^2J_{Pt\text{-}H}$ = 73 Hz), 2.64, 2.61, 2.45, 2.41, 2.40, 2.37 (s, 3H each, Tp′ CH_3), 2.44, 2.28 (s, 3H each, Ph-*C*H_3), 1.61 (s, 3H, C*H*$_3$C=N, $^3J_{Pt\text{-}H}$ = 14 Hz); ^{13}C (125 MHz, $CDCl_3$, 298 K) δ 152.8, 151.2, 148.5, 148.4, 144.3, 144.0 (Tp′ *C*CH_3), 145.9 (*C*=N, $^1J_{Pt\text{-}C}$ = 813 Hz), 143.8, 128.2, 127.0, 126.5, 122.2 (Ph), 108.6, 108.1, 107.8 (Tp′ CH), 27.8 (*C*H_3C=N, $^2J_{Pt\text{-}H}$ = 44 Hz), 19.8, 19.4 (Ph-*C*H_3), 18.5, 15.7, 14.9, 13.4, 12.9, 12.7 (Tp′ CH_3), -3.3 (Pt-Me, $^1J_{Pt\text{-}C}$ = 533 Hz); Anal. Calc for $C_{26}H_{37}BN_7IPt$: C 40.01, H 4.78, N 12.56. Found: C 40.70, H 4.34, N 12.11.

Synthesis of {Tp′Pt[C(CH_3)NHR]Me_2}{BF_4}, 7: HBF_4 (3 μL, 0.026 mmol) was added to a solution of **5a** (10 mg, 0.015 mmol) in 500 μL CD_2Cl_2 at -78°C. The solution was allowed to warm to room temperature and stirred for 5 minutes. Chromatography on alumina with 1:3 THF:CH_2Cl_2 yielded an off white powder (yield: 6 mg, 0.014 mmol, 53%). NMR: ^{1}H (500 MHz, $CDCl_3$, 298 K), δ 11.62 (s, 1H, N-H, $^3J_{Pt\text{-}H}$ = 52 Hz), 7.24 (t, 1H, *p*-Ph), 7.13 (d, 2H, *m*-Ph, 8 Hz), 5.89 (s, 2H, Tp′ CH), 5.84 (s, 1H, Tp′ CH), 2.40 (s, 9H, Tp′ CH_3), 2.39, 2.36 (s, 3H each, Tp′ CH_3), 2.19 (s, 6H, Ph-C*H*$_3$), 2.11 (s, 3H, C*H*$_3$C=N, $^3J_{Pt\text{-}H}$ = 18 Hz), 2.01 (s, 6H, Pt-Me, $^2J_{Pt\text{-}H}$ = 65 Hz); ^{13}C (125 MHz, $CDCl_3$, 298 K) δ 203.8 (*C*=N, $^1J_{Pt\text{-}C}$ = 1039 Hz), 151.3, 148.3, 144.9, 144.5 (Tp′ *C*CH_3), 136.1, 133.5,

129.7, 129.6 (Ph), 109.3, 108.0 (Tp′ CH), 30.6 (*C*H_3C=N, $^2J_{Pt\text{-}H}$ = 22 Hz), 18.7 (Ph-*C*H_3), 14.9, 13.5, 12.9 (Tp′ CH_3), -3.7 (Pt-Me, $^1J_{Pt\text{-}C}$ = 577 Hz); Anal. Calc for $C_{27}H_{41}B_2N_7F_4Pt$ • ½ CH_2Cl_2: C 41.34, H 5.31, N 12.28. Found: C 41.54, H 5.20, N 12.27.

Table 5.2. Crystal and Data Collection Parameters for Tp′Pt(C≡NR)Me, Tp′Pt(MeC=NHR)Cl, Tp′Pt(MeC=NR)Me_2, and Tp′Pt(MeC=NR)MeI.

EMPIRICAL FORMULA	$C_{25}H_{34}BN_7Pt$	$C_{25}H_{35}BClN_7Pt$	$C_{27}H_{40}BN_7Pt$	$C_{26}H_{37}BIN_7Pt$
Complex	**2**	**4**	**5a**	**6**
Mol wt	638.47	674.93	668.54	780.41
Color	Colorless	Colorless	Yellow	Yellow
Temperature	100 K	100(2) K	100(2) K	100(2) K
Wavelength	1.54178 Å	1.54178 Å	1.54178 Å	1.54178 Å
Cryst Syst	Monoclinic	Monoclinic	Triclinic	Triclinic
Space Group	*P*1 21/n1	*C*1c1	*P*-1	*P*-1
a, Å	10.9514(2)	12.6745(50	10.9293(3)	11.0982(9)
b, Å	19.4849(5)	24.5151(11)	11.9574(3)	11.9831(9)
c, Å	12.2946(2)	9.8781(5)	22.0161(6)	12.5360(8)
α, deg	90	90	78.747(2)	86.822(5)
β, deg	93.8260(10)	119.460(2)	83.337(2)	75.098(5)
γ, deg	90	90	78.822(2)	76.798(5)
Vol. $Å^3$	2617.73(73)	2672.4(2)	2759.19(13)	1.568(2)
Z	4	4	4	2
Density (calculated)	1.620 Mg/cm^3	1.675 Mg/cm^3	1.609 Mg/m^3	1.832 Mg/cm^3
μ, mm^{-1}	10.226	10.951	9.728	17.888
F(000)	1264	1332	1336	840
Crystal size	0.05 x 0.10 x 0.10 mm^3	0.09 x 0.18 x 0.26 mm^3	0.15 x 0.10 x 0.02 mm^3	0.06 x 0.11 x 0.15 mm^3
2θ range	4.26 to 69.74°	3.61 to 66.59°	2.05 to 66.5°	4.23 to 66.50°
Index Ranges	-13<=h<=12 -23<=k<=21 -14<=l<=14	-15<=h<=15 -29<=k<=29 -11<=l<=11	-12<=h<=12 -14<=k<=14 -25<=l<=26	-11<=h<=12 -14<=k<=14 -14<=l<=14
Reflections Collected	25542	10350	19664	12151
Independent reflections	4844 [R(int) = 0.0327]	4127 [R(int) = 0.0229]	8967 [R(int) = 0.0606]	5141 [R(int) = 0.0510]
Data/restraints/parameters	4844/0/316	4127/2/325	88084/0/252	5141/36/403
Goodness-of-fit on F^2	1.065	1.028	1.035	1.088
Final R indices[I>2sigma(I)]	R1 = 0.0229 wR2 = 0.0550	R1 = 0.0180 wR2 = 0.0448	R1 = 0.0490 wR2 = 0.0985	R1 = 0.0525 wR2 = 0.1176
R indices (all data)	R1 = 0.0262 wR2 = 0.0564	R1 = 0.0182 wR2 = 0.0450	R1 = 0.0735 wR2 = 0.1061	R1 = 0.0612 wR2 = 0.1216
Largest diff. peak and hole	0.859 and -0.616 e $Å^{-3}$	0.762 and -0.794 e $Å^{-3}$	1.207 and -1.786 e $Å^{-3}$	3.168 and -1.460 e $Å^{-3}$

References

(1) Michelin, R. A.; Pombeiro, A. J. L.; Fatima, M.; da Silva, C. G. *Coord. Chem. Rev.* 2001, *218*, 75.

(2) Pombeiro, A. J. L.; da Silva, M.; Michelin, R. A. *Coord. Chem. Rev.* 2001, *218*, 43.

(3) Tamm, M.; Ekkehardt, H. F. *Coord. Chem. Rev.* 1999, *182*, 175.

(4) Singleton, E.; Oosthuizen, H. E. *Adv. Organomet. Chem.* 1983, *22*, 209.

(5) Treichel, P. M. *Adv. Organomet. Chem.* 1973, *1*, 21.

(6) Jovanovic, B.; Manojlovic-Muir, L.; Muir, K. W. *J. Organomet. Chem.* 1971, *33*, C75.

(7) Clark, H. C.; Manzer, L. E. *Inorg. Chem.* 1972, *11*, 503.

(8) Treichel, P. M.; Knebel, W. J. *Inorg. Chem.* 1972, *11*, 1285.

(9) Canovese, L.; Visentin, F.; Uguagliati, P.; Crociani, B. *J. Organomet. Chem.* 1997, *543*, 145.

(10) Canovese, L.; Visentin, F.; Uguagliati, P.; Crociani, B.; DiBianca, F. *J. Organomet. Chem.* 1997, *535*, 69.

(11) Cross, R. J.; Davidson, M. F.; Rocamora, M. *J. Chem. Soc.-Dalton Trans.* 1988, 1147.

(12) Balch, A. L. *J. Organomet. Chem.* 1972, *37*, C19.

(13) Rendina, L. M.; Vittal, J. J.; Puddephatt, R. J. *Organometallics* 1995, *14*, 1030.

(14) Zhang, S. W.; Takahashi, S. *Organometallics* 1998, *17*, 4757.

(15) Bertani, R.; Mozzon, M.; Michelin, R. A.; Benetollo, F.; Bombieri, G.; Castilho, T. J.; Pombeiro, A. J. L. *Inorg. Chim. Acta* 1991, *189*, 175.

(16) Durfee, L. D.; Rothwell, I. P. *Chem. Rev.* 1988, *88*, 1059.

(17) Adams, R. D.; Chodosh, D. F. *J. Am. Chem. Soc.* 1977, *99*, 6544.

(18) Adams, R. D.; Chodosh, D. F.; Golembeski, N. M. *J. Organomet. Chem.* 1977, *139*, C39.

(19) Adams, R. D.; Chodosh, D. F.; Golembeski, N. M.; Weissman, E. C. *J. Organomet. Chem.* 1979, *174*, 251.

(20) Garnovskii, D. A.; da Silva, M.; Pakhomova, T. B.; Wagner, G.; Duarte, M. T.; da Silva, J.; Pombeiro, A. J. L.; Kukushkin, V. Y. *Inorg. Chim. Acta* 2000, *300*, 499.

(21) Kukushkin, V. Y.; Pakhomova, T. B.; Bokach, N. A.; Wagner, G.; Kuznetsov, M. L.; Galanski, M.; Pombeiro, A. J. L. *Inorg. Chem.* 2000, *39*, 216.

(22) Wagner, G.; Pombeiro, A. J. L.; Kukushkin, Y. N.; Pakhomova, T. B.; Ryabov, A. D.; Kukushkin, V. Y. *Inorg. Chim. Acta* 1999, *295*, 253.

(23) Wagner, G.; Pombeiro, A. J. L.; Kukushkin, Y. N.; Pakhomova, T. B.; Ryabov, A. D.; Kukushkin, V. Y. *Inorg. Chim. Acta* 1999, *292*, 272.

(24) Kukushkin, V. Y.; Pakhomova, T. B.; Kukushkin, Y. N.; Herrmann, R.; Wagner, G.; Pombeiro, A. J. L. *Inorg. Chem.* 1998, *37*, 6511.

(25) Gamble, A. S.; White, P. S.; Templeton, J. L. *Organometallics* 1991, *10*, 693.

(26) Carmona, E.; Palma, P.; Poveda, M. L. *Polyhedron* 1990, *9*, 1447.

(27) Bianchini, C.; Masi, D.; Romerosa, A.; Zanobini, F.; Peruzzini, M. *Organometallics* 1999, *18*, 2376.

(28) Reinartz, S.; White, P. S.; Brookhart, M.; Templeton, J. L. *Organometallics* 2000, *19*, 3854.

(29) Engelman, K. L.; White, P. S.; Templeton, J. L. *Inorg. Chim. Acta* 2009, *362*, 4461.

(30) O'Reilly, S. A.; White, P. S.; Templeton, J. L. *J. Am. Chem. Soc.* 1996, *118*, 5684.

(31) Reinartz, S.; Brookhart, M.; Templeton, J. L. *Organometallics* 2002, *21*, 247.

(32) West, N. M.; Reinartz, S.; White, P. S.; Templeton, J. L. *J. Am. Chem. Soc.* 2006, *128*, 2059.

(33) Akita, M.; Ohta, K.; Takahashi, Y.; Hikichi, S.; Morooka, Y. *Organometallics* 1997, *16*, 4121.

APPENDIX A

Atomic coordinates (x 10^4) and equivalent isotropic displacement parameters ($Å^2$x 10^3) for Tp′Pt(HC≡CPh)(Me) (Chapter 2, **2e**). U(eq) is defined as one third of the trace of the orthogonalized U^{ij} tensor.

	x	y	z	U(eq)
Pt(1)	7141(1)	3328(1)	9358(1)	20(1)
C(1)	6302(9)	2872(3)	10137(13)	32(2)
C(2)	8105(8)	2929(3)	8513(12)	27(2)
C(3)	8636(7)	3017(3)	10099(12)	25(2)
C(4)	9615(7)	2983(3)	11655(12)	24(2)
C(5)	9926(7)	3277(3)	12876(12)	29(2)
C(6)	10949(8)	3247(3)	14245(13)	36(2)
C(7)	11609(8)	2927(3)	14428(14)	37(2)
C(8)	11288(9)	2626(3)	13218(14)	40(3)
C(9)	10305(8)	2647(3)	11845(14)	33(2)
N(11)	7948(6)	3849(2)	8549(9)	25(2)
N(12)	7302(6)	4182(2)	8382(9)	22(2)
C(13)	7898(8)	4471(3)	7871(12)	25(2)
C(14)	8904(8)	4323(3)	7714(13)	33(2)
C(15)	8915(7)	3937(3)	8140(11)	21(2)
C(16)	7441(9)	4869(3)	7561(14)	39(2)
C(17)	9853(8)	3647(3)	8122(13)	31(2)
N(18)	5557(5)	3529(2)	7521(9)	21(2)
N(19)	5292(6)	3918(2)	7520(9)	21(2)
C(20)	4291(7)	3978(3)	6246(11)	24(2)
C(21)	3922(8)	3634(3)	5419(12)	27(2)
C(22)	4743(7)	3360(3)	6271(11)	24(2)
C(23)	3760(9)	4374(3)	5899(12)	31(2)
C(24)	4756(8)	2943(3)	5868(13)	32(2)
N(25)	6689(6)	3706(2)	11307(9)	17(1)
N(26)	6260(6)	4065(2)	10768(9)	20(2)
C(27)	6038(8)	4252(3)	12162(12)	25(2)
C(28)	6340(8)	4019(3)	13644(11)	24(2)
C(29)	6763(7)	3678(3)	13051(12)	24(2)
C(30)	5554(9)	4649(3)	12025(13)	30(2)
C(31)	7203(8)	3319(3)	14128(11)	35(2)
B(32)	6121(8)	4198(3)	8795(12)	20(2)
C(33)	3719(9)	3638(3)	471(16)	43(3)
Cl(1)	2894(3)	4054(1)	361(5)	59(1)

Cl(2)	2919(3)	3222(1)	654(4)	50(1)
C(34)	960(9)	5621(3)	7183(16)	45(3)
Cl(3)	-498(2)	5692(1)	6226(5)	57(1)
Cl(4)	1335(3)	5128(1)	7183(5)	58(1)

Bond lengths [Å] and angles [°] for Tp′Pt(HC≡CPh)(Me) (Chapter 2, **2e**).

Pt(1)-C(2)	2.032(9)	C(16)-H(16B)	0.9800
Pt(1)-C(3)	2.061(8)	C(16)-H(16C)	0.9800
Pt(1)-C(1)	2.062(10)	C(17)-H(17A)	0.9800
Pt(1)-N(25)	2.175(6)	C(17)-H(17B)	0.9800
Pt(1)-N(18)	2.181(6)	C(17)-H(17C)	0.9800
Pt(1)-N(11)	2.227(8)	N(18)-C(22)	1.324(11)
C(1)-H(1A)	0.9800	N(18)-N(19)	1.397(10)
C(1)-H(1B)	0.9800	N(19)-C(20)	1.363(11)
C(1)-H(1C)	0.9800	N(19)-B(32)	1.553(12)
C(2)-C(3)	1.263(13)	C(20)-C(21)	1.377(13)
C(2)-H(2)	0.9500	C(20)-C(23)	1.520(12)
C(3)-C(4)	1.456(12)	C(21)-C(22)	1.411(13)
C(4)-C(5)	1.377(13)	C(21)-H(21)	0.9500
C(4)-C(9)	1.424(12)	C(22)-C(24)	1.489(13)
C(5)-C(6)	1.407(13)	C(23)-H(23A)	0.9800
C(5)-H(5)	0.9500	C(23)-H(23B)	0.9800
C(6)-C(7)	1.357(15)	C(23)-H(23C)	0.9800
C(6)-H(6)	0.9500	C(24)-H(24A)	0.9800
C(7)-C(8)	1.391(16)	C(24)-H(24B)	0.9800
C(7)-H(7)	0.9500	C(24)-H(24C)	0.9800
C(8)-C(9)	1.375(14)	N(25)-C(29)	1.330(11)
C(8)-H(8)	0.9500	N(25)-N(26)	1.377(9)
C(9)-H(9)	0.9500	N(26)-C(27)	1.345(11)
N(11)-C(15)	1.327(11)	N(26)-B(32)	1.559(11)
N(11)-N(12)	1.389(10)	C(27)-C(28)	1.374(12)
N(12)-C(13)	1.358(12)	C(27)-C(30)	1.497(13)
N(12)-B(32)	1.546(12)	C(28)-C(29)	1.417(13)
C(13)-C(14)	1.359(13)	C(28)-H(28)	0.9500
C(13)-C(16)	1.489(14)	C(29)-C(31)	1.520(13)
C(14)-C(15)	1.383(14)	C(30)-H(30A)	0.9800
C(14)-H(14)	0.9500	C(30)-H(30B)	0.9800
C(15)-C(17)	1.524(12)	C(30)-H(30C)	0.9800
C(16)-H(16A)	0.9800	C(31)-H(31A)	0.9800

C(31)-H(31B)	0.9800
C(31)-H(31C)	0.9800
B(32)-H(32)	1.0000
C(33)-Cl(1)	1.750(12)
C(33)-Cl(2)	1.772(11)
C(33)-H(33A)	0.9900
C(33)-H(33B)	0.9900
C(34)-Cl(3)	1.744(11)
C(34)-Cl(4)	1.779(12)
C(34)-H(34A)	0.9900
C(34)-H(34B)	0.9900

APPENDIX B

Atomic coordinates (x 10^4) and equivalent isotropic displacement parameters ($Å^2$x 10^3) for Tp′Pt(C≡N(2,6-$C_6Me_2H_3$))(Me) (Chapter 5, **2**). U(eq) is defined as one third of the trace of the orthogonalized U^{ij} tensor.

	x/a	y/b	z/c	U(eq)
Pt1	0.032325(11)	0.290048(7)	0.586364(10)	0.01495(5)
C1	0.9799(2)	0.3095(2)	0.4264(2)	0.0217(7)
C2	0.9768(2)	0.19940(17)	0.5590(2)	0.0172(7)
N3	0.9371(2)	0.14562(14)	0.5411(2)	0.0196(5)
C4	0.8862(2)	0.08041(17)	0.5229(2)	0.0181(7)
C5	0.8533(2)	0.06037(18)	0.4160(2)	0.0196(7)
C6	0.8032(2)	0.9953(2)	0.4012(2)	0.0232(7)
C7	0.7858(2)	0.9532(2)	0.4890(2)	0.0269(8)
C8	0.8175(2)	0.9744(2)	0.5944(2)	0.0263(8)
C9	0.8697(2)	0.03897(18)	0.6138(2)	0.0216(7)
C10	0.8717(2)	0.1070(2)	0.3209(2)	0.0262(8)
C11	0.9053(4)	0.0628(2)	0.7275(2)	0.0317(9)
B12	0.9635(2)	0.3859(2)	0.7859(2)	0.0198(8)
N13	0.0799(2)	0.39145(13)	0.6135(2)	0.0168(5)
N14	0.0293(2)	0.42511(13)	0.6981(2)	0.0163(5)
C15	0.0565(2)	0.49244(17)	0.6938(2)	0.0176(7)
C16	0.1279(2)	0.50236(18)	0.6065(2)	0.0191(7)
C17	0.1410(2)	0.43838(18)	0.5587(2)	0.0184(7)
C18	0.0118(2)	0.54234(17)	0.7744(2)	0.0199(7)
C19	0.2145(2)	0.4209(2)	0.4647(2)	0.0243(7)
N20	0.0813(2)	0.27653(13)	0.7528(2)	0.0175(5)
N21	0.0454(2)	0.32525(14)	0.8254(2)	0.0173(5)
C22	0.0954(2)	0.3097(2)	0.9262(2)	0.0215(7)
C23	0.1636(2)	0.2507(2)	0.9188(2)	0.0232(7)
C24	0.1531(2)	0.23166(18)	0.8088(2)	0.0196(7)
C25	0.0753(2)	0.3518(2)	0.0245(2)	0.0270(8)
C26	0.2111(2)	0.1731(2)	0.7526(2)	0.0262(8)
N27	0.7781(2)	0.40014(14)	0.6559(2)	0.0203(5)
N28	0.8384(2)	0.36029(14)	0.7349(2)	0.0192(5)
C29	0.7640(2)	0.3094(2)	0.7666(2)	0.0262(8)
C30	0.6543(2)	0.3154(2)	0.7058(2)	0.0278(8)
C31	0.6669(2)	0.3725(2)	0.6388(2)	0.0243(7)

	x/a	y/b	z/c	U(eq)
C32	0.8019(4)	0.2582(2)	0.8532(4)	0.0424(11)
C33	0.5759(2)	0.4035(2)	0.5561(2)	0.0330(9)

Bond lengths [Å] and angles [°] Tp′Pt(C≡N(2,6-$C_6Me_2H_3$))(Me) (Chapter 5, **2**).

Pt1-C2	1.891(3)	C2-Pt1-C1	86.29(14)
Pt1-N13	2.065(3)	C1-Pt1-N13	91.73(13)
C2-N3	1.150(4)	C1-Pt1-N20	176.20(13)
C4-C5	1.395(5)	N3-C2-Pt1	176.4(3)
C5-C6	1.388(5)	C5-C4-N3	118.7(3)
C6-C7	1.380(5)	N3-C4-C9	117.9(3)
C8-C9	1.396(5)	C6-C5-C10	121.4(3)
B12-N14	1.541(4)	C7-C6-C5	121.0(3)
B12-N28	1.550(5)	C7-C8-C9	120.3(3)
N13-N14	1.377(4)	C8-C9-C11	121.1(3)
C15-C16	1.383(5)	N14-B12-N21	108.1(3)
C16-C17	1.390(5)	N21-B12-N28	111.2(3)
N20-C24	1.336(4)	C17-N13-Pt1	134.5(2)
N21-C22	1.355(4)	C15-N14-N13	109.4(3)
C22-C25	1.489(5)	N13-N14-B12	121.6(3)
C24-C26	1.497(5)	N14-C15-C18	121.6(3)
N27-N28	1.377(4)	C15-C16-C17	106.4(3)
C29-C30	1.377(5)	N13-C17-C19	123.1(3)
C30-C31	1.397(5)	C24-N20-N21	107.5(3)
Pt1-C1	2.047(3)	N21-N20-Pt1	118.7(2)
Pt1-N20	2.097(3)	C22-N21-B12	130.6(3)
N3-C4	1.399(4)	N21-C22-C23	108.3(3)
C4-C9	1.400(5)	C23-C22-C25	128.6(3)
C5-C10	1.505(5)	N20-C24-C23	109.3(3)
C7-C8	1.382(5)	C23-C24-C26	129.6(3)
C9-C11	1.499(5)	C29-N28-N27	110.3(3)
B12-N21	1.542(5)	N27-N28-B12	118.2(3)
N13-C17	1.341(4)	N28-C29-C32	123.3(3)
N14-C15	1.347(4)	C29-C30-C31	105.8(3)
C15-C18	1.494(4)	N27-C31-C33	120.1(3)
C17-C19	1.492(4)	C2-Pt1-N13	175.79(12)
N20-N21	1.378(4)	C2-Pt1-N20	96.57(12)
C22-C23	1.376(5)	N13-Pt1-N20	85.25(11)
C23-C24	1.400(5)	C2-N3-C4	177.8(3)
N27-C31	1.336(4)	C5-C4-C9	123.5(3)
N28-C29	1.357(4)	C6-C5-C4	117.0(3)
C29-C32	1.496(6)	C4-C5-C10	121.6(3)
C31-C33	1.501(5)	C6-C7-C8	121.1(3)
C8-C9-C4	117.2(3)	C4-C9-C11	121.8(3)

N14-B12-N28	108.6(3)
C17-N13-N14	107.1(3)
N14-N13-Pt1	117.9(2)
C15-N14-B12	128.8(3)
N14-C15-C16	107.7(3)
C16-C15-C18	130.6(3)
N13-C17-C16	109.3(3)
C16-C17-C19	127.5(3)
C24-N20-Pt1	133.5(2)
C22-N21-N20	108.8(3)
N20-N21-B12	120.6(3)
N21-C22-C25	123.1(3)
C22-C23-C24	106.0(3)
N20-C24-C26	121.0(3)
C31-N27-N28	105.8(3)
C29-N28-B12	130.5(3)
N28-C29-C30	107.4(3)
C30-C29-C32	129.3(4)
N27-C31-C30	110.6(3)
C30-C31-C33	129.3(3)

APPENDIX C

Atomic coordinates (x 10^4) and equivalent isotropic displacement parameters ($Å^2$x 10^3) for Tp′Pt[C(Me)N(2,6-$C_6Me_2H_3$)H]Cl (Chapter 5, **4**). U(eq) is defined as one third of the trace of the orthogonalized U^{ij} tensor.

	x/a	y/b	z/c	U(eq)
Pt1	0.74980(2)	0.177597(5)	0.25181(2)	0.01276(5)
Cl1	0.71421(11)	0.16484(6)	0.00201(13)	0.0185(2)
C1	0.4780(4)	0.1979(2)	0.0582(5)	0.0225(9)
C2	0.5787(5)	0.1646(2)	0.1822(7)	0.0155(10)
C4	0.4330(2)	0.10060(17)	0.1966(5)	0.0177(8)
C5	0.3779(4)	0.06857(17)	0.0642(5)	0.0188(8)
C6	0.2660(4)	0.0453(2)	0.0237(5)	0.0241(9)
C7	0.2125(4)	0.0533(2)	0.1159(5)	0.0277(10)
C8	0.2700(4)	0.08507(18)	0.2478(7)	0.0226(10)
C9	0.3830(4)	0.10903(18)	0.2930(5)	0.0220(9)
C10	0.4387(4)	0.0575(2)	0.9683(5)	0.0239(9)
C11	0.4460(5)	0.1430(2)	0.4368(5)	0.0328(11)
N12	0.5519(2)	0.12320(13)	0.2431(4)	0.0157(7)
B13	0.9441(4)	0.11175(18)	0.5366(5)	0.0160(9)
N14	0.7864(4)	0.18554(17)	0.4737(5)	0.0157(10)
N15	0.8676(2)	0.14904(13)	0.5816(4)	0.0152(7)
C16	0.8720(4)	0.15870(18)	0.7187(5)	0.0178(8)
C17	0.7940(4)	0.20111(18)	0.6985(5)	0.0202(9)
C18	0.7426(2)	0.21676(18)	0.5435(5)	0.0181(8)
C19	0.9492(4)	0.12669(18)	0.8622(5)	0.0223(9)
C20	0.6565(4)	0.26241(18)	0.4586(5)	0.0233(9)
N21	0.9372(5)	0.18099(14)	0.3403(5)	0.0141(11)
N22	0.0057(2)	0.14863(13)	0.4680(4)	0.0153(7)
C23	0.1236(4)	0.15591(17)	0.5123(5)	0.0186(8)
C24	0.1310(4)	0.19298(18)	0.4114(5)	0.0181(8)
C25	0.0124(2)	0.20817(17)	0.3065(5)	0.0154(8)
C26	0.2240(4)	0.1268(2)	0.6464(5)	0.0248(9)
C27	0.9680(4)	0.24914(17)	0.1787(5)	0.0203(8)
N28	0.7619(2)	0.05040(13)	0.4222(4)	0.0174(7)
N29	0.8598(2)	0.07008(12)	0.4128(4)	0.0158(7)
C30	0.8758(4)	0.04061(18)	0.3084(5)	0.0191(8)
C31	0.7867(4)	0.0011(2)	0.2493(5)	0.0204(10)
C32	0.7197(4)	0.00840(18)	0.3233(5)	0.0170(9)

	x/a	y/b	z/c	U(eq)
C33	0.9732(4)	0.0507(2)	0.2659(5)	0.0272(10)
C34	0.6149(4)	0.97578(18)	0.3089(5)	0.0258(9)

Bond lengths [Å] and angles [°] for Tp′Pt[C(Me)N(2,6-$C_6Me_2H_3$)H]Cl (Chapter 5, **4**).

Pt1-C2	1.952(6)	Pt1-N14	2.014(5)
Pt1-N21	2.090(5)	Pt1-Cl1	2.3011(11)
C1-C2	1.503(7)	C1-H1A	0.98
C1-H1B	0.98	C1-H1C	0.98
C2-N12	1.307(7)	C4-C5	1.384(6)
C4-C9	1.395(6)	C4-N12	1.452(5)
C5-C6	1.392(6)	C5-C10	1.511(6)
C6-C7	1.391(6)	C6-H6	0.95
C7-C8	1.379(8)	C7-H7	0.95
C8-C9	1.402(6)	C8-H8	0.95
C9-C11	1.494(7)	C10-H10A	0.98
C10-H10B	0.98	C10-H10C	0.98
C11-H11A	0.98	C11-H11B	0.98
C11-H11C	0.98	B13-N29	1.548(6)
B13-N15	1.549(5)	B13-N22	1.552(5)
B13-H13	1.0	N14-C18	1.321(6)
N14-N15	1.385(6)	N15-C16	1.348(5)
C16-C17	1.380(6)	C16-C19	1.489(6)
C17-C18	1.391(6)	C17-H17	0.95
C18-C20	1.499(6)	C19-H19A	0.98
C19-H19B	0.98	C19-H19C	0.98
C20-H20A	0.98	C20-H20B	0.98
C20-H20C	0.98	N21-C25	1.333(6)
N21-N22	1.377(6)	N22-C23	1.346(5)
C23-C24	1.385(6)	C23-C26	1.492(6)
C24-C25	1.393(6)	C24-H24	0.95
C25-C27	1.490(6)	C26-H26A	0.98
C26-H26B	0.98	C26-H26C	0.98
C27-H27A	0.98	C27-H27B	0.98
C27-H27C	0.98	N28-C32	1.336(6)
N28-N29	1.376(4)	N29-C30	1.353(6)
C30-C31	1.380(7)	C30-C33	1.507(5)
C31-C32	1.378(7)	C31-H31	0.95
C32-C34	1.497(6)	C33-H33A	0.98
C33-H33B	0.98	C33-H33C	0.98
C34-H34A	0.98	C34-H34B	0.98
C34-H34C	0.98	C2-Pt1-N21	172.2(2)
C2-Pt1-N14	91.2(2)	C2-Pt1-Cl1	90.12(17)
N14-Pt1-N21	86.3(2)	N21-Pt1-Cl1	92.12(15)

N14-Pt1-Cl1	177.18(15)	C2-C1-H1B	109.5
C2-C1-H1A	109.5	C2-C1-H1C	109.5
H1A-C1-H1B	109.5	H1B-C1-H1C	109.5
H1A-C1-H1C	109.5	N12-C2-Pt1	117.4(4)
N12-C2-C1	119.3(5)	C5-C4-C9	122.8(4)
C1-C2-Pt1	123.3(4)	C9-C4-N12	118.5(4)
C5-C4-N12	118.6(3)	C4-C5-C10	121.2(4)
C4-C5-C6	118.3(4)	C7-C6-C5	120.6(4)
C6-C5-C10	120.5(4)	C5-C6-H6	119.7
C7-C6-H6	119.7	C8-C7-H7	120.1
C8-C7-C6	119.8(4)	C7-C8-C9	121.3(4)
C6-C7-H7	120.1	C9-C8-H8	119.3
C7-C8-H8	119.3	C4-C9-C11	121.4(4)
C4-C9-C8	117.2(4)	C5-C10-H10A	109.5
C8-C9-C11	121.4(4)	H10A-C10-H10B	109.5
C5-C10-H10B	109.5	H10A-C10-H10C	109.5
C5-C10-H10C	109.5	C9-C11-H11A	109.5
H10B-C10-H10C	109.5	H11A-C11-H11B	109.5
C9-C11-H11B	109.5	H11A-C11-H11C	109.5
C9-C11-H11C	109.5	C2-N12-C4	127.9(4)
H11B-C11-H11C	109.5	N29-B13-N22	109.8(3)
N29-B13-N15	109.3(3)	N29-B13-H13	110.0
N15-B13-N22	107.6(3)	N22-B13-H13	110.0
N15-B13-H13	110.0	C18-N14-Pt1	133.9(4)
C18-N14-N15	108.5(4)	C16-N15-N14	107.9(4)
N15-N14-Pt1	117.5(3)	N14-N15-B13	119.6(3)
C16-N15-B13	132.0(3)	N15-C16-C19	123.2(4)
N15-C16-C17	108.3(4)	C16-C17-C18	106.4(4)
C17-C16-C19	128.6(4)	C18-C17-H17	126.8
C16-C17-H17	126.8	N14-C18-C20	121.2(4)
N14-C18-C17	108.9(4)	C16-C19-H19A	109.5
C17-C18-C20	129.8(4)	H19A-C19-H19B	109.5
C16-C19-H19B	109.5	H19A-C19-H19C	109.5
C16-C19-H19C	109.5	C18-C20-H20A	109.5
H19B-C19-H19C	109.5	H20A-C20-H20B	109.5
C18-C20-H20B	109.5	H20A-C20-H20C	109.5
C18-C20-H20C	109.5	C25-N21-N22	108.1(5)
H20B-C20-H20C	109.5	N22-N21-Pt1	115.8(3)
C25-N21-Pt1	136.1(4)	C23-N22-B13	130.7(3)
C23-N22-N21	108.7(4)	N22-C23-C24	108.0(4)

N21-N22-B13	120.6(4)	C24-C23-C26	128.5(4)
N22-C23-C26	123.5(4)	C23-C24-H24	126.9
C23-C24-C25	106.3(4)	N21-C25-C24	108.8(4)
C25-C24-H24	126.9	C24-C25-C27	129.1(4)
N21-C25-C27	122.1(4)	C23-C26-H26B	109.5
C23-C26-H26A	109.5	C23-C26-H26C	109.5
H26A-C26-H26B	109.5	H26B-C26-H26C	109.5
H26A-C26-H26C	109.5	C25-C27-H27B	109.5
C25-C27-H27A	109.5	C25-C27-H27C	109.5
H27A-C27-H27B	109.5	H27B-C27-H27C	109.5
H27A-C27-H27C	109.5	C30-N29-N28	110.0(3)
C32-N28-N29	105.7(3)	N28-N29-B13	118.2(3)
C30-N29-B13	130.6(3)	N29-C30-C33	125.1(4)
N29-C30-C31	107.4(3)	C32-C31-C30	105.9(4)
C31-C30-C33	127.5(4)	C30-C31-H31	127.0
C32-C31-H31	127.0	N28-C32-C34	119.9(4)
N28-C32-C31	111.0(4)	C30-C33-H33A	109.5
C31-C32-C34	129.1(4)	H33A-C33-H33B	109.5
C30-C33-H33B	109.5	H33A-C33-H33C	109.5
C30-C33-H33C	109.5	C32-C34-H34A	109.5
H33B-C33-H33C	109.5	H34A-C34-H34B	109.5
C32-C34-H34B	109.5	H34A-C34-H34C	109.5
C32-C34-H34C	109.5		
H34B-C34-H34C	109.5		

APPENDIX D

Atomic coordinates (x 10^4) and equivalent isotropic displacement parameters ($Å^2$x 10^3) for Tp′Pt(MeC=N(2,6-$C_6Me_2H_3$))Me_2 (Chapter 5, **5a**). U(eq) is defined as one third of the trace of the orthogonalized U^{ij} tensor.

	x	y	z	U(eq)
Pt(1)	2472(1)	8281(1)	9004(1)	25(1)
C(1)	2303(9)	7042(6)	8509(4)	34(2)
C(2)	3305(8)	9164(6)	8216(3)	27(2)
C(3)	793(8)	9163(6)	8723(4)	29(2)
C(4)	-110(8)	9709(7)	9206(4)	31(2)
N(5)	529(7)	9272(5)	8161(3)	32(2)
C(6)	-591(9)	9879(7)	7917(4)	32(2)
C(7)	-677(9)	11022(7)	7629(4)	32(2)
C(8)	-1733(11)	11609(8)	7330(4)	46(3)
C(9)	-2702(10)	11057(8)	7313(4)	43(3)
C(10)	-2619(9)	9899(8)	7590(4)	36(2)
C(11)	-1584(9)	9313(7)	7894(4)	34(2)
C(12)	399(10)	11682(8)	7630(5)	48(3)
C(13)	-1528(10)	8043(8)	8179(5)	48(3)
B(14)	3565(10)	7685(8)	10345(5)	33(2)
N(15)	2769(7)	9503(5)	9580(3)	26(2)
N(16)	3317(7)	9009(6)	10126(3)	31(2)
C(17)	3537(8)	9847(7)	10413(4)	31(2)
C(18)	3152(8)	10880(7)	10044(4)	30(2)
C(19)	2681(9)	10637(7)	9537(4)	31(2)
C(20)	4107(9)	9606(7)	11012(4)	36(2)
C(21)	2170(11)	11487(7)	8996(4)	45(3)
N(22)	4298(6)	7303(5)	9251(3)	22(1)
N(23)	4528(7)	7115(5)	9871(3)	26(2)
C(24)	5622(8)	6391(7)	9968(4)	29(2)
C(25)	6139(9)	6153(7)	9398(4)	33(2)
C(26)	5287(8)	6720(7)	8972(4)	30(2)
C(27)	6159(9)	5999(7)	10579(5)	41(2)
C(28)	5433(10)	6671(7)	8284(4)	42(2)
N(29)	1703(7)	7314(5)	9863(3)	29(2)
N(30)	2338(8)	7214(5)	10393(3)	30(2)
C(31)	1767(9)	6598(7)	10889(4)	29(2)
C(32)	746(9)	6304(6)	10686(4)	34(2)
C(33)	736(9)	6756(6)	10052(4)	29(2)
C(34)	2218(10)	6337(7)	11523(4)	37(2)

C(35)	-184(9)	6665(7)	9615(4)	39(2)
Pt(2)	3649(1)	3110(1)	4072(1)	27(1)
C(41)	2741(9)	4022(7)	3320(4)	34(2)
C(42)	4393(9)	1858(7)	3563(4)	38(2)
C(43)	5166(8)	3866(6)	3724(4)	28(2)
C(44)	5776(9)	4308(7)	4204(4)	35(2)
N(45)	5539(7)	3970(5)	3167(3)	33(2)
C(46)	6592(9)	4477(7)	2905(4)	34(2)
C(47)	6443(10)	5653(7)	2611(4)	37(2)
C(48)	7469(12)	6095(8)	2328(5)	49(3)
C(49)	8660(10)	5430(9)	2321(5)	49(3)
C(50)	8802(10)	4278(9)	2581(4)	44(2)
C(51)	7791(9)	3776(7)	2884(4)	32(2)
C(52)	5146(11)	6363(7)	2587(5)	56(3)
C(53)	7988(10)	2484(7)	3148(4)	46(2)
B(54)	2350(10)	2713(8)	5463(4)	31(2)
N(55)	2790(7)	4407(5)	4632(3)	29(2)
N(56)	2172(7)	4026(6)	5189(3)	30(2)
C(57)	1459(8)	4928(7)	5426(4)	30(2)
C(58)	1627(9)	5914(7)	5019(4)	36(2)
C(59)	2465(10)	5575(7)	4538(4)	37(2)
C(60)	654(10)	4796(8)	6016(5)	46(2)
C(61)	3045(10)	6332(7)	4000(4)	44(2)
N(62)	4476(7)	2129(6)	4909(3)	32(2)
N(63)	3725(8)	2177(5)	5463(3)	33(2)
C(64)	4385(10)	1575(7)	5953(4)	36(2)
C(65)	5552(9)	1165(7)	5714(4)	35(2)
C(66)	5586(9)	1495(7)	5074(4)	35(2)
C(67)	3807(10)	1420(8)	6611(4)	48(3)
C(68)	6633(11)	1197(9)	4617(5)	60(3)
N(69)	2026(7)	2258(6)	4430(3)	32(2)
N(70)	1695(7)	2144(5)	5051(3)	29(2)
C(71)	732(9)	1572(7)	5203(4)	32(2)
C(72)	414(8)	1310(7)	4662(4)	32(2)
C(73)	1266(8)	1751(6)	4189(4)	26(2)
C(74)	144(10)	1314(7)	5843(4)	39(2)
C(75)	1301(9)	1663(8)	3513(4)	40(2)

Bond lengths [Å] and angles [°] for Tp′Pt(C=N(2,6-$C_6Me_2H_3$))Me_2 (Chapter 5, **5a**).

Pt(1)-C(3)	2.030(8)	C(31)-C(34)	1.489(11)
Pt(1)-C(1)	2.049(8)	C(32)-C(33)	1.396(12)
Pt(1)-C(2)	2.060(7)	C(33)-C(35)	1.503(11)
Pt(1)-N(22)	2.179(6)	Pt(2)-C(42)	2.032(8)
Pt(1)-N(29)	2.186(7)	Pt(2)-C(43)	2.040(8)
Pt(1)-N(15)	2.203(6)	Pt(2)-C(41)	2.042(8)
C(3)-N(5)	1.279(10)	Pt(2)-N(55)	2.173(7)
C(3)-C(4)	1.519(12)	Pt(2)-N(62)	2.174(7)
N(5)-C(6)	1.403(11)	Pt(2)-N(69)	2.207(7)
C(6)-C(7)	1.381(11)	C(43)-N(45)	1.238(11)
C(6)-C(11)	1.397(13)	C(43)-C(44)	1.535(11)
C(7)-C(8)	1.392(13)	N(45)-C(46)	1.417(12)
C(7)-C(12)	1.539(13)	C(46)-C(51)	1.413(13)
C(8)-C(9)	1.360(14)	C(46)-C(47)	1.415(12)
C(9)-C(10)	1.390(13)	C(47)-C(48)	1.364(15)
C(10)-C(11)	1.379(12)	C(47)-C(52)	1.506(14)
C(11)-C(13)	1.518(12)	C(48)-C(49)	1.388(15)
B(14)-N(30)	1.539(13)	C(49)-C(50)	1.372(13)
B(14)-N(16)	1.542(11)	C(50)-C(51)	1.398(13)
B(14)-N(23)	1.552(12)	C(51)-C(53)	1.524(11)
N(15)-C(19)	1.326(10)	B(54)-N(63)	1.516(12)
N(15)-N(16)	1.380(9)	B(54)-N(70)	1.543(11)
N(16)-C(17)	1.355(10)	B(54)-N(56)	1.552(11)
C(17)-C(18)	1.359(12)	N(55)-C(59)	1.354(10)
C(17)-C(20)	1.479(11)	N(55)-N(56)	1.370(10)
C(18)-C(19)	1.385(11)	N(56)-C(57)	1.356(10)
C(19)-C(21)	1.491(11)	C(57)-C(58)	1.363(12)
N(22)-C(26)	1.324(11)	C(57)-C(60)	1.481(13)
N(22)-N(23)	1.384(9)	C(58)-C(59)	1.387(14)
N(23)-C(24)	1.345(11)	C(59)-C(61)	1.501(13)
C(24)-C(25)	1.375(12)	N(62)-C(66)	1.348(11)
C(24)-C(27)	1.483(12)	N(62)-N(63)	1.393(10)
C(25)-C(26)	1.385(12)	N(63)-C(64)	1.370(11)
C(26)-C(28)	1.515(12)	C(64)-C(65)	1.359(14)
N(29)-C(33)	1.341(11)	C(64)-C(67)	1.505(13)
N(29)-N(30)	1.398(9)	C(65)-C(66)	1.386(12)
N(30)-C(31)	1.353(11)	C(66)-C(68)	1.470(14)
C(31)-C(32)	1.377(13)	N(69)-C(73)	1.328(11)

N(69)-N(70)	1.359(10)	C(19)-N(15)-N(16)	105.8(6)
N(70)-C(71)	1.339(12)	C(19)-N(15)-Pt(1)	138.2(6)
C(71)-C(72)	1.385(12)	N(16)-N(15)-Pt(1)	115.7(4)
C(71)-C(74)	1.481(12)	C(17)-N(16)-N(15)	110.0(6)
C(72)-C(73)	1.407(12)	C(17)-N(16)-B(14)	128.6(7)
C(73)-C(75)	1.507(11)	N(15)-N(16)-B(14)	121.4(6)
C(3)-Pt(1)-C(1)	88.1(3)	N(16)-C(17)-C(18)	107.1(7)
C(3)-Pt(1)-C(2)	88.0(4)	N(16)-C(17)-C(20)	123.5(7)
C(1)-Pt(1)-C(2)	89.2(3)	C(18)-C(17)-C(20)	129.4(7)
C(3)-Pt(1)-N(22)	176.6(3)	C(17)-C(18)-C(19)	106.8(7)
C(1)-Pt(1)-N(22)	89.1(3)	N(15)-C(19)-C(18)	110.4(7)
C(2)-Pt(1)-N(22)	89.9(3)	N(15)-C(19)-C(21)	122.6(7)
C(3)-Pt(1)-N(29)	95.5(3)	C(18)-C(19)-C(21)	127.0(7)
C(1)-Pt(1)-N(29)	91.8(3)	C(26)-N(22)-N(23)	105.7(7)
C(2)-Pt(1)-N(29)	176.4(3)	C(26)-N(22)-Pt(1)	137.1(6)
N(22)-Pt(1)-N(29)	86.6(3)	N(23)-N(22)-Pt(1)	116.9(5)
C(3)-Pt(1)-N(15)	96.4(3)	C(24)-N(23)-N(22)	110.4(7)
C(1)-Pt(1)-N(15)	175.2(3)	C(24)-N(23)-B(14)	129.2(7)
C(2)-Pt(1)-N(15)	92.6(3)	N(22)-N(23)-B(14)	120.3(7)
N(22)-Pt(1)-N(15)	86.4(2)	N(23)-C(24)-C(25)	106.8(7)
N(29)-Pt(1)-N(15)	86.1(2)	N(23)-C(24)-C(27)	124.9(8)
N(5)-C(3)-C(4)	122.1(8)	C(25)-C(24)-C(27)	128.3(8)
N(5)-C(3)-Pt(1)	121.1(7)	C(24)-C(25)-C(26)	106.6(8)
C(4)-C(3)-Pt(1)	116.8(5)	N(22)-C(26)-C(25)	110.4(8)
C(3)-N(5)-C(6)	125.6(8)	N(22)-C(26)-C(28)	124.0(8)
C(7)-C(6)-C(11)	118.3(9)	C(25)-C(26)-C(28)	125.5(8)
C(7)-C(6)-N(5)	120.2(9)	C(33)-N(29)-N(30)	105.6(7)
C(11)-C(6)-N(5)	121.1(7)	C(33)-N(29)-Pt(1)	138.0(6)
C(6)-C(7)-C(8)	121.2(9)	N(30)-N(29)-Pt(1)	116.4(5)
C(6)-C(7)-C(12)	120.5(8)	C(31)-N(30)-N(29)	110.3(7)
C(8)-C(7)-C(12)	118.3(8)	C(31)-N(30)-B(14)	129.1(7)
C(9)-C(8)-C(7)	120.2(9)	N(29)-N(30)-B(14)	120.5(7)
C(8)-C(9)-C(10)	119.2(9)	N(30)-C(31)-C(32)	107.1(7)
C(11)-C(10)-C(9)	121.1(9)	N(30)-C(31)-C(34)	123.4(8)
C(10)-C(11)-C(6)	119.9(8)	C(32)-C(31)-C(34)	129.5(8)
C(10)-C(11)-C(13)	119.0(9)	C(31)-C(32)-C(33)	106.9(8)
C(6)-C(11)-C(13)	121.0(8)	N(29)-C(33)-C(32)	110.1(8)
N(30)-B(14)-N(16)	109.8(7)	N(29)-C(33)-C(35)	122.2(8)
N(30)-B(14)-N(23)	109.5(7)	C(32)-C(33)-C(35)	127.7(8)
N(16)-B(14)-N(23)	109.2(7)	C(42)-Pt(2)-C(43)	86.5(4)

C(42)-Pt(2)-C(41)	88.7(4)	N(56)-C(57)-C(60)	123.8(8)
C(43)-Pt(2)-C(41)	88.7(4)	C(58)-C(57)-C(60)	129.0(8)
C(42)-Pt(2)-N(55)	177.5(3)	C(57)-C(58)-C(59)	106.7(8)
C(43)-Pt(2)-N(55)	95.9(3)	N(55)-C(59)-C(58)	110.1(8)
C(41)-Pt(2)-N(55)	91.5(3)	N(55)-C(59)-C(61)	121.7(9)
C(42)-Pt(2)-N(62)	93.2(3)	C(58)-C(59)-C(61)	128.1(8)
C(43)-Pt(2)-N(62)	95.4(3)	C(66)-N(62)-N(63)	105.5(7)
C(41)-Pt(2)-N(62)	175.6(3)	C(66)-N(62)-Pt(2)	138.3(7)
N(55)-Pt(2)-N(62)	86.4(3)	N(63)-N(62)-Pt(2)	116.0(5)
C(42)-Pt(2)-N(69)	91.9(3)	C(64)-N(63)-N(62)	109.7(8)
C(43)-Pt(2)-N(69)	178.4(3)	C(64)-N(63)-B(54)	128.7(8)
C(41)-Pt(2)-N(69)	91.1(3)	N(62)-N(63)-B(54)	121.1(7)
N(55)-Pt(2)-N(69)	85.6(3)	C(65)-C(64)-N(63)	107.0(9)
N(62)-Pt(2)-N(69)	84.9(3)	C(65)-C(64)-C(67)	130.6(9)
N(45)-C(43)-C(44)	123.4(8)	N(63)-C(64)-C(67)	122.4(9)
N(45)-C(43)-Pt(2)	121.8(6)	C(64)-C(65)-C(66)	107.7(8)
C(44)-C(43)-Pt(2)	114.8(6)	N(62)-C(66)-C(65)	110.0(9)
C(43)-N(45)-C(46)	123.9(7)	N(62)-C(66)-C(68)	122.7(9)
C(51)-C(46)-C(47)	119.4(9)	C(65)-C(66)-C(68)	127.3(9)
C(51)-C(46)-N(45)	119.6(7)	C(73)-N(69)-N(70)	107.2(7)
C(47)-C(46)-N(45)	120.7(9)	C(73)-N(69)-Pt(2)	135.5(6)
C(48)-C(47)-C(46)	119.2(10)	N(70)-N(69)-Pt(2)	117.2(5)
C(48)-C(47)-C(52)	121.7(9)	C(71)-N(70)-N(69)	110.4(7)
C(46)-C(47)-C(52)	119.0(9)	C(71)-N(70)-B(54)	129.3(7)
C(47)-C(48)-C(49)	122.2(9)	N(69)-N(70)-B(54)	120.2(7)
C(50)-C(49)-C(48)	118.8(10)	N(70)-C(71)-C(72)	107.7(8)
C(49)-C(50)-C(51)	121.6(10)	N(70)-C(71)-C(74)	123.7(8)
C(50)-C(51)-C(46)	118.6(8)	C(72)-C(71)-C(74)	128.6(9)
C(50)-C(51)-C(53)	119.7(9)	C(71)-C(72)-C(73)	105.3(8)
C(46)-C(51)-C(53)	121.6(8)	N(69)-C(73)-C(72)	109.4(7)
N(63)-B(54)-N(70)	109.8(7)	N(69)-C(73)-C(75)	125.5(8)
N(63)-B(54)-N(56)	111.1(8)	C(72)-C(73)-C(75)	125.1(8)
N(70)-B(54)-N(56)	107.0(7)		
C(59)-N(55)-N(56)	105.1(7)		
C(59)-N(55)-Pt(2)	136.4(6)		
N(56)-N(55)-Pt(2)	117.0(5)		
C(57)-N(56)-N(55)	110.9(7)		
C(57)-N(56)-B(54)	129.1(8)		
N(55)-N(56)-B(54)	120.0(6)		
N(56)-C(57)-C(58)	107.2(8)		

APPENDIX E

Atomic coordinates (x 10^4) and equivalent isotropic displacement parameters ($Å^2$x 10^3) for Tp′Pt(MeC=N(2,6-$C_6Me_2H_3$))MeI (Chapter 5, **6**). U(eq) is defined as one third of the trace of the orthogonalized U^{ij} tensor.

	x/a	y/b	z/c	U(eq)
Pt1	0.59049(4)	0.12325(3)	0.73465(3)	0.02676(12)
I1	0.65983(9)	0.32221(6)	0.71485(6)	0.0331(2)
C1	0.5014(16)	0.1621(13)	0.8881(13)	0.045(3)
Pt1A	0.59049(4)	0.12325(3)	0.73465(3)	0.02676(12)
I1A	0.4531(2)	0.1608(2)	0.94133(12)	0.0381(8)
C1A	0.642(3)	0.268(2)	0.7390(17)	0.037(3)
C2	0.4173(8)	0.1402(7)	0.5791(7)	0.0226(18)
C3	0.4316(9)	0.1973(8)	0.6805(8)	0.030(2)
N4	0.3545(8)	0.2831(7)	0.7287(7)	0.0336(18)
C5	0.2428(10)	0.3432(8)	0.6963(8)	0.036(2)
C6	0.2535(11)	0.4155(9)	0.6056(9)	0.041(2)
C7	0.1423(11)	0.4843(9)	0.5853(10)	0.043(3)
C8	0.0227(11)	0.4789(10)	0.6483(10)	0.047(3)
C9	0.0139(11)	0.4098(10)	0.7413(11)	0.051(3)
C10	0.1208(11)	0.3433(9)	0.7690(10)	0.044(3)
C11	0.3818(11)	0.4280(10)	0.5342(10)	0.050(3)
C12	0.1063(11)	0.2746(13)	0.8721(11)	0.069(4)
B13	0.7771(10)	0.8810(9)	0.6709(9)	0.031(2)
N14	0.7599(7)	0.0439(5)	0.7972(5)	0.0288(17)
N15	0.8167(8)	0.9330(5)	0.7636(5)	0.0302(17)
C16	0.9052(10)	0.8870(9)	0.8176(9)	0.037(2)
C17	0.9076(10)	0.9708(9)	0.8876(8)	0.038(2)
C18	0.8179(10)	0.0655(9)	0.8736(8)	0.036(2)
C19	0.9806(11)	0.7668(10)	0.8007(11)	0.051(3)
C20	0.7842(11)	0.1763(9)	0.9341(8)	0.040(2)
N21	0.5412(8)	0.9618(7)	0.7485(5)	0.0316(18)
N22	0.6381(8)	0.8685(5)	0.7153(5)	0.0304(17)
C23	0.5921(10)	0.7733(8)	0.7365(8)	0.035(2)
C24	0.4645(10)	0.8068(9)	0.7808(9)	0.041(2)
C25	0.4323(10)	0.9238(9)	0.7894(9)	0.040(2)
C26	0.6758(13)	0.6553(9)	0.7124(11)	0.055(3)
C27	0.3056(11)	0.0006(10)	0.8341(10)	0.052(3)
N28	0.7142(8)	0.0680(7)	0.5740(5)	0.0294(17)

	x/a	y/b	z/c	U(eq)
N29	0.7900(8)	0.9584(7)	0.5689(5)	0.0306(17)
C30	0.8713(10)	0.9392(10)	0.4680(8)	0.038(2)
C31	0.8483(11)	0.0360(11)	0.4052(9)	0.045(3)
C32	0.7515(10)	0.1152(10)	0.4723(9)	0.039(2)
C33	0.9676(11)	0.8311(10)	0.4373(10)	0.048(3)
C34	0.6937(11)	0.2341(10)	0.4445(10)	0.046(3)
C35	0.354(4)	0.482(5)	0.900(2)	0.115(4)
Cl1	0.2411(10)	0.5889(8)	0.8569(9)	0.075(2)
Cl2	0.3315(11)	0.4786(10)	0.0375(5)	0.116(3)
C36	0.326(4)	0.481(5)	0.910(3)	0.115(4)
Cl3	0.3008(9)	0.5786(7)	0.8052(8)	0.069(2)
Cl4	0.1923(13)	0.4832(11)	0.0109(8)	0.133(3)

Bond lengths [Å] and angles [°] for Tp′Pt(MeC=N(2,6-$C_6Me_2H_3$))MeI (Chapter 5, **6**).

Pt1-C1	1.951(15)	N28-N29	1.383(11)
Pt1-N21	2.114(8)	C30-C31	1.377(16)
Pt1-N14	2.217(8)	C31-C32	1.386(17)
C2-C3	1.535(12)	C35-Cl2	1.68(3)
N4-C5	1.428(13)	C36-Cl4	1.68(3)
C5-C10	1.425(15)	C1-Pt1-C3	92.3(6)
C6-C11	1.509(16)	C3-Pt1-N21	91.4(3)
C8-C9	1.387(18)	C3-Pt1-N28	96.4(3)
C10-C12	1.486(18)	C1-Pt1-N14	86.4(6)
B13-N22	1.539(13)	N21-Pt1-N14	88.6(3)
N14-C18	1.349(13)	C1-Pt1-I1	88.8(5)
N15-C16	1.334(13)	N21-Pt1-I1	178.2(2)
C16-C19	1.487(14)	N14-Pt1-I1	90.1(2)
C18-C20	1.489(14)	N4-C3-Pt1	120.3(8)
N21-N22	1.361(11)	C3-N4-C5	125.0(9)
C23-C24	1.354(15)	C6-C5-N4	120.2(10)
C24-C25	1.368(15)	C5-C6-C7	118.5(10)
N28-C32	1.368(13)	C7-C6-C11	119.4(10)
N29-C30	1.348(13)	C7-C8-C9	118.2(10)
C30-C33	1.476(15)	C9-C10-C5	118.1(11)
C32-C34	1.485(15)	C5-C10-C12	121.9(10)
C35-Cl1	1.75(2)	N29-B13-N15	110.2(8)
Pt1-C3	2.048(10)	C18-N14-N15	105.4(8)
Pt1-N28	2.166(7)	N15-N14-Pt1	115.3(6)
Pt1-I1	2.6480(9)	C16-N15-B13	129.6(8)
C3-N4	1.247(12)	N15-C16-C17	106.6(9)
C5-C6	1.388(15)	C17-C16-C19	130.1(10)
C6-C7	1.394(15)	N14-C18-C17	109.8(9)
C7-C8	1.373(17)	C17-C18-C20	126.4(10)
C9-C10	1.384(16)	C25-N21-Pt1	135.3(7)
B13-N29	1.533(14)	C23-N22-N21	109.4(8)
B13-N15	1.548(13)	N21-N22-B13	121.0(8)
N14-N15	1.373(10)	N22-C23-C26	122.5(10)
C16-C17	1.379(15)	C23-C24-C25	108.9(10)
C17-C18	1.364(15)	N21-C25-C27	123.6(10)
N21-C25	1.356(13)	C32-N28-N29	106.0(8)
N22-C23	1.340(13)	N29-N28-Pt1	115.8(6)
C23-C26	1.502(14)	C30-N29-B13	129.9(8)
C25-C27	1.483(14)	N29-C30-C31	108.2(9)

C31-C30-C33	128.8(10)
C1-Pt1-N21	92.3(5)
C1-Pt1-N28	171.3(6)
N21-Pt1-N28	87.4(3)
C3-Pt1-N14	178.7(3)
N28-Pt1-N14	84.9(3)
C3-Pt1-I1	90.0(3)
N28-Pt1-I1	91.3(2)
N4-C3-C2	124.3(9)
C2-C3-Pt1	115.4(6)
C6-C5-C10	120.3(10)
C10-C5-N4	118.6(9)
C5-C6-C11	121.9(10)
C8-C7-C6	122.4(10)
C10-C9-C8	122.2(11)
C9-C10-C12	120.0(11)
N29-B13-N22	110.8(8)
N22-B13-N15	108.3(7)
C18-N14-Pt1	138.5(6)
C16-N15-N14	110.9(8)
N14-N15-B13	119.4(7)
N15-C16-C19	123.3(10)
C18-C17-C16	107.3(9)
N14-C18-C20	123.8(9)
C25-N21-N22	107.5(8)
N22-N21-Pt1	117.1(6)
C23-N22-B13	129.5(8)
N22-C23-C24	107.1(9)
C24-C23-C26	130.3(10)
N21-C25-C24	107.1(9)
C24-C25-C27	129.4(10)
C32-N28-Pt1	137.8(7)
C30-N29-N28	109.8(8)
N28-N29-B13	120.3(7)
N29-C30-C33	123.0(10)
N28-C32-C31	109.3(9)
C31-C32-C34	127.9(10)
N28-C32-C34	122.7(10)
Cl2-C35-Cl1	112.6(16)